11281

UNIVERSIDAD NACIONAL AUTÓNOMA DE MÉXICO

INSTITUTO DE INVESTIGACIONES BIOMÉDICAS

MODIFICACIONES BIOQUíMICO-FUNCIONALES EN LA CORTEZA VISUAL DE GATO COMO RESULTADO DE UNA LESIÓN ISQUÉMICA FOCAL CORTICAL

T E S I S

QUE PARA OBTENER EL GRADO DE

DOCTOR EN CIENCIAS BIOMÉDICAS

P R E S E N T A:

PSIC. ANGÉLICA ZEPEDA RIVERA

DIRECTORA DE TESIS: DRA CLORINDA ARIAS ÁLVAREZ

BIOMEDICAS

MÉXICO, D.F. 2004

Miembros del Jurado

Dr. Ranulfo Romo Trujillo

Dra. Clorinda Arias Álvarez

Dr. José Miguel Cervantes Alfaro

Dr. Julio Morán Andrade

Dr. Ricardo Tapia Ibargüengoytia

Dra. Lourdes Massieu Trigo

Dr. Miguel Morales Mendoza

El presente trabajo se realizó en el Departamento de Biología Celular y Fisiología del Instituto de Investigaciones Biomédicas de la UNAM, bajo la dirección de la Dra. Clorinda Arias y en el Departamento de Neurofisiología del Instituto Max-Planck de Neurobiología en Munich, Alemania, bajo la dirección del Dr. Frank Sengpiel y el Dr. Tobias Bonhoeffer. El trabajo se llevó a cabo con el apoyo del departamento de becas al extranjero del Consejo Nacional de Ciencia y Tecnología (CONACYT); CONACYT (Proyecto 36250M); de la DGEP; del PAEP (Proyecto 202373); Graduierten Kollege Sensorische Interaktion der Systemen München y la Deutsche Akademische Austausch Dienst, DAAD.

A mi esposo Luis por su apoyo, dedicación, amor y paciencia a lo largo de estos años.

A nuestro bebé, por traer su luz a nuestras vidas.

Agradecimientos

A la Dra. Clorinda Arias, por aceptarme en su laboratorio, por su confianza y su apoyo incondicional. Por esas largas pláticas y por sus enseñanzas no solo de ciencia, sino de la vida y de la amistad.

A Luis, por ser un gran maestro y el mejor compañero de vida.

A mis papas, Edith y Eduardo por su apoyo constante, su interés y su amor ilimitado.

A Bea, mi hermana quien es y ha sido un gran ejemplo en mi vida.

A Montse, por su fidelidad, su compañía y por su amistad incondicional.

A Perla y Miguel por su paciencia y sus pláticas en los momentos de angustia.

A mis compañeros del laboratorio.

Al Dr. Gabriel Gutiérrez y a los miembros de su laboratorio por su interés y por ayudar a mejorar este trabajo.

A los miembros del jurado, cuyos comentarios me permitieron enriquecer este trabajo.

INDICE

RESUMEN

Los mapas corticales representan la activación selectiva de grupos neuronales ante numerosas características de la información sensorial proveniente del mundo externo. Dichos mapas constituyen un mosaico dinámico, que puede modificarse como consecuencia de procesos como el desarrollo, el entrenamiento, el aprendizaje y lesiones. La reorganización funcional de las representaciones en la corteza visual ha sido ampliamente explorada después de lesiones periféricas (retinianas), sin embargo, el estudio de la plasticidad cortical visual en respuesta a lesiones centrales ha recibido poca atención no obstante su relevancia clínica. El objetivo de este trabajo fue explorar la capacidad de reorganización de algunos mapas corticales visuales en respuesta a una lesión isquémica focal en corteza visual primaria de gato y correlacionar la reorganización funcional con procesos de cambios morfológicos y moleculares de reparación asociados a ella. Para ello, se indujo una lesión fotoquímica focal en la corteza visual primaria de gato y se exploró, por medio de la técnica de imagenología óptica de señales intrínsecas, la organización funcional cortical alrededor de la lesión inmediatamente después de producirla y 1, 2 y 5 semanas posteriores. El volumen de lesión en el tejido se determinó por medio de una tinción de violeta de cresilo e histoquímica para citocromo oxidasa. Para evaluar la posible correlación entre la reorganización funcional y los cambios morfológicos y bioquímicos alrededor de la lesión, se analizó la expresión de la proteína fibrilar acídico glial (GFAP), la proteína asociada a microtúbulos MAP-2, la proteína específica de núcleos neuronales NeuN, la proteína asociada al crecimiento axónico GAP-43, la subunidad $\alpha 1$ del receptor $GABA_A$ y la subunidad R1 del receptor glutamatérgico NMDA; además, se evaluaron los niveles de aminoácidos en el borde de la lesión. Funcionalmente se observó que la lesión fotoquímica genera un área silente de actividad, la cual disminuye a lo largo del tiempo debido a un proceso de cicatrización y a la reorganización funcional de los mapas corticales. Los resultados histológicos muestran una

lesión bien delimitada formada por un centro de núcleos picnóticos rodeado de astroglia anisomórfica. El proceso de reorganización funcional se acompañó de: 1) el incremento gradual en el contenido de MAP-2 entre las semanas 1 y 5 post lesión (sPL); 2) un incremento de estructuras dendríticas alrededor de la lesión y un decremento paralelo de células inmunopositivas a GFAP; 3) un incremento máximo de GAP-43 a las 2sPL; 4) un incremento paralelo en el contenido de NMDAR1 y glutamato entre las semanas 1 y 5 PL; 5) un incremento de los niveles de $GABA_A\alpha 1$ entre las semanas 1 y 2 PL y la permanencia de niveles bajos de GABA entre las semanas 1 y 5 PL. Los resultados descritos muestran que diferentes representaciones visuales corticales se reorganizan como resultado de una lesión isquémica focal y que la reorganización correlaciona en el tiempo con rebrote dendrítico y cambios diferenciales en elementos asociados a la neurotransmisión excitadora / inhibidora, lo que sugiere su participación en los mecanismos que determinan la reorganización funcional cortical.

ABSTRACT

Cortical maps represent the selective activation of neuronal groups in response to numerous features of sensorial information. Maps constitute a dynamic mosaic susceptible of modifications due processes such as development, training and lesions. Visual cortex reorganization has been extensively studied after peripheral (retinal) lesions, but plasticity after focal cortical lesions have received less attention despite their clinical relevance. In this study, we investigated the reorganization of different cortical maps at different time points after a focal ischemic lesion in the primary visual cortex (V1) and addressed some of the morphological and molecular changes previously associated with functional repair. We induced a focal photochemical lesion in V1 of kittens and assessed, through optical imaging of intrinsic signals, the functional cortical layout immediately afterwards and at 1, 2 and 5 weeks after lesion. We analyzed histologic sections and evaluated temporal changes of functional maps. We calculated the volume of the lesion form Nissl stained sections and sections processed for cytochrome oxidase hystochemistry and addressed whether functional reorganization correlated in time with changes in the expression of microtubule associated protein (MAP-2), growth associated protein (GAP-43), the neuronal specific nuclear protein NeuN, glial fibrillary acidic protein (GFAP), $GABA_A$ receptor subunit $\alpha 1$ ($GABA_A\alpha 1$), subunit 1 of the NMDA receptor (NMDAR1) and in neurotransmitter levels at the border of the lesion. Functional results showed that the photochemical lesion produces a silent area, which shrinks with time due to a scar formation process and to functional reorganization of cortical maps. Histology results showed a well delimited lesion with a core of pycnotic nuclei surrounded by anisomorphic astroglia. Functional reorganization was accompanied by: 1) a gradual increase in MAP-2 contents within 1 and 5 weeks post-lesion (wPL); 2) an increase of dendritic structures surrounding the lesion and a parallel decrease of GFAP immunopositive cells; 3) an increase of GAP-43 after 2wPL and a subsequent decrease in protein levels; 4) a parallel

increase in NMDAR1 and glutamate contents between weeks 1 and 5 PL; 5) an increase in $GABA_A\alpha 1$ levels between weeks 1 and 2 PL, but low levels of GABA from week 1 to 5 PL. The above described results show that visual cortex representations may reorganize after a focal ischemic lesion and that reorganization correlates in time with dendritic sprouting and with modifications in the excitatory / inhibitory neurotransmission systems thus suggesting mechanisms by which plasticity of cortical representations may occur.

Organización de la tesis

El presente trabajo está dividido en 6 secciones: Introducción, Hipótesis y Objetivos, Anexo metodológico, Resultados experimentales, Discusión y Conclusiones.

En la introducción se revisa la organización general del sistema visual enfatizando la organización funcional de la corteza visual y la plasticidad de la representaciones corticales visuales. Así mismo, se exponen los principales mecanismos de plasticidad nerviosa que se han asociado a la reorganización funcional cortical y finalmente, se revisa el tema de la isquemia cerebral y el empleo de la lesión fotoquímica como modelo experimental para la inducción de un evento isquémico cortical.

La siguiente sección expone la hipótesis de trabajo de la tesis y los objetivos de ésta última. Posteriormente se incluye el trabajo titulado: "Optical imaging of intrinsic signals: Recent developments in the methodology and its applications" (*J Neurosci Methods* (2004) en prensa) el cual provee una revisión detallada de la técnica de imagenología óptica de señales intrínsecas que se empleó para evaluar la reorganización *in vivo* de los mapas corticales visuales en respuesta a una lesión isquémica. El resto de la metodología empleada en este trabajo se puede consultar en los trabajos que componen la sección de resultados. Esta sección se presenta mediante dos trabajos originales, el primero de ellos titulado: "Reorganization of Visual Cortical Maps After Focal Ischemic Lesions" (*J Cereb Blood Flow Metab* (2003) 23:811-820*)* y el segundo titulado: "Functional Reorganization of Visual Cortex Maps After Ischemic Lesions is Accompanied by Changes in Expression of Cytoskeletal Proteins and NMDA and $GABA_A$ Receptor Subunits" (*J Neurosci* (2004) 24:1812-21).

En la discusión se enmarcan los resultados de la tesis en un contexto más amplio de lo tratado en cada uno de los trabajos de Resultados y se finaliza con la sección de Conclusiones y Perspectivas.

INTRODUCCIÓN

El sistema visual

Organización general de la vía visual

En los mamíferos, la sensación final de un estímulo visual ocurre en la corteza visual primaria, también denominada V1 o corteza estriada. La entrada de la información visual inicia con la activación de los fotorreceptores de la retina, quienes forman una capa continua en la parte posterior del ojo. Los fotorreceptores transducen la energía luminosa en cambios del potencial membrana, información que envían a través de sus axones a las células horizontales y bipolares; estas últimas establecen sinapsis con las células amacrinas y ganglionares. Los axones de las células ganglionares establecen conexiones sinápticas con las células del núcleo geniculado lateral (NGL) del tálamo y en el tracto final de la vía visual, los axones de las neuronas del NGL proyectan hasta la corteza visual primaria. Para algunos autores, la corteza visual primaria del mamífero incluye a las áreas corticales 17 y 18 debido a que son estas quienes reciben información directa del NGL y sin dicha entrada de información, las células en estas áreas no presentan actividad eléctrica. Sin embargo, debido a que el área 18 recibe a su vez información de la corteza estriada y está funcionalmente implicada en etapas posteriores del procesamiento visual existe aun controversia con respecto a su inclusión como parte de la corteza primaria.

El área 17 del gato es el área visual más extensa y abarca entre 300 y 400 mm^2 de superficie cortical por lo que ocupa la mayor parte de la corteza superior al sulco esplenio, el área que se encuentra por encima del giro fusiforme. La mayor parte del área 17 no es visible en el cerebro expuesto, sin embargo una zona pequeña de esta área se puede observar en la superficie dorsal del cerebro en la unión con los giros marginal y posteromedial. El área 18 es una región inmediatamente lateral al área 17 que ocupa una gran parte de la porción expuesta del giro marginal y está flanqueada lateralmente por el área 19 (Fig 1) (Payne y Peters, 2002).

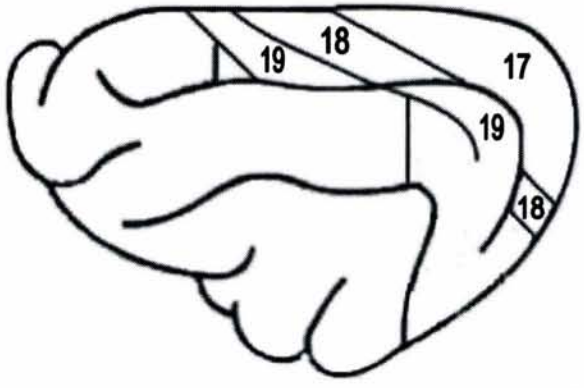

Fig 1 Esquema de una vista dorsolateral del hemisferio cortical izquierdo del gato en el que se muestra la posición típica del área 17 y regiones que le circundan. Modificado de Payne y Peters (2002).

Organización celular de la corteza visual

Con base en preparaciones con tinciones de Nissl, se ha determinado que el área 17 contiene seis capas corticales, aun cuando las capas 4, 5 y 6 se han subdividido cada una en 2 subcapas (Fig 2). Esta laminación se basa esencialmente en la disposición de los cuerpos celulares de las células piramidales y células espinosas estrelladas, que son excitadoras y representan el 80% de la población total de neuronas en el área 17 (Gabbott y Somogyi, 1986). Estas células son la fuente y los efectores de la transmisión sináptica excitadora, mientras que el 20% de células restantes son de tipo GABAérgico y son las efectoras de la inhibición intracortical. A estas células también se les conoce como neuronas de circuitos locales, células estrelladas o interneuronas y sus axones están generalmente distribuidos localmente dentro de la corteza cerebral (Somogyi et al., 1982; Farinas y DeFelipe, 1991).

La corteza estriada tiene un grosor aproximado de 1.5 mm y la capa más superficial, o capa 1 cuenta sólo con algunas neuronas inhibidoras, algunas de ellas tipo neurogliaformes y astrocitos. La capa 2 está poblada de células piramidales pequeñas que están concentradas en su borde más dorsal. A medida que se continúa en profundidad, las células piramidales pequeñas se hacen menos notorias y se observan células piramidales grandes, las cuales continúan hasta la capa 3, por lo que no existe una distinción clara entre las capas 2 y 3. Sin embargo, existe un grupo de células en la capa 3, de tipo

piramidal, cuyos axones no sólo se extienden verticalmente hacia la materia blanca, sino también horizontalmente hacia las diferentes capas. Estas ramas horizontales suelen formar grupos de terminales que contactan espinas dendríticas de células piramidales. Se ha propuesto, que la función principal de los axones horizontales es activar otras células piramidales con características fisiológicas similares como son la preferencia de orientación de los estímulos, la dominancia ocular, la preferencia de dirección de movimiento u otras propiedades de los campos receptivos (*vide infra*) (Payne y Peters, 2002).

En la capa 2/3 también se encuentran células GABAérgicas tipo canasta grande y candelabro; los botones sinápticos de las primeras establecen contacto sináptico solamente con los segmentos iniciales axónicos de las células piramidales, mientras que los de las segundas forman sinapsis con soma y dendritas proximales de células piramidales (Somogyi et al., 1983; Kisvarday et al., 1993). Además de la inhibición lateral que ejercen estas células, se encuentran las células de doble bouquet, cuyos axones establecen sinapsis con dendritas y espinas dendríticas de células de la capa 4, por lo que se ha sugerido que juegan un papel en la inhibición cortical en el cerebro (Payne y Peters, 2002).

La capa 4 cortical es la más gruesa de todas y contiene, en su mayoría, células espinosas estrelladas pequeñas; los somas de estas células participan en la formación de sinapsis simétricas, mientras que sus dendritas, que contienen espinas, reciben un gran número de terminales axónicas de neuronas espinosas que forman sinapsis asimétricas. Aquí también se encuentran células GABAérgicas del tipo de canasta grandes y pequeñas; estas últimas establecen sinapsis con dendritas y espinas dendríticas (Kisvarday et al., 1985).

La Capa 5 contiene células piramidales pequeñas, medianas y grandes que se caracterizan por tener dendritas apicales largas que terminan en las capas 1-4. La capa 6 contiene principalmente células piramidales pequeñas y medianas con núcleos celulares redondos. Dichos núcleos se encuentran dispuestos en grupos de columnas verticales separadas por espacios claros en las que no se observan procesos dendríticos o axónicos.

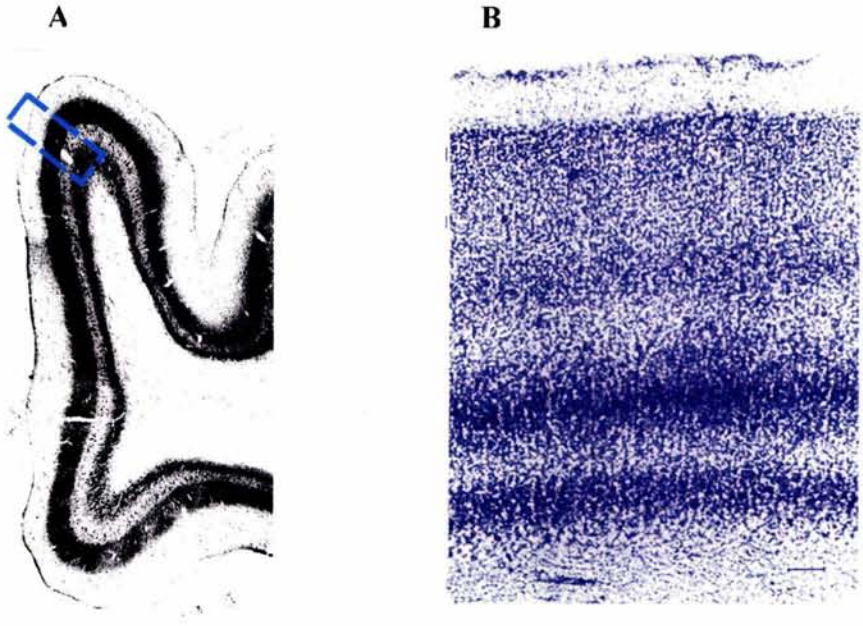

Fig 2. Distribución de capas celulares en la corteza visual primaria del gato. **(A)** Fotomicrografía de un corte coronal teñido con plata. El recuadro enmarca una zona de área 17 correspondiente a la sección amplificada que se muestra en **(B). (B)** Micrografía de un corte coronal de área 17 teñido con violeta de cresilo. A la izquierda se indica la numeración de las capas corticales.

Organización funcional de la corteza visual

Una de las características más sobresalientes de la arquitectura funcional de la neocorteza es que las neuronas con propiedades de respuesta similares están agregadas en forma de columnas que se extienden perpendiculares a la corteza cerebral desde la pía madre hasta la superficie de la materia blanca. Esta organización columnar la describió por primer vez Vernon Mountcastle en la corteza somatosensorial (Mountcastle, 1957) y ha sido subsecuentemente descrita en otras áreas primarias sensoriales y motoras.

Con respecto a la corteza visual, se ha descrito que las células del área cortical 17 se agrupan de acuerdo a sus características funcionales formando columnas que se extienden perpendiculares a la corteza. Cada columna responde a elementos particulares de los objetos visuales, como su ubicación espacial, la orientación espacial del objeto, la dirección de su movimiento y su frecuencia espacial (Hubel y Wiesel, 1962; Hubel y Wiesel, 1963). La organización de dichas columnas entre si en la corteza visual conforma los denominados mapas corticales visuales.

El estudio sistemático de las columnas funcionales inició con registros electrofisiológicos empleando electrodos de profundidad. Sin embargo, el mapeo electrofisiológico de alta resolución de las propiedades de respuesta celulares en regiones grandes de la corteza visual se dificulta debido a que la técnica requiere mucho tiempo por lo que resulta poco factible hacer un muestreo suficientemente grande de células.

Otra técnica que se empleó en forma alternativa a los registros electrofisiológicos fue la de la histoquímica para 2-deoxyglucosa, por medio de la cual se realizan mapeos de regiones metabólicamente activas. Esta técnica permite la visualización de la arquitectura funcional con una resolución suficientemente alta, pero tiene la desventaja de que sólo se puede estudiar la activación de un solo tipo de mapa cortical (máximo 2) y no permite realizar estudios crónicos. Alternativamente a estos métodos, se han empleado técnicas de imagenología óptica para estudiar la arquitectura funcional de la corteza visual. La técnica de imagenología óptica de señales intrínsecas ha sido la más empleada para este propósito. Dicha técnica permite realizar estudios crónicos con una alta resolución (80 um) y se basa en la detección de cambios sutiles en la refracción de luz que genera el tejido cortical eléctrica y metabólicamente activo (Bonhoeffer y Grinvald, 1996) (ver Trabajo 1). En la siguiente sección se detallará la organización funcional de los mapas que se han descrito, mediante diversas técnicas, principalmente de imagenología, en la corteza visual primaria del gato.

El mapa retinotópico

La sensación visual inicia en la retina, donde los fotorreceptores forman una capa continua en la parte posterior del ojo. Con ayuda de la óptica del ojo, la capa de fotorreceptores captura la imagen del campo visual sin interrupciones entre los puntos de la imagen, excepto en el área donde se localiza el disco óptico o fóvea. Esta información de posición se mantiene en un arreglo retinotópico y se transmite vía talámica a la corteza visual primaria, donde se forma una representación continua del campo visual denominado mapa visuotópico o retinotópico (Daniel y Whitteridge, 1961; Tusa et al., 1978).

Los primeros estudios sobre la organización funcional de la corteza visual se llevaron a cabo mediante el registro electrofisiológico de las células con microelectrodos. Por medio de esta técnica Hubel y Wiesel (Hubel y Wiesel, 1959; Hubel y Wiesel, 1962; Hubel y

Wiesel, 1965) describieron por primer vez los mapas de organización visuotópica y establecieron un mapa del campo visual con respecto a la superficie de la corteza visual. Así, se determinó que en el mapa visuotópico, puntos adyacentes en el campo visual están representados como puntos adyacentes en la corteza y que el orden espacial del campo visual se mantiene sin distorsión significativa y con el mismo orden en la corteza.

Estudios recientes con imagenología óptica de señales intrínsecas han demostrado que en efecto, líneas adyacentes en el campo visual están representadas con una progresión continua en el área 17 de la corteza visual (Bosking et al., 2002; Zepeda et al., 2003) (Fig. 3).

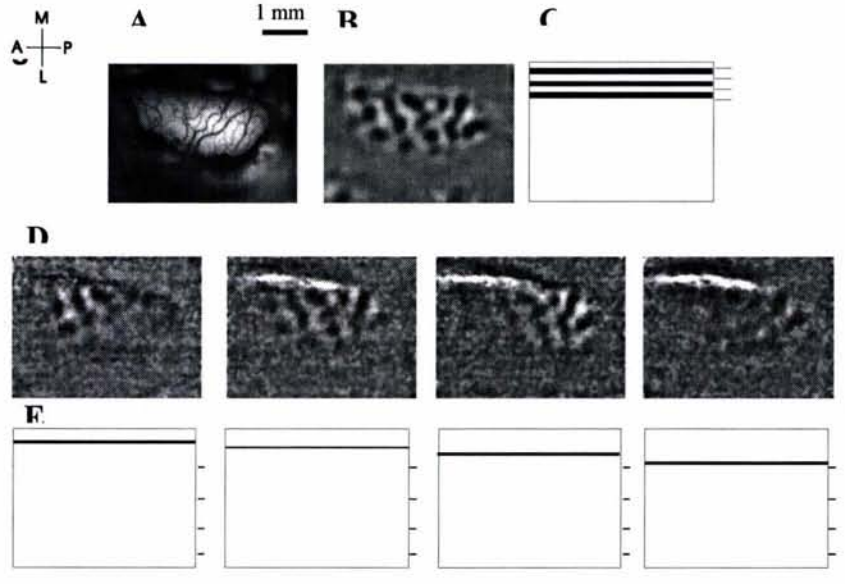

Fig 3. Mapa retinotópico en corteza visual primaria de gato obtenido por medio de la técnica de imagenología óptica de señales intrínsecas. **(A)** Vista dorsal del patrón de vasos corticales de la región correspondiente al área de la que se obtuvieron los mapas. (A:anterior; P: posterior; M:medial; L: lateral). **(B)** Mapa de orientación preferente evocado ante la presentación del estímulo mostrado en **(C)**. Las áreas negras corresponden a los grupos de células que responden preferentemente a estímulos de 0^0; **(C)** Estímulo visual presentado en la pantalla de una computadora y que consiste en barras en movimiento de 0^0 de orientación que evoca respuesta celular en el área cortical correspondiente. Las líneas a la derecha representan los cuadrantes en los que se puede presentar el estímulo dependiendo de punto de fijación visual del animal. **(D)** Respuesta celular ante cada uno de los estímulos representados en **(E)**. Note que los dominios celulares que se activan cambian dependiendo de la posición del estímulo presentado en **(E)**. **(E)** Estímulos visuales de 0^0 de orientación y 1^0 de ancho que se presentan aleatoriamente para evocar el mapa retinotópico cortical. Note que estímulos adyacentes evocan respuesta en regiones corticales adyacentes (Zepeda y Sengpiel, datos no publicados).

El mapa de orientación preferente

Hubel y Wiesel (Hubel y Wiesel, 1962; Hubel y Wiesel, 1963) describieron por primer vez dominios celulares en la superficie cortical que se extendían en un sistema columnar y respondían selectivamente a la orientación de un contorno. Esta misma disposición columnar fue descrita por medio de la técnica de 2-deoxyglucosa (Albus y Sieber, 1984) y

más recientemente mediante el empleo de la técnica de imagenología óptica de señales intrínsecas (Bonhoeffer y Grinvald, 1991) (Ver trabajo 1).

Las imágenes obtenidas por medio de imagenología muestran que cada dominio de orientación preferente tiene una forma redonda o elongada y que los dominios están dispuestos en forma radial o de "rehilete" alrededor de llamados centros de orientación (Bonhoeffer y Grinvald, 1991). Cada rehilete está compuesto de un grupo completo de dominios que responden a todas las orientaciones de un contorno y cada orientación está representada una sola vez en cada rehilete. Como se observa en la figura 4, el cambio entre una y otra orientación es muy sutil y no se observan fracturas evidentes entre cada dominio. La densidad de los centros de orientación varía entre animales, sin embargo, en el área cortical 17 se puede encontrar un promedio de 2.0 a 2.6 centros por mm^2 (Bonhoeffer et al., 1995).

El mapa de dirección preferente

La mayoría de las neuronas de la corteza visual del gato muestran preferencia por estímulos en movimiento en relación a estímulos estáticos. Más aún, estas células generalmente responden selectivamente a la dirección del movimiento y tienden a agruparse según su preferencia por una u otra dirección formando así dominios de preferencia por dirección de movimiento (Payne et al., 1981; Swindale et al., 1987). La disposición de los dominios en este mapa también cambia sutilmente entre la preferencia por distintas direcciones, sin embrago, se ha observado una coincidencia espacial entre aquellas regiones donde la selectividad por una dirección particular es baja con regiones con cambios rápidos en la preferencia por una dirección (Shmuel y Grinvald, 1996).

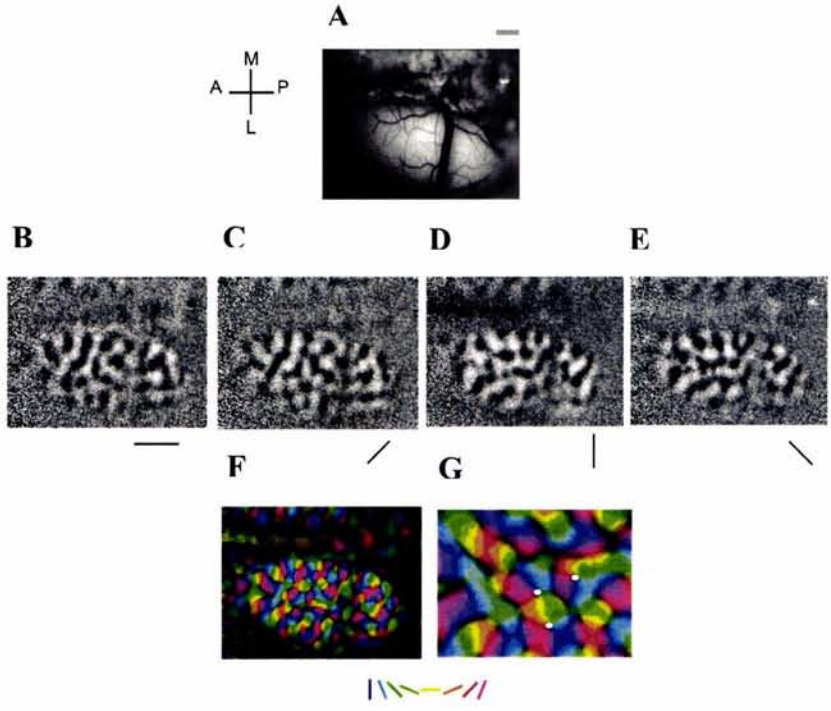

Fig 4. Mapas de orientación preferente en corteza visual primaria de gato obtenido por medio de la técnica de imagenología óptica de señales intrínsecas. **(A)** Vista dorsal del patrón de vasos corticales de la región correspondiente al área de la que se obtuvieron los mapas. (A:anterior; P: posterior; M:medial; L: lateral). **(B-E)** mapas de orientación preferente correspondientes a la región cortical mostrada en **(A).** Las áreas negras corresponden a los grupos de células que responden preferentemente a estímulos de 0^0 **(B)**, 45^0 **(C)**, 90^0 **(D)** y 135^0 **(E).** Las barras muestran la orientación del estímulo preferido. **(F-G)** Mapas en los que se muestra la preferencia de grupos celulares a diferentes orientaciones. Cada color corresponde a una orientación particular (codificadas en las barras inferiores). **(G)** Magnificación de **(F)**. Los círculos blancos muestran la localización de los centros de rehilete. Note la distribución ordenada de los diferentes grupos celulares alrededor de dichos centros. Escala: 1mm (Zepeda y Sengpiel, datos no publicados).

Las columnas de frecuencia espacial

Las neuronas de la corteza visual primaria se pueden activar óptimamente con frecuencias espaciales particulares y se ha demostrado que la respuesta neuronal a frecuencias altas o bajas está dispuesta en forma de dominios o parches. Sin embargo, aún no se ha logrado un consenso en cuanto al mapa que pudieran formar los dominios en la superficie cortical. Así, se ha planteado que los dominios con preferencia por frecuencias espaciales bajas están rodeados por una región contigua de células con preferencia por frecuencias altas (Hubener et al., 1997; Shoham et al., 1997), pero también se ha sugerido que el mapeo de la frecuencia espacial en el área 17 es un continuo similar al de los mapas de

orientación y dirección preferente (Everson et al., 1998; Issa et al., 2000). En estos trabajos se utilizó la técnica de imagenología óptica de señales intrínsecas (ver Trabajo1, sección Materiales y métodos) para estudiar la organización de los dominios de frecuencia espacial, sin embargo, dado que la técnica no ha permitido resolver la organización de este tipo de mapas, pudiera resultar valioso el combinarla con un registro electrofisiológico detallado de neuronas únicas para determinar cual de los esquemas propuestos describe mejor la disposición de los dominios de frecuencia espacial de la corteza visual del gato.

Relaciones funcionales entre mapas corticales visuales

Un elemento característico de la corteza visual es que agrupa un número de mapas de respuestas variadas que representan un parámetro particular del campo visual (posición, orientación, etc). Así todos los mapas anteriormente descritos coexisten en una misma región cortical y tienen un arreglo geométrico particular entre sí (Hubener et al., 1997). Más aún, cada punto del mundo visual se analiza por un conjunto circunscrito de células corticales (Hubel y Wiesel, 1962). Esto es, la imagen completa de un punto en el espacio puede ser analizada por un área de 2x2 mm en la que se encuentran contenidos por lo menos un grupo de cada una de las columnas funcionales anteriormente descritas.

La cobertura uniforme de un estímulo depende, hasta cierto punto, de cómo la preferencia de orientación y el espacio visual están mapeados cada uno entre sí. Como se mencionó anteriormente, estudios de imagenología han mostrado que el mapa de orientación preferente no es homogéneo: en algunas regiones la progresión de la preferencia de orientación es lenta y suave, mientras que en otras regiones como los centros de rehilete, sitios vecinos prefieren orientaciones ortogonales (Bonhoeffer y Grinvald, 1991). Sin embargo, estas dos representaciones son independientes, ya que si el mapa retinotópico siguiera la misma arquitectura funcional que el mapa de orientación, entonces las irregularidades de este último correlacionarían con fracturas en el mapa visual, lo cual se ha comprobado que no ocurre (Bosking et al., 2002). Más aún, se ha demostrado que no hay una relación consistente entre la tasa de cambio de la preferencia por una orientación y la tasa de cambio por la preferencia de una posición en el espacio (Bosking et al., 2002).

En cuanto a la dirección del movimiento, esta es una propiedad que está íntimamente asociada con la preferencia de orientación en el área visual 17 y muchas neuronas selectivas a orientación prefieren el movimiento de un estímulo en una u otra de las direcciones perpendiculares a la orientación de preferencia. La complementariedad de los mapas de preferencia de orientación y selectividad a dirección se demostró en un estudio realizado por Shmuel y Grinvald (Shmuel y Grinvald, 1996) que describe que cada dominio de orientación consiste de dos subregiones, cada una de las cuales prefieren movimiento en direcciones opuestas, aún cuando formen parte del mismo dominio de orientación.

El significado funcional de las relaciones específicas entre los distintos sistemas columnares para el procesamiento de la información visual, pudiera ser que las relaciones ortogonales entre las columnas confieren la ventaja de permitir diferentes combinaciones de las propiedades de los estímulos para que estas se representen en el área cortical más pequeña posible. Este arreglo de columnas en la corteza visual podría permitir que cada punto del campo visual se analice con respecto a todas las combinaciones de parámetros, es decir, que la cobertura del estímulo en el espacio visual esté maximizada. De hecho Hubel y Wiesel propusieron que un pedazo de 2x2 mm de corteza estriada, al que denominaron módulo cortical, es necesario y suficiente para analizar la imagen de un punto en el espacio, ya que su remoción conlleva a la percepción de un punto ciego en el espacio visual (Hubel y Wiesel, 1962).

La plasticidad de las representaciones corticales visuales

Las representaciones corticales visuales están compuestas de grupos grandes de neuronas, cada una de las cuales cuenta con un campo receptivo (CR). El CR es el área en la retina que, cuando se estimula, provoca actividad en una neurona visual (Eysel, 2002).

Con base en una serie de estudios que muestran que el CR de las células corticales pueden modificarse en cuestión de minutos u horas, se ha propuesto que los CR representan una propiedad neuronal dinámica (Sillito, 1974a, b). Así mismo, se ha demostrado que la organización de los mapas corticales visuales es relativamente constante a través del tiempo, si bien constituye un mosaico dinámico que puede sufrir cambios como consecuencia de procesos de entrenamiento y aprendizaje (Sengpiel et al.,

1998; Sengpiel et al., 1999). Esto es, las representaciones visuales, como el resto de las representaciones sensoriales y motora corticales son plásticas.

La plasticidad nerviosa se ha definido como el cambio duradero en las propiedades de las neuronas corticales; por ejemplo, en la fortaleza de sus conexiones internas, sus patrones representacionales, o sus propiedades morfológicas y funcionales (Donoghue et al., 1996).

La plasticidad de las representaciones corticales visuales ha sido ampliamente estudiada precisamente en relación al desarrollo (Godecke y Bonhoeffer, 1996; Godecke et al., 1997), al entrenamiento (Blakemore y Cooper, 1970; Singer et al., 1981; Sengpiel et al., 1999) y a otras manipulaciones que incluyen la privación monocular (Godecke y Bonhoeffer, 1996), el apareamiento de estimulación visual y eléctrica (Fregnac et al., 1988; Schuett et al., 2001) y la microestimulación intracortical (Godde et al., 2002). Más aún, la plasticidad cortical visual en respuesta a lesiones periféricas (retineanas) ha sido ampliamente abordada (Kaas et al., 1990; Eysel et al., 1999). Sin embargo, el tema de la reorganización visual posterior a lesiones focales ha recibido poca atención, no obstante su relevancia en la medicina.

Lesiones de corteza visual

Las lesiones nerviosas focales cerebrales provocan deficiencias asociadas a un deterioro sensorial, motor o cognitivo dependiendo del sitio del daño. En el caso de las lesiones de corteza visual, éstas pueden provocar síntomas muy diversos dependiendo de las áreas afectadas y los estudios que han evaluado las consecuencias de lesiones masivas han estado enfocados a evaluar la compensación conductual y reorganización en áreas visuales corticales alejadas de la lesión (Spear et al., 1988; Orban et al., 1990; Vandenbussche et al., 1991; MacNeil et al., 1996; Illig et al., 2000; Payne y Lomber, 2002). Sin embargo, como se mencionó, el estudio de la reorganización funcional en áreas aledañas a lesiones focales es muy limitado (Eysel y Schweigart, 1999). Las repercusiones funcionales de este tipo de lesiones cobran importancia debido a que el daño focal de corteza visual produce un escotoma o punto ciego en el campo visual de los individuos que la padecen. Debido a la organización retinotópica de la corteza visual primaria, todos los elementos de un punto determinado del mundo visual se representan y analizan en una

región definida de la corteza, llamada hipercolumna (Hubel y Wiesel, 1974). Así, la lesión focal de la corteza visual destruye las células blanco de las fibras geniculocorticales en una región retinotópica determinada, privando al individuo de visión en el área del campo visual correspondiente. Sin embargo, el déficit funcional generado por la lesión puede disminuir con el paso del tiempo de forma natural o como producto del entrenamiento tanto en infantes como en adultos (Zihl y von Cramon, 1985; Kasten et al., 1998). Debido a que el tejido destruido no tiene la capacidad de restaurar la función alterada, se postula que la compensación perceptual posterior a una lesión se debe a la reorganización anatómico-funcional de áreas corticales aledañas al daño o de estructuras funcionales asociadas al área lesionada. El proceso que permite al individuo compensar las discontinuidades que existen en su campo visual y percibir estímulos en un área del campo visual donde no hay entrada de información visual, se denomina "filling in" o "completado de imagen". Funcionalmente, el individuo percibe el área del escotoma como invadida por el patrón de las áreas circundantes del campo visual y deja de percibir el punto ciego, posiblemente como resultado de la reorganización de las estructuras centrales visuales.

En un estudio reciente, Eysel y Schweigart (1999) mostraron que 55 días después de producida una lesión focal en corteza visual primaria en gato, las células de alrededor de la lesión mostraban un incremento en sus campos receptivos, sugiriendo un posible mecanismo por el que ocurriría el fenómeno de "filling in". Sin embargo, en este trabajo no se evaluaron los posibles mecanismos celulares asociados a la reorganización de los CR visuales. No obstante, estudios de este mismo grupo (Mittmann et al., 1994; Mittmann y Eysel, 2001) sugieren que la compensación visual posterior a una lesión puede resultar de: a) la activación de neuronas silentes ubicadas en el área de penumbra (la zona circundante a la lesión que ha sobrevivido el daño primario producto de la isquemia) y/o; b) el alargamiento del campo receptivo (CR) neuronal (área restringida de respuesta de una neurona) en el borde de la lesión. Ambas posibilidades pudieran relacionarse tanto con modificaciones a nivel anatómico de las células sanas alrededor de la lesión, como a cambios en el balance de los sistemas excitador/inhibidor de comunicación neuronal (Mittmann et al., 1994; Buonomano y Merzenich, 1998; Mittmann y Eysel, 2001).

Los estudios antes mencionados proveen un importante marco de referencia para comprender la reorganización funcional visual posterior a una lesión focal visual, sin

embargo, no ofrecen evidencia que muestre si el mapa cortical asociado al déficit funcional se reorganiza, como sucede en los sistemas motor (Jones y Schallert, 1994; Nudo et al., 1996a) y somatosensorial (Nguyen et al., 2000). Más aún, no abordan la reorganización de los mapas funcionales posterior a una lesión en conjunto con algunos de los mecanismos de plasticidad nerviosa que pudieran estar asociados a ella.

La plasticidad nerviosa y la reorganización funcional

Los mecanismos de neuroplasticidad que presentan las células nerviosas como consecuencia del desarrollo, de modificaciones en el ambiente del individuo o a partir de un proceso lesión son muy similares, es decir, los mecanismos de plasticidad que un organismo despliega durante la ontogenia son los mismos que se observan durante un proceso de neuroreparación.

Aún cuando se sabe poco sobre los mecanismos generales que subyacen a la neuroplasticidad, se conocen algunos de los eventos comunes que participan en la remodelación de los circuitos neuronales. Las dos formas principales de plasticidad que se han descrito son 1) el rebrote, por medio del que terminales axónicas y procesos dendríticos crecen y forman nuevas conexiones con sitios sinápticos vacantes y 2) el desenmascaramiento funcional de sinapsis silentes, que implica modificaciones en el balance de la neurotransmisión excitadora e inhibidora y que conlleva a la activación de vías preexistentes (Buonomano y Merzenich, 1998). Tanto las modificaciones morfológicas, como neuroquímicas pueden mediar la reorganización funcional. No obstante, el fenómeno no se debe limitar a uno solo de los mecanismos mencionados, sino que se debe tener presente que en él coexisten eventos que dan lugar a su expresión. Así, en el caso de la neuroreparación, hay que tomar en cuenta la evidencia experimental reciente sobre el papel de la glia y de la neurogénesis, que pudieran también contribuir en la restauración de circuitos neuronales dañados y en la reorganización funcional.

Con respecto a la reorganización cortical posterior a lesiones retineanas, se ha propuesto que tanto el rebrote, como la modulación de la neurotransmisión juegan un papel importante. Sin embargo, cada uno de ellos parecería actuar con una temporalidad distinta. Así, las modificaciones plásticas de corto plazo pudieran estar dadas por ajustes dinámicos en los sistemas de neurotransmisión excitadora e inhibidora resultado de una

modulación rápida de la efectividad de conexiones preexistentes, donde la actividad excitadora subumbral pudiera tornarse supraumbral ya sea por medio de la supresión de la inhibición o de la potenciación de conexiones excitadoras (Chino et al., 1992).

A largo plazo, la plasticidad cortical posterior a una lesión periférica se ha asociado a modificaciones del citoesqueleto neuronal que dan lugar a la elongación y ramificación de axones y dendritas y a un subsecuente proceso de sinaptogénesis (Darian-Smith y Gilbert, 1994).

Mecanismos morfológicos asociados a la plasticidad nerviosa: Rebrote dendrítico y elongación axónica

El citoesqueleto es una estructura altamente dinámica que se reorganiza continuamente. Varias líneas de evidencia indican que cambios en la estructura del citoesqueleto neuronal proveen el soporte de los dramáticos cambios morfológicos que ocurren durante el desarrollo neuronal. En un proceso de lesión en el SNC el citoesqueleto de las neuronas afectadas tanto por daño primario, como por daño secundario, puede resultar alterado. Esto se traduce en la desestabilización de las proteínas del citoesqueleto, la cual puede resultar en la degeneración retrógrada o anterógrada de la célula, en la desaparición de terminales axónicas y en el consecuente incremento de sitios postsinápticos vacantes.

Durante el proceso de degeneración muchas células morirán, sin embrago aquellas que sobreviven al daño pueden presentar un proceso de regeneración presináptico o postináptico denominado rebrote axónico o dendrítico respectivamente. Este proceso requiere de cambios concertados tanto de señales que operan en la superficie neuronal como de respuestas que se dan al interior de la célula e implica que las proteínas del citoesqueleto que conforman microtúbulos, neurofilamentos y microfilamentos se reensamblen hasta alcanzar cierto grado de estabilidad. Una vez que las proteínas del citoesqueleto se reorganizan y estabilizan, el axón y las dendritas pueden reestablecer conexiones sinápticas específicas y funcionales.

Las neuronas que sobreviven al daño pueden presentar un proceso de rebrote dendrítico el cual se ha planteado como un posible mecanismo celular para reestablecer la comunicación sináptica de las neuronas que han quedado desaferentadas (Jones y Schallert, 1992; Buonomano y Merzenich, 1998).

Los microtúbulos (Mts), los filamentos más gruesos del citoesqueleto, son estructuras dinámicas huecas, que crecen y se contraen por medio de la adición o substracción de subunidades de α y β tubulina. El grado de rigidez o plasticidad de estas estructuras confiere a la neurona propiedades dinámicas, favorece el desarrollo de polaridad neuronal y regula aspectos funcionales como el transporte axonal. La estabilidad de los Mts depende en gran medida de las proteínas asociadas a éstos, llamadas frecuentemente MAPs estructurales, que modulan la polimerización, estabilidad y arreglo de los MTs en el citoplasma.

Existen diversos tipos de MAPs, cada una de ellas con diferentes isoformas. De estas proteínas, la fosfoproteína MAP-2 se encuentra distribuida de manera prominente en soma y dendritas, pero no en axones. La función de esta proteína ha sido particularmente asociada a fenómenos como el establecimiento de la polaridad neuronal, el crecimiento dendrítico, la plasticidad neuronal y la regeneración dendrítica posterior a lesiones centrales (Sanchez et al., 2000).

Diversos trabajos han documentado que después de un proceso de daño isquémico cortical, MAP-2 desaparece del área central de la lesión, pero que esta muestra una sobreexpresión progresiva en el área de penumbra isquémica entre 7 y 14 días posteriores a la lesión (Bidmon et al., 1998; Li et al., 1998). Más aún, se ha demostrado que existe una coincidencia temporal entre la reorganización del árbol dendrítico y la recuperación funcional motora post-lesión (Kolb y Gibb, 1993; Jones y Schallert, 1994). Sin embargo, el estudio de la reorganización dendrítica posterior a lesiones corticales es escaso.

Si bien es cierto que los resultados de los trabajos mencionados no implican que la sobreexpresión de MAP-2 en células aledañas a una lesión sea un indicador de reorganización funcional, si permiten inferir que, posterior a la lesión, se está gestando un proceso de plasticidad estructural asociado a la polimerización y estabilización de Mts de dendritas previamente existentes o en formación.

Los axones, como las dendritas son estructuras que están en constante remodelación. El crecimiento axónico es un evento principalmente asociado a la formación circuitos neuronales durante el desarrollo y durante la regeneración nerviosa.

La regeneración axónica puede ocurrir en forma de: a) *Rebrote colateral*, en el que las terminales de neuronas intactas generan rebrotes que repueblan las sinapsis que quedaron vacantes a consecuencia de la pérdida de terminales o de la muerte de sus neuronas aferentes y; b) *rebrote regenerativo* en donde un axón dañado no sufre degeneración retrógrada, sino que da lugar a un cono de crecimiento que reinerva el blanco denervado (Fawcett et al., 2001b).

Diversos estudios han mostrado que después de lesiones periféricas y centrales a los sistemas motor y somatosensorial, ocurren procesos de regeneración axónica que implican modificaciones tanto de terminales tálamo-corticales (Jones y Pons, 1998), como cortico-corticales (Florence et al., 1998).

El proceso de rebrote axónico normalmente concluye con un proceso llamado sinaptogénesis en el que la formación de nuevas sinapsis reemplaza a las que se han perdido por la degeneración retrógrada de axones destruidos (Stroemer et al., 1995; Bergado-Rosado y Almaguer-Melian, 2000).

En el caso de las lesiones del sistema visual, se ha sugerido que la remodelación topográfica después de lesiones retineanas (Kaas et al., 1990; Chino et al., 1992; Gilbert y Wiesel, 1992) depende de a) circuitos viables remanentes que proveen de una conectividad cruzada en el área reorganizada (Calford et al., 1999); b) la reconexión funcional a nivel del NGL (Eysel, 1982) y; c) el rebrote axónico de conexiones laterales (Gilbert y Wiesel, 1992; Darian-Smith y Gilbert, 1994, 1995).

En experimentos en los que la reformación de mapas de la corteza visual se indujo por medio de lesiones a la retina, Darian-Smith y Gilbert (1994) mostraron, mediante el marcaje de axones tálamo-corticales que el escotoma cortical no se "rellenaba" por el rebrote de terminales de dichos axones, pero si por la ramificación axónica de conexiones cortico-corticales.

El proceso del rebrote regenerativo o elongación axónica correlaciona con cambios notables y específicos en la síntesis de algunas proteínas características de axones denominadas "proteínas asociadas al crecimiento". Una de estas proteínas, quizá las más estudiada, es la GAP-43 (Growth Associated Protein-43) (Skene, 1989).

GAP-43 es una fosfoproteína asociada a la membrana que se localiza en la parte intracelular de la membrana plasmática de neuronas y que interviene en el proceso de

crecimiento de la terminal presináptica por medio de una asociación con el citoesqueleto. (McGuire et al., 1988).

En la neocorteza y el hipocampo, los niveles más altos de GAP-43 se observan durante las dos primeras semanas de vida, coincidentes con el periodo de ramificación de la terminal axónica y de sinaptogénesis (Linden et al., 1988). Sin embargo esta proteína, cuyo papel en el proceso de crecimiento neurítico ha sido ampliamente documentado (Aigner et al., 1995; Aigner y Caroni, 1995) también se sobre expresa en neuronas aledañas a una lesión isquémica del SNC (Stroemer et al., 1995; Li et al., 1998). Stroemer et al. (1995) demostraron que los tiempos de expresión máxima de la proteína, correspondían a aquellos en los que los sujetos lesionados mostraban una curva significativa de recuperación de la función alterada consecuente al daño. Además, reportan que la sobre expresión de GAP-43 ocurre durante un periodo específico como producto de la lesión y que el proceso se atenúa una vez que inicia el proceso de formación de nuevas sinapsis identificadas mediante inmunohistoquímica para la sinaptofisina, una proteína asociada a vesículas presinápticas.

Papel de la glía en la plasticidad nerviosa

Las células gliales y neuronales mantienen una estrecha relación funcional y estructural. Los astrocitos representan a un tipo de células gliales que proveen el soporte estructural a las neuronas, modulan el ambiente que las rodea, liberan factores de crecimiento diversos y permiten la comunicación entre neuronas y vasos sanguíneos.

El papel de la glia en un proceso de lesión y regeneración es aun controversial. Está bien documentado que uno de los eventos tempranos asociados a una lesión nerviosa es la formación de la cicatriz glial formada principalmente por astrocitos y microglía reactivos, fibroblastos y moléculas de matriz extracelular (para una revisión, véase (Nieto-Sampedro et al., 2002). Se ha propuesto que el papel esencial de la cicatriz glial es el de aislar al tejido sano del daño secundario. La cicatriz consiste esencialmente en una acumulación de astrocitos fibrosos hipertróficos en la superficie de la lesión. Fibroblastos del tejido conjuntivo adyacente proliferan sobre la capa de astrocitos fibrosos, depositan colágeno y completan la formación de una nueva frontera con el resto del tejido sano.

Los astrocitos, componentes mayoritarios de la cicatriz glial, son posiblemente las células que poseen mayor plasticidad del SNC, ya que son capaces de cambiar en número y morfología en respuesta a perturbaciones del microambiente neuronal. Tras una lesión muestran un gran incremento en la expresión de filamentos intermedios, lo que les confiere el aspecto 'fibroso' que les da el nombre de astrocitos "fibrosos" o "reactivos". Los filamentos intermedios son reconocidos por anticuerpos contra la proteína fibrilar ácida de la glía (GFAP), el marcador más típico de los astrocitos reactivos.

Los astrocitos que proliferan en el SNC de mamíferos adultos pueden originarse: a) por desdiferenciación de astrocitos maduros a astroblastos; b) a partir de precursores de astrocitos, conservados en el adulto; c) a partir de nuevos astroblastos, derivados de células madre, y d) de todas estas posibilidades (Bovolenta et al., 1993).

La formación de la cicatriz glial puede tener efectos tanto permisivos como inhibidores de la extensión neurítica debido a que la reacción glial inflamatoria presenta infiltración leucocitaria y producción de citotoxinas, pero también factores antinflamatorios, antioxidantes, neurotróficos y neuritogénicos. Los astrocitos presentan una dualidad de propiedades benéfico/deletéreas especialmente notorias cuando se considera la restitución de funciones biológicas tras una lesión. El tipo de agresión al que es sometido el SNC determina la composición celular de la 'cicatriz glial'. Sus componentes astrocitarios mayoritarios son de dos tipos: astrocitos fibrosos hipertróficos y astroblastos. El origen y las propiedades de interacción con neuritas de ambos tipos celulares son también diferentes, incluso opuestos. Se ha propuesto que los astrocitos fibrosos hipertróficos en la 'cicatriz glial', expresan proteoglicanos inhibidores de la iniciación, adhesión, crecimiento y orientación de las neuritas que son un obstáculo para la regeneración de axones lesionados. Por otro lado, los astroblastos, que expresan proteoglicanos promotores del crecimiento, son un sustrato excelente para el crecimiento de axones y dendritas (neuritas) (Bovolenta et al., 1993). Sin embargo, se ha probado que los astrocitos reactivos expresan moléculas de adhesión celular, moléculas de matriz extracelular (ECM), factores de crecimiento y, receptores a factores de crecimiento que sólo se encuentran presentes en astrocitos inmaduros, astrocitos intactos o neuronas (Ridet et al., 1997; McGraw et al., 2001). En suma, la coexistencia de factores

favorecedores e inhibidores, tanto de la muerte neuronal como de la regeneración axonal, definen una situación de equilibrio durante el proceso de cicatrización en el SNC. La evidencia que contrapone los efectos permisivos y negativos de los astrocitos en un proceso de regeneración nerviosa, puede reconciliarse partiendo de que estas células pudieran ejercer diferentes efectos en las neuronas dependiendo del tiempo que haya transcurrido a partir de la lesión. Así, es posible que en los primeros días que suceden a la lesión, la cicatriz glial en efecto restringa el reestablecimiento de comunicación intercelular. Sin embargo, tanto la retracción de los astrocitos, como su disminución en número y la secreción de diferentes moléculas quimiotácticas en días posteriores a la lesión, podrían generar un ambiente más permisivo tanto para la extensión neurítica, como para el reestablecimiento sináptico entre células sobrevivientes al daño (Raivich et al., 1999).

Modificaciones neuroquímicas asociadas a la plasticidad neuronal

Las eventos plásticos anteriormente descritos están principalmente relacionados con cambios morfológicos neuronales y morfo-funcionales de las células gliales. Sin embargo, las neuronas también pueden sufrir modificaciones a nivel funcional, que generen cambios en los circuitos preestablecidos.

En la corteza cerebral del mamífero la mayoría de las sinapsis inhibidoras son GABAérgicas y las excitadoras, glutamatérgicas. La inhibición está mediada por los receptores $GABA_A$ y $GABA_B$, mientras que la excitación está mediada a través de los receptores al ácido α-amino 3-hidroxi-5-metil-4-isoxasol-propriónico (AMPA), al kainato (no NMDA) y al N-metil-D-aspartato (NMDA).

La especificidad de la transmisión excitadora e inhibidora en las células corticales y su modulación contribuyen a la arquitectura funcional de los campos receptivos, por lo que el fenómeno de plasticidad sináptica se ha asociado a nivel celular con la reorganización del área de respuesta de las células que componen un mapa cortical.

Desde un punto de vista más funcional, la recuperación de circuitos neuronales después de lesiones, se ha asociado a un fenómeno denominado desenmascaramiento de vías (Jacobs y Donoghue, 1991; Schieber y Hibbard, 1993) que implica modificaciones en la modulación espacio-temporal del balance excitación/inhibición de circuitos neuronales específicos.

La comunicación química interneuronal involucra principalmente la excitación o inhibición eléctrica de las neuronas. El balance entre excitación e inhibición de los circuitos neuronales puede variar como consecuencia de eventos patológicos o traumáticos resultando en la sobreexcitación, desinhibición o inhibición de circuitos específicos. Estos desajustes pueden resultar a su vez de la disponibilidad y liberación de neurotransmisores y de la regulación a la alta o a la baja de sus receptores específicos.

El sistema de neurotransmisión inhibidora predominante del sistema nervioso central es el GABAérgico. El ácido γ-amino butírico (GABA) ejerce su acción principal a través del receptor $GABA_A$. Este neurotransmisor y sus receptores definen el campo receptivo (CR) de las células corticales, es decir, delimitan el área de respuesta de cada neurona (Jones, 1993).

En una variedad de trabajos se ha demostrado que el tamaño del CR depende de la funcionalidad del receptor $GABA_A$; en células corticales visuales, el antagonismo del receptor induce el alargamiento de los CR (Sillito, 1974a,b, 1975a,b; Jacobs y Donoghue, 1991) (ver (Eysel, 2002).

El fenómeno de crecimiento de los CR corticales también se ha observado en células aledañas a lesiones centrales (Nudo et al., 1996a; Eysel y Schweigart, 1999) y se ha propuesto que este evento está asociado a modificaciones en la eficacia sináptica. En este sentido, lo que se propone es que la inhibición que normalmente delimita los CR disminuye, promoviendo el desenmascaramiento de conexiones corticales preexistentes.

Recientemente, el grupo de Eysel (Mittmann et al., 1994; Mittmann y Eysel, 2001) mostró que lesiones focales en la corteza visual de ratas adultas inducen hiperexcitabilidad, probablemente debida a una disminución de la inhibición GABAérgica y a un incremento de la transmisión excitatoria mediada por el glutamato a través de su receptor NMDA . Este mismo grupo demostró también, que los CR de células que rodean una lesión focal en corteza visual de gato aumentan. Por ello, se ha propuesto que la desinhibición neuronal asociada tanto al alargamiento de los CR, como a la facilitación sináptica que ocurre en la periferia de una lesión cortical, podría resultar de la regulación a la baja de receptores $GABA_A$ y/o de la reducción en la afinidad del GABA por éstos (Schiene et al., 1996; Redecker et al., 2000). Así mismo, se ha demostrado que tanto las conexiones inhibidoras, como las excitadoras, tienen el potencial de modificar la

selectividad de orientación de una célula por medio de las sinapsis locales provenientes de la misma columna o de columnas aledañas con la misma orientación (Eysel, 2002). De hecho, un estudio posterior demostró que el efecto inhibidor más importante provenía de células con orientaciones aledañas a la óptima, lo cual pudiera sugerir que una disminución en la eficacia del sistema inhibidor conlleve a la plasticidad de la preferencia de orientación de una célula cortical y su red cortical local. Así, mientras la inyección del antagonista del receptor $GABA_A$, bicuculina, reduce y hasta provoca la pérdida de selectividad de orientación de una célula (Sillito, 1975b), las conexiones excitadoras incrementan la selectividad de orientación de una célula por medio de los receptores glutamatérgicos tipo NMDA (Eysel, 2002). Esto es, la funcionalidad de un circuito neuronal también puede sufrir alteraciones a partir del incremento de la eficacia excitadora, principalmente regulada por el sistema glutamatérgico en el SNC. El glutamato, a través de una variedad de receptores específicos, ionotrópicos y metabotrópicos, promueve modificaciones de largo plazo en la excitabilidad y morfología neuronal, así como en la estructura y función sináptica (Michaelis, 1998).

Existe evidencia que indica que neuronas aledañas a una lesión cortical en individuos que no han sido sometidos a procesos de aprendizaje o memoria muestran potenciación sináptica probablemente como un mecanismo compensatorio de la pérdida sináptica (Schiene et al., 1999; Neumann-Haefelin y Witte, 2000; Mittmann y Eysel, 2001). El incremento de la eficacia sináptica puede estar dado a partir de la activación de sinapsis silentes, mediada por receptores NMDA (Rumpel et al., 1998; Rumpel et al., 2000). Esta activación excitadora puede ser el resultado de i) modificaciones funcionales del receptor; ii) cambios en la composición de subunidades o número de receptores del tipo NMDA; iii) la regulación a la alta de los receptores o; iv) el agrupamiento postsináptico de los receptores (Michaelis, 1998; Que et al., 1999a).

La modulación de los receptores NMDA también se ha asociado a los cambios morfológicos que sufren las células nerviosas ante situaciones diversas, ya que el bloqueo de estos receptores impide la inducción de la proteína GAP-43 y el crecimiento axónico colateral (McNamara y Routtenberg, 1995). Se ha postulado que el mecanismo de acción de estos receptores es a través de la entrada de Ca^{2+} a las terminales post-sinápticas lo

que puede activar, entre otros mecanismos, enzimas que modifican a proteínas morforeguladoras del citoesqueleto (Montoro et al., 1993; Sanchez et al., 1997).

De forma alternativa o concomitante a la regulación a la baja de los receptores $GABA_A$, los receptores NMDA pueden sufrir una regulación a la alta como parte de un proceso de potenciación sináptica. Estos últimos también podrían mediar la estabilización de proteínas del citoesqueleto, particularmente a través de la regulación del contenido o grado de fosforilación de MAP-2 (Sanchez et al., 1997) en un proceso de reorganización funcional, por lo que resulta importante explorar su expresión temporal en el modelo de lesión que aborda este trabajo.

Modelos de lesión nerviosa: La isquemia cortical como modelo de lesión para el estudio de la plasticidad nerviosa

Las lesiones al SNC pueden tener orígenes muy diversos. Sin embrago, las dos causas principales de daño resultan de traumatismos craneoencefálicos y de eventos isquémicos. En el presente trabajo se empleó un modelo de isquemia denominado "lesión fotoquímica" (*vide infra*) debido a que permite inducir un foco isquémico focal cortical sin manipular el tejido y por tanto evita riesgos de lesión mecánica por manipulación.

En los humanos, se observan dos tipos principales de isquemia: la isquemia global transitoria y la isquemia focal prolongada. La isquemia global ocurre cuando hay una falla circulatoria generalizada, como es el caso del ataque cardíaco, mientras que la isquemia focal ocurre cuando un área circunscrita del cerebro pierde su flujo sanguíneo debido al bloqueo o ruptura de una arteria. Los eventos focales pueden estar asociados a un bloqueo permanente o transitorio de la arteria seguido de un proceso de reperfusión una vez que el trombo desbloquea la arteria (Fawcett et al., 2001a).

La isquemia cerebral se origina por la disminución del flujo sanguíneo hasta un nivel suficiente (20-40 mmHg) para interferir con la función del sistema nervioso (Castillo, 2000). Este decremento es el resultado de la alteración del equilibrio de numerosos factores hemodinámicos y puede conducir a la aparición, en las

neuronas y en la glia, de una serie de alteraciones metabólicas y bioquímicas que concluirán en la necrosis celular (Siesjo, 1984).

En un evento isquémico primario se combinan diferentes procesos que incluyen la anoxia, la vasoconstricción y la formación del edema, así como una cascada de procesos tóxicos que incluyen la excitotoxicidad, la toxicidad metabólica, la activación de proteasas y el estrés oxidante, los cuales convergen para producir la degeneración nerviosa.

La disminución del flujo sanguíneo por debajo de un determinado umbral (20-12 ml/100g/min) en una zona del parénquima cerebral origina inmediatamente alteraciones de la transmisión sináptica y si el flujo sanguíneo disminuye a menos de 12ml/100g/min) puede provocar supresión de la actividad electrencefalográfica (Castillo, 2000).

Las alteraciones funcionales aparecen inmediatamente después del comienzo de la isquemia y son únicamente dependientes del flujo, mientras que las alteraciones estructurales requieren más tiempo y son dependientes tanto del tiempo, como del flujo.

La obstrucción de un vaso sanguíneo cerebral ocasiona un gradiente isquémico que da lugar a una isquemia intensa en el centro del territorio vascular y a una isquemia menos pronunciada en la periferia del mismo. Las células del núcleo isquémico, con un flujo inferior al umbral del infarto, mueren en pocos minutos. En la zona periférica, con un flujo por debajo del umbral de isquemia, se originan alteraciones de la actividad funcional de las neuronas, pero con conservación de una actividad metabólica mínima que preserva su integridad estructural durante algún tiempo. Esta zona se denomina penumbra isquémica (Ginsberg y Pulsinelli, 1994). La importancia del concepto de penumbra isquémica radica en la hipótesis de que las neuronas localizadas en la periferia del infarto que sobreviven al período isquémico pueden recuperarse al reestablecerse las condiciones hemodinámicas y se restaure un flujo sanguíneo cerebral que permita un aporte normal de glucosa y oxígeno.

El fallo bioenergético ocasionado por la disminución del flujo sanguíneo cerebral ocasionará la lesión celular, fundamentalmente a través de: el desarrollo de

acidosis, las alteraciones en el equilibrio de los flujos iónicos y la entrada de calcio iónico (Ca^2+) en la célula. La isquemia condiciona la activación de la glucólisis anaerobia, con producción de ácido láctico y reducción del pH intra y extracelular.

Durante la isquemia, la neurona es incapaz de mantener la polarización de la membrana, lo que condiciona la apertura de los canales de Ca^2+ dependientes de voltaje y el desbloqueo de los canales de Ca^2+ acoplados a receptores. Estos mecanismos ocasionan un incremento de la concentración del Ca^2+ intracelular de aproximadamente el doble o más de su valor inicial; esta concentración todavía no es capaz de iniciar el proceso de la muerte celular, pero si de originar una brusca despolarización de la membrana (Castillo, 2000).

La intensa despolarización de la membrana neuronal condiciona el aumento de la liberación de cantidades excesivas de glutamato y otros aminoácidos excitadores. El glutamato estimula receptores ionotrópicos, fundamentalmente el AMPA y el NMDA, así como receptores metabotrópicos. La estimulación del receptor AMPA aumenta la concentración de sodio intracelular y ocasiona edema celular. La estimulación de los receptores NMDA es responsable del aumento de Ca^2+ intracelular y de la iniciación de la cascada isquémica dependiente de este catión que contribuye importantemente a la muerte neuronal (Ginsberg, 1997).

El edema que aparece durante la isquemia cerebral es el resultado de la acumulación de líquido en el interior de las células y en el intersticio celular o de ambos. En el primer caso recibe el nombre de edema citotóxico y en el segundo, de edema cerebral vasogénico.

Las características bioquímicas del sistema nervioso, entre ellas su elevada concentración en lípidos y su alto requerimiento energético, lo hacen particularmente sensible a la lesión mediada por radicales libres. En la isquemia cerebral, la formación de radicales libres de oxígeno puede exceder la capacidad antioxidante de la neurona y ocasionar alteraciones en algunos constituyentes celulares, como proteínas, ácidos nucléicos y lípidos. Los radicales libres de oxígeno responsables del estrés oxidante en las neuronas son el anión superóxido, el radical hidroxilo, el peróxido de hidrógeno, el óxido nítrico y el peroxinitrito.

La lesión fotoquímica

Los modelos experimentales de isquemia cerebral tienen por objetivo reproducir algunos de los eventos fisiopatológicos que ocurren durante un proceso isquémico, el cual puede ocurrir a partir de la hemorragia de vasos cerebrales, o bien por medio de la oclusión trombótica o embólica de vasos cerebrales.

La lesión fotoquímica es un modelo de lesión isquémica focal que se basa en la peroxidación de la membrana lipídica de las células endoteliales y la consecuente formación de trombos.

La reacción fotoquímica se induce al inyectar un derivado de fluoresceína, rosa de bengala (disodio tetraiodotetraclorofluoresceína), al torrente sanguíneo y concomitante a la inyección, irradiar el área cortical a lesionar con una luz verde de 562 nm de longitud de onda. La absorción de luz provoca que la molécula del rosa de bengala done electrones al oxígeno molecular para crear oxígeno en singulete, el cual es altamente reactivo y peroxida algunos constituyentes de las membranas celulares, particularmente los ácidos grasos insaturados y algunas proteínas (Watson, 1998). La reacción fotoquímica produce defectos endoteliales que facilitan la adhesión y agregación plaquetaria hasta el punto de la oclusión del vaso, modelando así una lesión de tipo tromobótica. El depósito plaquetario ocurre principalmente en la superficie cortical, donde la interacción fotoquímica es máxima. Sin embargo, el infarto se desarrolla en capas corticales más profundas debido a la compresión edematosa.

Las principales ventajas de este modelo son su reproducibilidad, la poca invasividad y su duración a largo plazo. Más aún, la lesión se puede localizar en regiones corticales específicas y tanto el área como el volumen de la lesión se pueden controlar por medio de variables como la concentración del rosa de bengala, la intensidad de la luz y la duración de la irradiación. Sin embargo, esta lesión no asemeja en su totalidad los eventos celulares desencadenados por un proceso isquémico no inducido experimentalmente, ya que en un evento trombótico natural, la formación de oxígeno en singulete no representa uno de los principales eventos asociados al daño celular; la muerte celular ocurre tanto por necrosis, como

por apoptosis y normalmente, se genera un área de penumbra isquémica cuya presencia puede influir de forma importante en el desarrollo tanto del daño, como del proceso de recuperación.

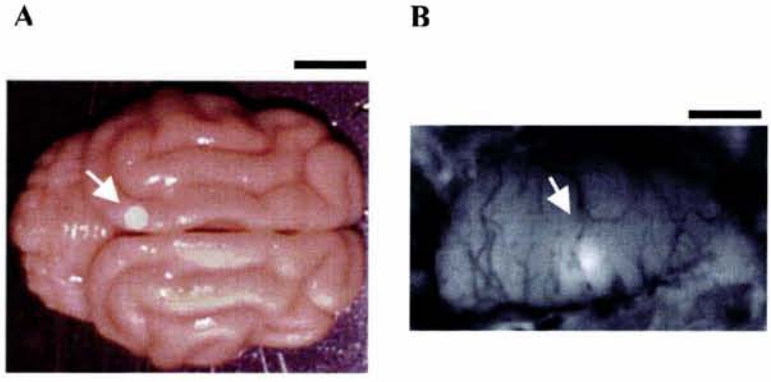

Fig 5. Lesión fotoquímica. **(A)** Vista dorsal de un cerebro perfundido de gato. El punto blanco representa el área donde se indujo la lesión fotoquímica (indicada con flecha). **(B)** Vista dorsal del cerebro del un gato inmediatamente después de producida la lesión fotoquímica (indicada con una flecha). Note la palidez del tejido en el área de la lesión con respecto al resto de la corteza. La región en la que se observa oclusión de vasos sanguíneos corresponde al área blanca marcada en **(A).** Esacala en (A): 1cm, (B) 1mm (Zepeda y Sengpiel, datos no publicados).

En el presente trabajo se exploraron algunas modificaciones morfológico-funcionales inducidas por una lesión isquémica focal cortical en la corteza visual primaria del gato. Las posibles modificaciones funcionales se estudiarán mediante la técnica de imagenología óptica de señales intrínsecas (ver Trabajos 2 y 3). Esta técnica permite visualizar longitudinalmente los mapas corticales visuales *in vivo* con una alta resolución espacial y temporal.

En paralelo a los estudios de imagenología se valorarán las posibles modificaciones morfológicas y moleculares de las células circundantes a la lesión isquémica.

Desde el punto de vista morfológico, se explorarán los patrones temporales de expresión y contenido de las proteínas MAP-2, asociada al rebrote dendrítico, GAP-43, asociada a la elongación axónica y GFAP, asociada a la activación astrocítica y a la generación de cicatrices en el SNC.

Desde el punto de vista neuroquímico se valorará el contenido de la subunidad $\alpha 1$ del receptor $GABA_A$ ($GABA_A\alpha 1$) y 1 del receptor NMDA (NMDAR1) fundamentales para la comunicación inhibidora y excitadora, respectivamente. El desbalance en la comunicación

excitadora/inhibidora puede, como se mencionó anteriormente, modificar la eficacia sináptica en los circuitos neuronales.

Este estudio pretende así, establecer un correlato espacio-temporal entre la reorganización funcional posterior a una lesión cortical visual y algunos mecanismos anatómicos y moleculares previamente asociados a la plasticidad nerviosa.

HIPÓTESIS

Los mapas corticales visuales retinotópicos y de orientación preferente tienen la capacidad de reorganizarse después de una lesión focal cortical y esta reorganización correlaciona con modificaciones celulares asociadas a procesos de plasticidad nerviosa.

OBJETIVO GENERAL

Explorar a lo largo del tiempo, la capacidad de reorganización de los mapas corticales visuales de orientación en respuesta a una lesión isquémica focal de corteza visual primaria y valorar algunos de los cambios anatómicos, celulares y moleculares asociados a ella.

OBJETIVOS PARTICULARES

1. Estudiar por medio de la técnica de imagenología óptica de señales intrínsecas, cambios en los mapas corticales visuales retinotópicos y de orientación en gatos (8-12 semanas de edad) después de una lesión isquémica focal cortical a través del tiempo (1, 2 y 5 semanas).

2. Evaluar posibles modificaciones indicativas de cambios morfológicos, en el patrón de expresión espacio-temporal (1, 2 y 5 semanas post-lesión) de MAP-2 y GFAP en áreas aledañas a la lesión isquémica por medio de inmunofluorescencia y microscopía confocal.

3. Evaluar los posibles cambios temporales (1, 2 y 5 semanas post-lesión) del contenido de MAP-2 y GAP-43 (asociados a elongación dendrítica y crecimiento axonal, respectivamente) y de las subunidades $GABA_A\alpha 1$ y NMDAR1 (asociados a cambios en la transmisión excitadora/inhibidora) en células aledañas a la lesión, por medio de la técnica de Western Blot y densitometría.

4. Evaluar posibles cambios temporales (1, 2 y 5 semanas post-lesión) en el contenido total de neurotransmisores en áreas inmediatas a la lesión por medio de la técnica de cromatografía líquida de alta presión (HPLC).

OPTICAL IMAGING OF INTRINSIC SIGNALS: RECENT DEVELOPMENTS IN THE METHODOLOGY AND ITS APPLICATIONS

[§]Angelica Zepeda, [§]Clorinda Arias and [#]Frank Sengpiel

[§]Departamento de Biología Celular y Fisiología. Instituto de Investigaciones Biomédicas, Universidad Nacional Autónoma de México, México, DF, México

[#]Cardiff School of Biosciences, Cardiff University, Museum Avenue, Cardiff CF10 3US, UK

Corresponding author: Frank Sengpiel

Cardiff School of Biosciences

Museum Avenue

Cardiff CF10 3US

Tel +44-29-2087 5698

Fax +44-29-2087 4094

Email SengpielF@cf.ac.uk

Abstract
Since optical imaging of intrinsic signals (OI) was first developed in the 1980s, significant advances have been made regarding our understanding of the origins of the recorded signals. The technique has been refined and the range of its applications has been broadened considerably. Here we review recent developments in methodology and data analysis as well as the latest findings on how intrinsic signals are related to metabolic cost and electrophysiological activity in the brain. We give an overview of what optical imaging has contributed to our knowledge of the functional architecture of sensory cortices, their development and plasticity. Finally, we discuss the utility of OI for functional studies of the human brain as well as in animal models of neuropathology.

Keywords: optical imaging, intrinsic signals, event-related, Fourier analysis, functional architecture, development, plasticity

I. Introduction

In recent years, functional brain imaging techniques have taken over more and more from classical physiological approaches such as extracellular single-cell recordings in studies of the mammalian brain *in vivo*. Functional imaging techniques rely on a similar fundamental approach to understanding brain organization; however they greatly differ in their spatial and temporal resolutions. Their principal advantages are reduced invasiveness, the ability to functionally characterize large areas of the brain in response to a set of stimuli, and the relative ease of longitudinal studies by repeated imaging of an individual subject.

In the last decade, imaging studies have shed light on the functional organization of the normal brain and more recently, on the reorganization of the injured cortex. These studies have been performed using functional magnetic resonance imaging (fMRI), near-infrared spectroscopy (NIRS) and optical imaging of intrinsic signals (OI), all of which are based on changes in blood oxygenation and in optical or magnetic properties of neural tissue caused by physiological activity.

The primary use of optical imaging in the past twelve years or so has been the visualization of functional cortical maps and their architecture. Prior to the advent of OI, the functional cortical architecture had been assessed mainly with electrophysiological techniques (extracellular single- and multi-unit recordings) and through 2-deoxyglucose (2-DG) labeling. However, despite their uses, these techniques have major limitations. Electrophysiological mapping of a large area of cortex is invasive, time-consuming and subject to sampling bias, whereas 2-DG mapping can generally only be performed for one particular stimulus (very rarely for two) and maps can only be analyzed *post mortem*. Thus, chronic experiments are not feasible.

Optical imaging of intrinsic signals, a technique developed by Grinvald and colleagues (Grinvald et al., 1986; Ts'o et al., 1990; Frostig et al., 1990; Bonhoeffer and Grinvald, 1996; Grinvald et al., 1999) has been used very successfully to study both acutely and chronically the principles underlying organization and functional architecture of different cortical regions in several species, including humans; cortical development and sensory information processing in vivo. The technique employs appropriate sensory stimuli to obtain high resolution functional maps from a relatively large area. A number of maps in response to a set of stimuli can be obtained from the same cortical area, which can be imaged repeatedly over a period of weeks or even months. Optical imaging is probably the technique that best combines spatial resolution, coverage and speed for functional mapping of the mammalian cortex.

The aim of this review is to provide an overview of recent developments in the methodology of optical imaging of intrinsic signals and to introduce some of its recent applications. In the following section, we will first describe the main principles of the technique and important experimental aspects. We will then discuss the latest advances in OI data analysis and focus on its contributions to various fields of neuroscience. A more comprehensive description of the technique can be found in Bonhoeffer and Grinvald (1996) and Grinvald et al. (1999).

II. Methodological and technical aspects of optical imaging based on intrinsic signals

a. Sources of intrinsic signals

Optical imaging of intrinsic signals (OI) is the visualization of changes of intrinsic optical properties of neural tissues, in particular light reflection, due to neuronal activity. The surface of the brain is illuminated and images are recorded with a CCD camera while the subject is being stimulated.

The sources of the intrinsic signal include reflectance changes from several optically active processes (Cohen, 1973), which correlate indirectly with neuronal firing. At least three characteristic physiological parameters affect the degree to which incident light is reflected by the active cortex. These are: a) changes in the blood volume, b) chromophore redox, including the oxy/deoxy hemoglobin ratio (oxymetry, see below), intracellular cytochrome oxidase and electron carriers and, c) light scattering *(see below)* (Frostig et al., 1990; Narayan et al., 1994a; Narayan et al., 1994b).

The first two factors rely principally on the increased metabolic demand of active cerebral tissue (i.e. of neurons) and on subsequent deoxygenation of hemoglobin in the micro-capillaries. Neuronal activity causes hydrolysis of ATP (see below) and the regeneration of ATP by glucose metabolism requires oxygen (1 mol of O_2 per 6 mol of ATP). Oxy-hemoglobin molecules in the capillaries within an active cortical area are the primary source of oxygen. Therefore during metabolic demand, a flux of oxygen from the capillaries to a depleted region causes a highly localized increase in deoxy-hemoglobin concentration. That the very first event following a sensory stimulus is indeed a local decrease in oxygen concentration was recently shown by Vanzetta and Grinvald (1999), who directly assessed of micro-capillary oxygen concentration by measuring the quenching of a phosphorescent probe. Optical imaging makes use of the different absorption spectra of oxy-hemoglobin and deoxy-hemoglobin, the latter having a higher absorption coefficient at wavelengths of 600 nm and above. Active cortical regions can therefore be distinguished from less active areas since the former reflect less red light than the latter (Grinvald et al., 1986; Frostig et al., 1990). The difference in reflectance change between active and inactive regions is known as the "mapping signal" (see below).

Local rise of deoxy- hemoglobin, or depletion of oxy-hemoglobin, is followed within 1-2 sec by local capillary recruitment and dilation of adjoining arterioles (Malonek et al., 1997). The resulting increase in local blood flow and volume of oxygenated blood causes a decrease in deoxy-hemoglobin and an increase in oxy-hemoglobin, albeit less well co-localized with the area of initial oxygen consumption. Thus, a close relationship exists between locally increased neuronal activity and the hemodynamic response. This so-called neurovascular coupling provides a link between local neuronal activity and cerebral microcirculation (Villringer and Dirnagl, 1995).

Various functional imaging techniques utilize different aspects of this link. While the early decrease in blood oxygen, or increase in deoxy-hemoglobin, forms a major signal component in optical imaging of intrinsic signals (see above), the blood oxygenation level-dependent (BOLD) signal measured in fMRI is attributable to the delayed and prolonged *increase* in blood oxygenation. Due to the recruitment of arterioles in the vicinity of the original site of oxygen consumption, the spatial resolution of this delayed signal is somewhat limited and does not allow visualization of individual functional domains in the cortex. However, high-field fMRI measurements (at up to 9.4 T) have confirmed the presence of an "initial dip", that is a short latency *decrease* in blood oxygenation corresponding to an increase in deoxy-hemoglobin

concentration (Kim et al., 2000). As this is confined to the site of neuronal activity, it allows functional imaging with a much higher spatial resolution than imaging based on later increases in blood flow and volume. Indeed, high-field fMRI that utilizes only the initial dip is capable of resolving individual cortical modules, such as orientation columns in cat primary visual cortex (Kim et al., 2000), similar to optical imaging of intrinsic signals. A recent study in humans comparing spatiotemporal patterns of fMRI signals and intrinsic optical signals (measured intra-operatively) also supported the conclusion that the initial fMRI dip and the intrinsic OI signal result from the same physiological events (Cannestra et al., 2001).

The third factor determining cortical surface reflectance, light scattering, was first discovered in the crab leg nerve by Hill and Keynes (1949) and has proven to be a particularly useful signal for functional mapping because of its relatively tight spatial and temporal coupling with neural activity. In optical imaging of the living brain, the incident light is scattered to some extent as it penetrates and is reflected through the neural tissue. Light scattering increases as a consequence of increased activity and may result from ion and water movement, expansion and contraction of extracellular spaces, capillary expansion or neurotransmitter release (for review see Cohen, 1973). Activity-related light scattering has been associated with changes in membrane potential (Stepnoski et al., 1991) and glial swelling (MacVicar and Hochman, 1991).

How does each of the signal components contribute to the "mapping signal" visualized in the functional maps, i.e. the stimulus-specific differential activation pattern? The different components of the intrinsic signal have different time-courses and their relative contribution depends on the wavelength used for illumination. The increase in light scattering reaches its maximum within 2-3 seconds of stimulus onset, while the deoxy-hemoglobin (oxymetry) component peaks after 4-6 seconds. The blood-volume related oxy-hemoglobin signal rises even more slowly, after an initial dip, and follows closely the global signal, beginning to decrease 1-3 seconds after stimulus offset (Bonhoeffer & Grinvald 1996). By injecting fluorescent dyes into the bloodstream, Frostig et al. (1990) demonstrated that blood volume changes alone can yield a functional map. However, the mapping signal is dominated by other mechanisms, including changes in the cytochrome oxidase redox state and more importantly, a decrease in oxygen saturation of hemoglobin due to increased oxygen consumption as well as increased light scatter. The oxymetry signal and even more so the light scattering component, which is more directly related to electrical activity, have a higher spatial resolution. Therefore, optical imaging using near-infrared wavelengths (700 nm and above) usually provides better functional maps (but see section *III.a.iv.* for auditory cortex) with reduced blood vessel artifacts despite a lower absolute signal magnitude (McLoughlin and Blasdel, 1998). In a recent study, Shtoyerman et al. (2000) estimated the individual contributions of the oxy-hemoglobin and the deoxy-hemoglobin concentrations to functional maps in awake monkeys and found that ocular dominance domains appear sharper in the deoxy-hemoglobin maps, confirming that the signals from the changes in concentration of deoxy-hemoglobin co-localize better with electrical activity than the signals from changes in oxy-hemoglobin concentration.

b. Correlation of intrinsic signals with metabolic cost and physiological activity

Regardless of the sources of the intrinsic signals, a second important question is which aspects of neuronal activity contribute to them, and to which degree? Activity comprises not only the generation and propagation of action potentials but also the synaptic transmission, postsynaptic potentials, vesicle and receptor recycling, etc. A recent theoretical paper by Attwell and Laughlin (2001) has shed some light on this issue. The

authors considered metabolic costs in terms of ATP of glutamatergic synaptic transmission and action potential propagation in the rodent cerebral cortex on the basis of available neuroanatomical and biophysical data.

Attwell and Laughlin (2001) estimated the resting consumption of ATP by neurons at $3.4x10^8$ sec^{-1} and that of glia cells at $1.0x10^8$ sec^{-1}. At an average firing rate of 4 spikes/sec, a pyramidal neuron consumes an additional $2.8x10^9$ ATP sec^{-1}. Just over half of this cost is attributable to the propagation of the action potentials, the remainder to synaptic transmission. The cost of the latter is dominated by the energy required to restore postsynaptic ion gradients, which outweighs presynaptic glutamate recycling and Ca^{2+} pumping by more than 10:1 (Fig. 1). These figures suggest that only just over 10% of neuronal energy consumption are due to maintaining the resting state, and the overall cortical energy consumption is more or less proportional to the average firing rate. ATP consumption in the cortex measured in vivo (Clarke and Sokoloff, 1999) would then correspond to an average spike rate of about 5-6 sec^{-1}. That this is close to observed values confirms the validity of the calculations. Estimates of energy consumption for non-pyramidal neurons, such as inhibitory (GABAergic) interneurons, are not yet available. However, assuming that values are similar to those for pyramidal cells, roughly half of the metabolized ATP is required at the synapses and the other half for spike propagation. This suggests that processes which do not result in action potentials being generated, i.e. subthreshold excitatory as well as inhibitory inputs, contribute very significantly to overall metabolic costs and therefore presumably to the intrinsic signals that form the substrate of OI. Since the above considerations pertain primarily to the oxymetry component of intrinsic signals, it is impossible to quantify the contribution of synaptic events, when light scattering changes are a major aspect of the overall signal.

A direct consequence of there being contributors other than action potentials to the intrinsic signal is the fact that the spatial extent of intrinsic signals elicited by a sensory stimulus is larger than the area of cortex where neurons respond to that stimulus with action potentials. In most cases, the so-called "point-spread" of the imaging signal, i.e. the area of cortex activated by a very small (near point-sized) stimulus, is larger than the point-spread for action potentials. In cat visual cortex, Das and Gilbert (1995) found that the optical response to a very narrow bar stimulus (width, 0.1°) extended over a cortical region of on average 3.9 mm diameter, corresponding to 2.25 – 6° of visual space (depending on eccentricity), while receptive field diameters of single neurons were 0.3° to 1° wide and spikes were recorded from an average cortical area 0.74 mm in diameter. Das and Gilbert (1995) concluded that the optical point-spread is up to 20 times larger in area than the suprathreshold neuronal activity. Bosking and colleagues (2002), in a study of retinotopy and orientation selectivity in tree shrew visual cortex, found a similar point-spread of the optical signal, as 0.25° wide bars panning over 1° of visual space elicited responses from an area of V1 corresponding to 4.9° of visual space. In contrast to results reported by Das and Gilbert (1995) for the cat, however, this was only marginally wider than the width of positional tuning as determined by multi-unit recording, suggesting species differences.

c. Protocol for an optical imaging experiment

This section will briefly describe the standard protocol for OI experiments (for more details, see Bonhoeffer and Grinvald, 1996; Grinvald et al., 1999), and we will point out recent methodological and technical advances.

i. Surgery and animal preparation

Anesthesia in cat, monkey and ferret is generally induced with a mixture of ketamine and xylazine (Bonhoeffer and Grinvald, 1996; Chapman and Bonhoeffer, 1998); pentobarbitone and urethane have been used in rat experiments (Masino and Frostig, 1996; Polley et al., 1999; Meister and Bonhoeffer, 2001). After initial anesthesia, the animal is intubated (chronic experiments) or tracheotomized (acute experiments). It is then mounted on a stereotaxic apparatus and connected to a respirator which delivers a mixture of N_2O and O_2 supplemented by halothane (or isoflurane) as necessary to maintain adequate anesthesia. In imaging studies of auditory cortex, both pentobarbitone and the steroid saffan (alphaxalone/alphadolone) have been used successfully, since halothane was found to depress responses (Versnel et al., 2002). A combination of ketamine and urethane has been used in mice, which will breathe spontaneously and need not be artificially respirated (Schuett et al., 2002).

To date, the question whether different anesthetics result in qualitatively or quantitatively different functional images has not been addressed systematically. However, subtle differences between halothane and isoflurane in their effects on visual cortical adaptation have recently been described (Sengpiel and Bonhoeffer, 2002).

CO_2, ECG, temperature and, when neuromuscular blockers are used, EEG are continuously monitored to ensure adequate anesthesia. Access to the cortex can be achieved by opening (e.g. Bonhoeffer and Grinvald, 1996) or thinning the skull (Masino et al., 1993; Masino and Frostig, 1996; Bosking et al., 1997; Polley et al., 1999) above the region of cortex to be studied. In mice, it is even possible to image through the exposed but intact skull (Schuett, Bonhoeffer et al., 2002; Kalatsky and Stryker, 2003). Under favorable conditions, optical imaging can provide activity maps with a spatial resolution of up to 80-100 μm. In order to achieve this resolution, it is important to minimize movement of the brain, which normally occurs due to heartbeat and respiration-related pulsations. Craniotomy is usually performed in large species (i.e. monkey, cat) and it is often required to open the rather opaque dura in order to get good quality images. One of the disadvantages of performing a durotomy in chronic experiments is the possible growth of opaque tissue on top of the cortical surface, which makes imaging difficult. In addition, capillary proliferation may occur in the growing membrane, thus increasing the risk for hemorrhage when resecting it. Another major problem of durotomy is that the exposed cortex becomes more susceptible to infections even when working under sterile conditions and when applying topical anti-inflammatory (e.g. dexamethasone) and antibiotic drugs. Recently, two different groups (Arieli et al., 2002; Chen et al., 2002) developed a transparent dural substitute for long-term imaging experiments, which allowed cortical imaging for up to 1 year after implantation without complications. The artificial dura is either made out of silicone (Arieli et al., 2002) or polyurethane (Chen et al., 2002) and is about 0.1-0.2 mm thick. The main advantages of using the dural substitute in chronic experiments are, 1) protection of the cerebrum against inflammation, 2) prevention of leakage of the cerebrospinal fluid, and 3) transparency, which allows maintaining the cortex in a good optical condition for long periods by preventing growth over the exposed cortex. In addition, an elastic dural substitute has proven useful to allow microelectrodes to pass through without suffering any damage (Arieli et al., 2002).

Different types of chamber system or cranial window have now been developed to both protect the brain and minimize movement. In larger animals (cats, adult ferrets, monkeys) a chamber made of titanium is used, which has an inlet and an outlet to which tubing is attached in order to fill the chamber with silicone oil (Bonhoeffer and Grinvald, 1996). It is then sealed with a glass coverslip which is pressed onto a silicone

gasket with a threaded ring. It is mounted onto the skull with dental cement and internal gaps between the skull and the chamber are sealed with melted dental wax.

Recently, Arieli and Grinvald (Arieli and Grinvald, 2002) designed a skull-mounting 'sliding-top cranial window' to facilitate the combination of optical imaging with various microelectrode-based techniques in chronic and acute experiments in the cerebral cortices of cats and monkeys. This assembly has allowed gaining insights in the relationship between neuronal morphology of single neurons and functional cortical architecture as well as between the dynamic state of the cortical networks and the functional response to a stimulus.

Alternatively to the chamber system, it has been possible to obtain cortical functional maps in ferrets and rats through a layer of agarose and a glass coverslip placed over the exposed cortex (Chapman and Bonhoeffer, 1998; Meister and Bonhoeffer, 2001; Schuett et al., 2001; Schwartz and Bonhoeffer, 2001) and through saline contained in a wall of Vaseline or through agarose and a coverslip to cover the thinned bone (Bosking et al., 1997; Polley et al., 1999). In mice, the cortex can be imaged through the intact skull, once the skin has been retracted; transparency of the bone is maintained by applying silicone oil directly to the skull (Schuett et al., 2002). This method is therefore ideally suited for chronic imaging.

ii. Data acquisition

The camera

Different types of cameras, such as photodiode arrays (Grinvald et al., 1986) and video cameras (Blasdel and Salama, 1986) have been used for functional brain imaging. Nowadays, most imaging systems contain charge-coupled device (CCD) type sensors. Photons reflected from the cortex strike the CCD faceplate liberating electrons that accumulate in SiO2 "wells", at a rate proportional to incident photon intensity. Slow-scan digital CCD cameras have been widely used for intrinsic signal imaging (Ts'o et al., 1990). They provide good signal-to-noise ratios at a high spatial resolution, and their main disadvantage, the low image acquisition or frame rate (< 10 Hz), is not critical for imaging of the rather slow intrinsic signals. In contrast, video cameras with CCD-type sensors are much faster (≥ 25 Hz) and have an even better signal-to-noise ratio at the light levels typical of an OI experiment. In the past, they were hampered by 8-bit frame grabbers, which could not digitize intensity changes of less than 1/256 (with the typical signal amplitude in OI being only ~1/1000). However, this problem can be overcome by differential subtraction of a stored (analog) reference image, resulting in an effective 10- to 12-bit digitization. This image enhancement is no longer necessary, as precision video cameras with 10-bit digitization have been developed, allowing optical imaging at up to 60 Hz. However, for imaging of voltage-sensitive dyes, much higher frame rates are desirable; cameras offering up to 1700 Hz are now available (Shoham et al., 1999).

Illumination and filters

Optimal illumination of the area of interest is crucial for the quality of the maps. The proper wavelengths of the illuminating light depend on the sources of intrinsic signals of interest (*see below*). One should also bear in mind that light of longer wavelengths will penetrate deeper into the tissue.

Even illumination is best achieved by using at least two fiber-optic light guides directed at the region of interest, whereas a high quality regulated DC power supply is essential for guaranteeing a stable light intensity.

Band-pass interference filters are used to limit the wavelength of the illuminating light. The most frequently used filters are: 1) green filter, 546 nm (30 nm

wide) - best for obtaining the blood vessel / surface picture; 2) orange filter, 605 nm (5-15 nm wide) - at this wavelength the oxymetry component dominates the signal; 3) red filter, 630 nm (30 nm wide) - at this wavelength the intrinsic signal is dominated by changes in blood volume and the oxygenation saturation level of hemoglobin; 4) near infrared filters, 700 to 850 nm (30 nm wide) - at these wavelengths, the light scattering component dominates the intrinsic signal, while the contribution of hemoglobin signals is much reduced (Frostig et al., 1990; Blood et al., 1995; Narayan et al., 1995). Optical imaging can thus be used to map different physiological processes depending on the specific wavelength chosen for illumination.

An alternative to the use of light guides (in combination with band-pass filters) is the illumination by a ring of light-emitting diodes (LEDs) of specific wavelengths (e.g. Mayhew et al., 1996).

Timing of data acquisition

A number of major biological signal sources in OI are not associated with neural activity but with respiratory and cardiovascular events and are therefore "noise". The most prominent ones are the so-called vasomotion signal as well as heartbeat and ventilation artifacts at their respective fundamental frequencies and harmonics (see Kalatsky and Stryker 2003). The vasomotion signal represents a low frequency (peaking near 0.1 Hz) oscillation resulting from modulations of regional cerebral blood flow (Mayhew et al., 1996). Although heartbeat and respiration artifacts occur at frequencies higher than vasomotion, they all fall within the category of "slow" noise of a periodicity that is within one or two orders of magnitude of the time-course of the neural signals.

In order to minimize their effects on functional maps, it is beneficial to synchronize heartbeat and respiration with image acquisition. This is achieved by triggering both the respirator and the image acquisition off the heartbeat, a measure that can reduce slow noise by up to a factor of 1.5 (Grinvald et al., 1991). Of course, accumulation of a large number of trials should average out periodic artifacts. Alternatively, temporal filtering of the intrinsic signal may be employed to remove periodic artifacts (see section on data analysis below).

Under optimal conditions, albeit noisy functional maps can be obtained in a single trial. Generally, between 20 and 100 responses to any stimulus condition are averaged in order to improve the signal-to-noise ratio. Since the spatial localization to the site of neural activity is better for the early intrinsic signal components (oxymetry, light scattering) than the later components (blood flow), stimuli are typically limited to 3-4 sec duration, while data acquisition may be slight longer, depending on the time course of the mapping signal. Inter-stimulus intervals may also vary. However, a minimum of about 7-8 sec is required for "metabolic relaxation", i.e. recovery to near baseline (Bonhoeffer and Grinvald, 1996). On the other hand, inter-stimulus interval should not be too long in order to maximize the number of images collected and to avoid systematic errors resulting from slow drifts in the baseline state of the cortex. Frequently, the end of the inter-stimulus interval is utilized to record one or more "first frames", the mean of which may be subtracted from subsequent frames collected during stimulus presentation in order to correct for relatively time-invariant biological noise (Bonhoeffer and Grinvald, 1996).

Basic experimental setup

Once the animal is anesthetized, it is held in a stereotaxic frame. The brain is illuminated with light of the appropriate wavelength and images are acquired by the camera positioned above the cortex. The camera must be firmly mounted in a vibration-

free device. The best arrangement should have the camera attached to a holder that allows tilting the camera to any desired angle. The camera holder should have, preferably, an xyz-translator for fine positioning and focusing. It is advisable to focus on the cortical surface first in order to choose a region of interest and capture a picture of the blood vessels, which can later be used to relate activity maps with anatomical landmarks. Lens aperture should be reduced during the recording of the blood vessel pattern to avoid blurring along the edges of the image due to the curvature of the cortex. For recording activity maps, the camera should be focused 300-700 μm below the cortical surface, and the lens apertures should be fully open; a "macroscope" assembly providing high numerical aperture is ideal for maximal light yield and a shallow depth of focus (Ratzlaff and Grinvald, 1991).

iii. Data analysis

In the living brain, intrinsic signals are very small. Change in light intensity at 605 nm due to neuronal activity is at best about 0.5% of the total intensity of the reflected light (and typically under 0.1%). Thus, intrinsic signals are not apparent but have to be extracted from the images with the appropriate analysis procedures (Bonhoeffer and Grinvald, 1996).

Like all functional imaging techniques, OI maps the differences found in a certain brain region between the basal activity level under a resting or control condition and an activated state following a specific stimulus. The choice of baseline condition and the method of extracting the stimulus-induced signal from biological as well as shot noise (the stochastic fluctuations of light emission) are therefore critical for meaningful data interpretation, since the measurement of absolute signal strength is not possible.

Event-related imaging

The standard form of stimulus presentation and image analysis is one of event-related imaging. In other words, for each stimulus, the change of the reflectance signal of the individual pixels in the image is recorded during and/or after the presentation of the stimulus, and the signals are averaged over a number of trials. This procedure is equivalent to the way peri-stimulus time histograms are obtained for single-cell responses. Typically, absorption begins to increase about 0.5 sec after stimulus onset and reaches a maximum after 3-4 sec (see Fig. 2F).

Whereas in single-cell recordings the spontaneous activity in the absence of explicit stimulation provides a simple baseline, a similar control condition for intrinsic-signal images is far harder to define because of the rather indirect relation between neuronal activity and the mapping signal. The equivalent of "spontaneous activity" is the "blank image" obtained from the unstimulated cortex. The difficulty with using the "blank" as a control arises from the fact that most adequate stimuli (e.g. visual stimuli in case of the primary visual cortex) will cause an overall elevation in absorption. This global response includes regions where at the level of neuronal (spiking) activity there is no response at all to the stimulus (see Fig. 2F).

In order to remove the DC response from the images and to extract only the stimulus selective response components, images can alternatively be divided by the "cocktail blank", which is the sum of the responses to all stimuli in a set (Bonhoeffer and Grinvald, 1993). For this procedure to have valid results, two important conditions must be met. First, the stimuli used must cover the stimulus space evenly. For example, in a set of oriented gratings, the orientations must cover the range of 180° in steps of equal size. The use of only a subset of stimuli can significantly affect the map obtained (Issa et al., 2000). Second, the sum of the responses to all stimuli must be uniform

across the imaged region. If it is patchy, division by the "cocktail blank" will result in a patchy map even for a stimulus which itself elicited no response at all (Bonhoeffer and Grinvald, 1993, 1996). In the case of "orthogonal" stimuli that elicit responses from largely non-overlapping populations of neurons, difference images present an alternative to the cocktail-blank procedure. Examples are the subtraction (or division: for very small differences, as is the case in OI, the results are interchangeable, see Bonhoeffer and Grinvald, 1996) of responses to horizontal vs. vertical gratings or left-eye vs. right-eye stimulation in order to obtain orientation and ocular dominance maps, respectively.

In addition to division by the "blank" control image (or as an alternative to it), the so-called "first-frame" subtraction has proved useful. In this approach, the reflectance image is recorded for a few frames prior to the actual stimulus onset, and is subtracted from the post-stimulus frames (Bonhoeffer and Grinvald, 1996). This method very successfully removes artifacts that are more or less time-invariant within the duration of the stimuli.

Fig 2 shows orientation preference maps of cat primary visual cortex. Fig. 2A represent single condition activity maps for four different orientations in both cortical hemispheres (B). These iso-orientation maps each represent the summed responses to 96 presentations of the same stimulus orientation; they were divided by the "blank" response (the response to a uniform grey screen). In Fig. 2C, the same summed responses were divided by the "cocktail blank" (Bonhoeffer and Grinvald, 1993). The differences between the more globalized responses in (A) and the more orientation-specific responses in (C) are evident. They can be quantified by calculating two-dimensional correlation coefficients between maps obtained with orthogonal orientations: these tend to be positive in case of blank divided images and negative in case of cocktail-blank divided images. Fig. 2D represents the orientation preference "angle map" obtained by pixel-by-pixel vectorial addition (Blasdel and Salama, 1986) of the single condition maps shown in (C). The colors in the image code for the angle of the preferred grating orientation. Additional information may be provided by displaying the magnitude of the resulting vector as brightness. The resulting "polar map" (Ts'o et al., 1990) shows the preferred orientation as color hue and the magnitude of the vector as brightness (Fig. 2E).

An alternative method to derive secondary parameter maps (such as the "angle map" of orientation preference mentioned above) is pixel-by-pixel analysis of responses to a set of stimuli. Here the responses of each image pixel are treated much in the same way as responses of a single neuron to a set of stimuli, and tuning functions previously described for single neurons can be fitted to those pixel responses. For example, (Swindale et al., 2003) fitted circular normal functions to pixel responses for a set of grating stimuli varying in orientation and direction of drift in order to calculate maps of orientation and direction preference as well as tuning width, revealing spatial relationships between these parameters not evident with traditional vector averaging. Similarly, we have recently determined, on a pixel-by-pixel basis, contrast-response functions and orientation tuning curves in cat V1, using hyperbolic ratio and Gaussian functions, respectively (Carandini and Sengpiel, 2004). We found that the fit parameters describing contrast responses were more or less uniform over the cortical surface. Moreover, stimulus contrast had no impact on maps of orientation preference: the orientation selectivity of each pixel, just as that of single neurons, was contrast-invariant.

Principal component analysis and related methods

As described above, intrinsic optical signals consist of a number of components, both stimulus-related and stimulus-independent, that exhibit distinct spatial and temporal patterns. Principal component analysis (PCA) is used to decorrelate signals of different origins in a linear mixture of signals, which are assumed to be orthogonal, and to find directions of extremal variance in the data space. Signal recovery from OI data by means of spatial PCA was developed by Sirovich and Everson (1992) and improved further by combining it with the standard difference image method (Gabbay et al., 2000). PCA over time (rather than space) of cortical images acquired in the absence of any stimulus and subsequent selection of components that are most strongly correlated with the surface vasculature pattern allows removal of blood vessel artifacts from images by linear extraction (Schuett et al., 2000). An example of the effectiveness of this procedure is illustrated in Fig. 3.

Blind source separation (BSS) describes a group of signal-processing techniques that can be regarded as extensions of PCA, making additional assumptions about the statistical structure of the signal sources in order to recover them from the mixtures. Independent component analysis (ICA; Bell and Sejnowski, 1995) and extended spatial decorrelation (ESD; Stetter et al., 2000) assume that the different sources are statistically independent and mutually uncorrelated, respectively. These methods improve the extraction of the stimulus-related spatial signal from OI data.

Periodic stimulation imaging

This recently developed approach (Kalatsky and Stryker, 2003) is comparable to the standard mode of image acquisition in fMRI (Engel et al., 1994, Boynton et al., 1996). Instead of measuring a response following each individual stimulus, stimuli are presented in periodic fashion over a longer period of time. This kind of stimulation results in a periodically modulated reflectance signal for each pixel in the image, which can be decomposed into sine waves of different frequencies using Fourier analysis (Fig. 4). The only frequency of interest is that corresponding to the stimulus presentation, while those relating e.g. to the heart and respiration rate and to vasomotion can be filtered out. In theory, then, the amplitude and phase of the pixel response over time at the stimulus frequency can be used to determine response strength and stimulus preference, respectively. One obvious advantage of this paradigm is the fact that absolute response levels play no part in the analysis, as only relative response modulation is assessed. Moreover, response components whose periodicity does not match that of the stimulus (such as heartbeat and respiration artifacts) can be removed easily. Finally, data can in principle be acquired in a much shorter period of time than is possible in event-related imaging (Kalatsky and Stryker, 2003). However, there are some caveats too. First, signal components whose frequency is very close to that of the stimulus cannot be filtered out but will contaminate the results. The frequency of stimulation should therefore be different from that the major hemodynamic components. Still, even after removal of slow changes in image intensity, an analysis of response amplitude versus phase will often show that response phases are not represented equally (as would be expected for a stimulus set such as orientation). Second, an unknown lag time (hemodynamic delay) between stimulus and intrinsic signal response means that response phases cannot be translated directly into an absolute stimulus preference map. This can be overcome (at the expense of doubling the data acquisition time) by cycling through the stimulus set both in ascending and descending order or by measuring the hemodynamic delay separately using just a single stimulus (Kalatsky and Stryker, 2003). It is important to keep in mind that the former method will only yield valid

results if the order of stimulus presentation does not itself affect responses. Third, if the stimuli in a periodic set are not equally efficacious at driving cortical responses, the stimulus-phase relationship may not be straightforward, as the phase lag may not be the same for all stimuli. For example, following a brief period of monocular deprivation, we found that responses through the two eyes in kitten V1 to alternating stimulation, using a contrast-reversing checkerboard, were not precisely in anti-phase, as would have been expected (F. Sengpiel, unpublished observation), presumably because of latency differences between the deprived and the non-deprived eye. The additional possibility of response delay differences at map edges is discussed by Mrsic-Flogel and colleagues (Mrsic-Flogel et al., 2003).

III. Applications of optical imaging of intrinsic signals

When intrinsic optical imaging was first developed, it helped understanding the detailed functional architecture of cat and monkey visual cortex (Grinvald et al., 1986; Ts'o et al., 1986; Frostig et al., 1990; Ts'o et al., 1990). However, nowadays, optical imaging has become an important tool for *i)* studying the functional architecture of motor, somatosensory, auditory cortices and the olfactory bulb, *ii)* assessing cortical maps in awake animals, and *iii)* investigating functional cortical development and plasticity under normal and pathological conditions and following environmental manipulations. Lately, the technique has also been used to visualize the spread of focal epileptic seizures and the reorganization of functional cortical maps in the surrounding of a focal ischemic injury, and it has been adapted to image the human cortex intra-operatively. In this section we will discuss some of the more recent insights into the functional organization of the brain gained be means of optical imaging of intrinsic signals.

a. Acute experiments in sensory cortices

i. Studies on functional architecture of visual cortex

The functional architecture of visual cortex had been extensively studied long before optical imaging was developed. Using electrophysiological techniques, Hubel and Wiesel (1962) first reported the existence of orientation preference and ocular dominance columns, which were confirmed using transneuronal labeling and 2-deoxyglucose (2DG) mapping techniques (Singer, 1981; Singer et al., 1981); Payne (1981) and Tolhurst (1981) described clustering of cells according to preferred direction of motion; and using the 2DG technique, Tootell (1981) described spatial frequency columns.

Optical imaging of intrinsic signals has provided a powerful tool for establishing the precise layout and the interrelationship of the aforementioned cortical feature representations (Grinvald et al., 1986; Ts'o et al., 1990; Bonhoeffer and Grinvald, 1991; Grinvald et al., 1991; Hübener et al., 1997; White et al., 2001) which had remained elusive using classical techniques. The main advantage of optical imaging in that respect is that it allows to visualize maps for all the above mentioned maps in the same subject at the same imaging time, which in turn facilitates establishing geometric relationships between different columnar systems (Bartfeld and Grinvald, 1992; Shmuel and Grinvald, 1996; Weliky et al., 1996; Hübener et al., 1997; Kim et al., 1999; Bosking et al., 2002; Landisman and Ts'o, 2002). Importantly, Hübener and colleagues (1997) reported that most columnar systems tend to intersect each other at right angles more frequently than would be expected in a random arrangement.

Knowledge of these relationships has enabled researchers to test and validate the hypothesis of coverage optimization (Swindale, 2000; Swindale et al., 2000), which is

at the heart of the "ice-cube model" (Hubel and Wiesel, 1977) of the primary visual cortex. Interestingly, no local spatial relationship appears to exist between retinotopic and orientation preference maps, at least not in tree shrew V1, while coverage uniformity is maintained (Bosking et al., 2002). An alternative interpretation of how multiple features may be represented in the visual cortex has recently been put forward. Basole and colleagues (2003) suggest that rather than reflecting the intersection of multiple maps, population activity may be better described by a single, spatiotemporal energy map.

The development of optical imaging has made it possible to visualize not only the layout of orientation preference and ocular dominance maps within area 17 and 18 in a number of species including cat, ferret, macaque, tree shrew, barn owl and marmoset monkey (Grinvald et al., 1991; Bonhoeffer et al., 1995; Bosking et al., 1997; Issa et al., 1999; Shmuel and Grinvald, 2000; Shtoyerman et al., 2000; Liu and Pettigrew, 2003) but also maps of direction of motion preference (Shmuel and Grinvald, 1996; Weliky et al., 1996), spatial frequency preference (Shoham et al., 1997; Issa et al., 2000), form processing modules in macaque area V4 (Ghose and Ts'o, 1997), clusters of color selective neurons in V1 (Landisman and Ts'o, 2002) and a hue-selective organization within the thin cytochrome oxidase stripes of V2 (Xiao et al., 2003) have been described. More recently, retinotopic maps in macaque monkey V1 (Blasdel and Campbell, 2001), owl monkey V3 (Lyon et al., 2002), mouse (Schuett et al., 2002; Kalatsky and Stryker, 2003), tree shrew (Bosking et al., 2000) and cat (Zepeda et al., 2003) have also been reported. Furthermore, optical imaging has been employed to reveal the functional architecture of owl monkey area MT (Malonek et al., 1994), to resolve the relationship between columnar systems in area V2 of the squirrel monkey (Malach et al., 1994) and to demonstrate the distributed processing of object features in macaque inferotemporal cortex (Wang et al., 1996; Tsunoda et al., 2001).

By combining optical imaging with other techniques, it has been possible to reveal properties of individual neurons at identified locations within the maps and to describe cortical characteristics at an even finer spatial scale (e.g. Malach et al., 1993; Maldonado et al., 1997; Yousef et al., 1999; Ts'o et al., 2001). Together with anterograde and retrograde labeling techniques, optical imaging has provided detailed information regarding the anatomical underpinnings of functional maps, thus shedding light on how excitatory horizontal (Bosking et al., 1997; Malach et al., 1997) and lateral inhibitory (Kisvarday et al., 1994; Kisvarday et al., 1997) as well as callosal connections (Bosking et al., 2000) contribute to neuronal response properties.

ii. Studies on functional architecture of somatosensory cortex

Among somatosensory areas, optical imaging has been applied mainly to mapping of the primary somatosensory cortex of rodents (S1) and monkeys (S-I).

In the rat, S1 is dominated by the representation of facial whiskers in discrete cytoarchitectonic units known as barrels, first described by Woolsey and Van der Loos (1970). Through optical imaging of intrinsic signals, it has been possible to show the functional representation of individual whiskers in rat and gerbil barrel cortex (Grinvald et al., 1986; Masino et al., 1993; Narayan et al., 1994a; Narayan et al., 1994b; Blood et al., 1995; Narayan et al., 1995; Peterson and Goldreich, 1998; Polley et al., 1999; Hess et al., 2000; Brett-Green et al., 2001), and it has been possible to resolve the areal extent and point-spread of single whisker representations in primary somatosensory cortex of rats (Chen-Bee, 1996; Chen-Bee et al., 1996; Masino and Frostig, 1996; Brett-Green et al., 2001; Sheth et al., 2003). Optical imaging results are in good agreement with functional maps obtained using voltage-sensitive dyes (Takashima et al., 2001).

However, signals from whisker stimulation obtained through optical imaging are often larger than expected when compared to electrophysiological mapping (Narayan et al., 1994b; Brett-Green et al., 2001). This divergence of activity may be a basic functional feature of the whisker-to-barrel projection (Brett-Green et al., 2001). The large areal extent of the functional representation of single whiskers obtained through optimal imaging may result from horizontal activity spread through excitatory connections in layers 2/3, which increases in extent with the degree of whisker deflection, as revealed by voltage-sensitive dye imaging (Petersen et al., 2003). However, the apparently very large single-whisker activation areas obtained in the above OI studies may also be a consequence of the fact that images of the unstimulated state of the barrel cortex were subtracted from images in response to single-whisker stimulation, rather than images from "orthogonal" stimulus conditions, as is commonly done in imaging studies of the visual cortex (e.g. horizontal vs. vertical gratings or left-eye vs. right eye stimulation) in order to enhance map contrast and domain delineation (Frostig et al., 1990). It is certainly problematic that results vary significantly with the method of analysis used (Schulze and Fox, 2000).

In somatosensory cortex, the topographic map of the body surface has been well established using electrophysiological techniques (Woolsey et al., 1942; Nelson et al., 1980; Pons et al., 1985; Pons et al., 1987). A number of groups have studied the cortical somatosensory topographic map of rat, cat, squirrel monkey, macaque and human using optical imaging (Gochin et al., 1992; Tommerdahl et al., 1993; Godde et al., 1995; Tommerdahl et al., 1996; Tommerdahl et al., 1998; Tommerdahl et al., 1999a,b; Chen et al., 2001; Shoham and Grinvald, 2001; Tommerdahl et al., 2002). Results have revealed that, consistent with electrophysiological observations, somatotopic representation of the finger pads exhibits an orderly medial to lateral progression from the D5 to D1 finger pads (Nelson et al., 1980; Sur et al., 1982; Pons et al., 1987). However, as for the visual cortex, electrophysiological methods do not allow to resolve whether different tactile features form multiple functional domains within the primary sensory cortex. In an attempt to reveal the organization of response of different sensory stimuli in somatosensory cortex of cat and squirrel monkey, Tommerdahl et al. (1993; 1996; 1998; 1999a,b) have addressed S-I cortical responses to cutaneous flutter, vibration, tapping, and skin heating while Chen et al (2001) have additionally addressed the cortical representation of pressure. Results from these groups have shown that area 3a in the anterior parietal cortex has a leading role in the processing of skin-heating stimuli (Tommerdahl et al., 1996), and that high-frequency ($\geq$ 200 Hz) vibrotactile stimuli activate neurons in cortical regions other than areas 3b and 1 (Tommerdahl et al., 1999a) whereas in area 3b the sensation of pressure, flutter and vibration preferentially activate one receptor population even when functional cortical representations for each sensation overlap (Chen et al., 2001). Thus, in accordance with a previous study by Tommerdahl et al. (1993), which proposed that activation of a mini-column in S-I encodes information about the physical properties of tactile stimuli, the authors suggest that initial cortical processing could involve the separation of sensory information into distinct functional maps. Interestingly, they report that under barbiturate anesthesia, the functional activation of the finger pads for all sensations were discrete and exhibited minimal overlap between them. However, under isoflurane anesthesia, the representation of finger pads on adjacent fingers had a higher degree of overlap than with Pentothal anesthesia even though the general topography was still maintained (Chen et al., 2001). As for barrel cortex studies, no orthogonal stimulus conditions are available for analysis (see above). Thus, alternative analyses such as the first–frame or blank subtraction and subtracting the sum of images obtained for one

stimulus condition (e.g., pressure) from that obtained under another have been used for data analysis.

iii. Studies on functional architecture of olfactory bulb

Olfactory sensory neurons that express a given odorant receptor are widely distributed within the olfactory epithelium. The olfactory epithelium projects to the olfactory bulb in the forebrain, where axons from olfactory sensory neurons expressing the same odorant receptor converge onto single glomeruli (Mombaerts, 1999). It has been suggested that glomeruli are functional units in olfactory processing (Hildebrand and Shepherd, 1997). In recent years, the central organization of odorant representation has received particular attention. However, until the development of imaging techniques, the relationship between the molecular biology of odorant receptors and the functional organization of the olfactory system remained poorly understood (for review, see Bozza and Mombaerts, 2001).

Using electrophysiological techniques, 2-deoxygluocose autoradiography, c-fos expression and functional magnetic resonance imaging, a number of groups have provided insights into the organization of groups of glomeruli with respect to odor molecules (Sharp et al., 1975; Sharp et al., 1977; Imamura et al., 1992; Guthrie et al., 1993; Johnson et al., 1998; Yang et al., 1998). However the spatial resolution of these techniques, did not allow assessment of responses of individual glomeruli to different odors.

Spatiotemporal activity patterns in the olfactory bulb were first studied in salamanders using voltage-sensitive dyes (Kauer, 1988). In a recent study in rats, Rubin and Katz (1999) used optical imaging of intrinsic signals to visualize the patterns of activation of different glomeruli in response to a wide range of odorants. The study provided refined information of odorant organization; odorants are represented by distributed patterns of activated glomeruli that are bilaterally symmetric, and distinct patterns of glomerular activity correlate with differences in odorant concentration and odorant identity. Further studies showed that odorants with different functional groups activate distinct domains in the olfactory bulb and that subtle changes in odorant structure such as length or configuration of carbon chains elicit distinct activity patterns (Uchida et al., 2000; Meister and Bonhoeffer, 2001). For example, short chain lengths of aliphatic aldehydes are mapped in the middle of each olfactory bulb, whereas glomeruli responding to the longest aldehydes are found near the lateral edge of the bulb. Thus, an ordered representation or map of odors exists in the olfactory bulb, based on the aliphatic chain length. Moreover, from the dynamics of the responses, Meister and Bonhoeffer (2001) concluded that the signals probably derived from afferents of the olfactory sensory neurons rather than from second-order neurons. (Note that in this respect, the olfactory bulb differs from sensory neocortex, where intrinsic signals are dominated by postsynaptic events.)

Histochemical analysis using cytochrome oxidase showed that functional glomeruli matched in size and distribution anatomically defined glomeruli (Belluscio and Katz, 2001; Meister and Bonhoeffer, 2001). Thus, these studies have provided important information regarding the molecular basis of odorant representations and the functional architecture of the olfactory bulb.

iv. Studies on functional architecture of auditory cortex

Classical electrophysiological studies in the cat auditory cortex (Rose, 1949; Merzenich et al., 1973, 1975) described a core primary auditory area (AI) surrounded by an

anterior auditory field (AAF), a ventral secondary area (AII), and a posterior ectosylvian field forming a belt around the core.

Based on extensive electrophysiological mapping studies, a precise cochleotopic map of tone representation was first described in cat auditory cortex by Merzenich and colleagues (1975). In pioneering optical imaging studies, Bakin et al (1996) reported a suprathreshold tonotopic organization of rat and guinea pig auditory cortex, while Hess and Scheich (1996) described frequency- and intensity-dependent spatiotemporal activity patterns in A1 of awake gerbils.

In a later study, Harrison and colleagues (1998) assessed sound frequency and intensity responses in primary auditory cortex of the anesthetized chinchilla and detected intrinsic activity in an area corresponding to the electrophysiologically defined AI cortex. In agreement with electrophysiological data, the authors found a low- to high-frequency tonotopic (or cochleotopic) organization along the anteroposterior axis of AI. More recently, Harel et al. (2000) defined auditory areas AII and AAF in chinchilla on the basis of intrinsic activity, and they were able to show, within AI, AII, and AAF, a tonotopic organization based on pure tones at octave-spaced frequencies from 500 Hz to 16 kHz. They found the maps in AI and AII to be arranged orthogonal to each other.

In addition to the study of cochleotopic maps, optical imaging has been employed to address the effects of acute electrical cochlear stimulation on the topography of the cat auditory cortex (Dinse et al., 1997). The authors report that systematic variation of the cochlear frequency sites evoked a corresponding shift of the response areas that matched the underlying frequency organization, thus suggesting the utility of optical imaging in mapping response areas evoked by electrical cochlear stimulation.

Even though progress has been made in the study of the auditory cortex using optical imaging of intrinsic signals, reports are sparse compared to those on other sensory cortical areas. There may be several reasons for this. First, optimal stimuli for evoking sustained activity in primary and secondary areas have been difficult to determine; typically acoustic stimuli produce short bursts of relatively few spikes, which are likely associated with only a moderate increase in metabolic demand. The resulting low signal-to-noise ratio may be responsible for the low spatial resolution (400 μm) and the considerable overlap in intrinsic signal evoked by tones of different frequencies (e.g. Spitzer et al., 2001).

Second, in areas outside of AI, anesthesia may induce the enhancement of inhibitory mechanisms thus leading to a reduction in tonic responses (Zurita et al., 1994; Harel et al., 2000). Neural activity in secondary areas may be so weak that the associated metabolic demand is not sufficient to initiate a measurable hemodynamic response to acoustic stimuli.

Two recent approaches promise an improved signal quality in intrinsic signal imaging of auditory cortex. First, Versnel et al. (2002) carried out a systematic study comparing the efficacy of different types of sound stimuli to evoke intrinsic cortical signals in AI of anesthetized ferrets. They found tone-pip trains as well as frequency-modulated tones to be optimal. Furthermore, green illuminating light (546 nm) appeared to yield more consistent results than the wavelengths of 600–700 nm used in imaging of visual areas, despite strongly increased vascular artifacts and the additional drawback that the spatial correlation of the optical activity with neural activity is smaller and the activated area is larger. Another, perhaps even more promising innovation is the use of continuous periodic stimulation originally described by Kalatsky and Stryker (2003) in an imaging study of the visual cortex (see above). Both Kalatsky and Stryker (2002) and

Mrsic-Flogel, Grothe and Hübener (pers. comm.) have been able to rapidly obtain high-quality tonotopic maps from rat and gerbil AI, respectively, using ascending and descending tone-pip stimuli.

b. Chronic experiments in intact animals

One of the greatest advantages of optical imaging is that it allows the repeated recording of multiple activity maps in single animals and enables studying the functional architecture of particular cortical areas over a period of weeks or even months. Chronic experiments using optical imaging have been designed to study the ontogenetic development of cortical maps as well as to explore functional maps in behaving animals and to follow up functional maps in experimental models of monocular deprivation, ischemia and epilepsy.

i. Developmental studies

Optical imaging of the brain, especially in young animals, is a relatively non-invasive procedure, nevertheless chronic imaging requires some methodological changes and special care must be taken in order to minimize the risk of infection. Ideally, the dura should be left intact, so as not to expose the brain itself. This is usually possible in studies of young cats or ferrets, where the dura is translucent enough unless excessive growth occurs following the initial exposure.

Chronic optical imaging studies have elucidated the development of orientation selectivity in the visual cortex of cats and ferrets (Chapman et al., 1996; Chapman and Bonhoeffer, 1998; Gödecke et al., 1997). Orientation preference maps appear very early in development, at around the time of eye-opening, and although it has to be borne in mind that a normally reared animal will have some patterned visual experienced through the closed eyelids (Krug et al., 2001), orientation maps have even been observed in the absence of any visual experience following dark-rearing (White et al., 2001). However, normal visual input and normal patterns of neuronal activity are necessary for the maturation and maintenance of orientation maps (Crair et al., 1998; Chapman and Gödecke, 2000; White et al., 2001).

An important issue in cortical development is the question of map stability over time. Chapman et al. (1996), Gödecke et al. (1997) and Shtoyerman et al. (2000) have all demonstrated the stability of orientation preference maps in the developing visual cortex of young cats and ferrets as well as in V1 of adult macaque monkeys. Moreover, Kim and Bonhoeffer (1994) and Gödecke and Bonhoeffer (1996) showed that even in the absence of any common visual experience more or less identical orientation maps develop independently through left- and right-eye stimulation (see also next section).

ii. Visual and somatosensory cortex plasticity

Optical imaging is an excellent tool for assessing plasticity of visual cortical maps in response to various manipulations of the visual input (Sengpiel et al., 1998; Sengpiel et al., 1999; Dragoi et al., 2000; Schuett et al., 2001).

Acute as well as chronic experiments have focused on the plasticity of orientation preference and, to a lesser extent, ocular dominance maps. A wide range of experimental manipulations including strabismus (Löwel et al., 1998; Sengpiel et al., 1998; Engelmann et al., 2002), monocular and binocular deprivation (Crair et al., 1997; Crair et al., 1998; Gödecke et al., 1997; Issa et al., 1999), reverse lid-suture (Gödecke and Bonhoeffer, 1996), stripe-rearing (Sengpiel et al., 1999), dark-rearing (White et al., 2001), pattern adaptation (Dragoi et al., 2000) as well as a combination of visual and

electrical stimulation (Schuett et al., 2001) have generally led to the conclusion that while e.g. the size of individual functional domains can be affected dramatically, the overall layout of the maps (e.g. periodicity of modules) appears to be remarkably stable, although it can reorganize to some extent after focal ischemic injury (Zepeda et al., 2003).

Optical imaging has also served to elucidate the role of neurotrophins and their receptors in visual cortical plasticity. In a recent study, Gillespie and coworkers (2000) examined the functional effects of infusion of NT-4/5, NGF, and neurotrophin-3 (NT-3) on ocular dominance plasticity caused by monocular visual deprivation during the critical period in kittens. This study revealed that visual cortex receiving an NT-4/5 (but not NT-3) infusion for 2 days at the peak of the critical period, showed enhanced cortical responses to the deprived-eye, but that orientation preference maps were lost within the infused region.

Before studying plasticity of somatosensory cortex representations through optical imaging it was important to establish the stability and dynamics of optical signals from somatosensory cortex over time. Masino and Frostig (1996) found that stimulation of a single whisker consistently activated a surprisingly large area of barrel cortex. While location of the functional representation and time course of the stimulus-related intrinsic signal response were consistent, nonsystematic changes both in the shape and the areal extent of the whisker representation, as well as the amplitude of the intrinsic signal were observed. Therefore, quantitative imaging results from barrel cortex must be interpreted with care, since optimal methods for data analysis have not yet been established. The possible reasons have been discussed earlier (see section *III.a.ii*). Despite these caveats, several groups have attempted to study plasticity of the somatosensory system using optical imaging.

Prakash et al. (1996) explored the effects of the topical application of different neurotrophins on the barrel cortex. They showed that topical application of BDNF resulted in a rapid and long-lasting decrease in the size of a whisker representation, and a decrease in the amplitude of the activity-dependent intrinsic signal. In contrast, NGF application provoked a rapid but transient increase in the size of a whisker representation, accompanied by an increase in the amplitude of the activity-dependent intrinsic signal. Thus, neurotrophins exert differential effects on the activity and functional organization of whisker representations.

Studies on reorganization after peripheral deafferentation (Polley et al., 1999) have shown that after whisker removal, plastic changes are expressed either as an expansion or a contraction of the spared whisker's functional representation depending on the animal's usage of its whiskers during the period of sensory deprivation. The reason as to why providing the animals with an opportunity to use their spared whisker in active exploration results in a decrease in its functional representation remains unknown.

iii. Studies in awake animals

Despite the fact that most imaging studies aimed at exploring the functional modularity in sensory neocortex, the study of such cortical modules in relation to perceptual and cognitive behavior in awake animals and humans is recent (Grinvald et al., 1991; Haglund et al., 1992; Vnek et al., 1999; Cannestra et al., 2000; Shtoyerman et al., 2000; Sato et al., 2002; Siegel et al., 2003). Anesthetized subjects are unsuitable for many types of studies, such as motivation, attention or arousal affecting sensory processing and perception, motor function, consciousness, and other cognitive functions. In addition, long-term plastic changes related to memory and learning or recovery of

function after trauma or stroke are difficult to pinpoint without imaging. Studies in human subjects are limited to noninvasive approaches (EEG, fMRI); electrical recording or anatomical techniques are not an option. Therefore, for the foreseeable future, the awake monkey model is likely to remain the preparation of choice to understand better the functional organization of the primate brain.

Experiments in awake and behaving monkey required a number of additional issues to be solved. Among them probably the most important concerned the elimination of the noise resulting from movement and the large optical noise produced by cardiac and respiratory pulsations. Another important issue that had to be addressed was the effect of anesthesia on the characteristics of the intrinsic optical signal. In order to resolve these problems and to investigate if imaging in awake animals was feasible, the first studies aimed at comparing cortical activity obtained in the awake versus the anesthetized animal. In a pioneering study, Grinvald et al., (1991) performed optical imaging of ocular dominance columns in V1 of untrained monkeys, by taking images of the exposed cortex while the animal was viewing video movies alternatively with each eye. They used a chamber like that described in section *II.c.i.,* which diminished movement related to pulsation and maintained the cortex in a closed environment whenever the subject was not in the recording apparatus. They also described that movement-related noise could be almost completely avoided by: i) mounting the monkey-chair to a heavy anti-vibration table; ii) holding the head of the monkey by restricting its movement and; iii) using rigid bars to anchor the head holder, the monkey-chair and the lens of the camera to each other. By this procedure they were able to obtain high resolution maps of ocular dominance columns, and observed that it was not necessary to synchronize respiratory and cardiac cycles to image acquisition.

This study revealed that although the intrinsic optical signals in the awake animal were similar to the anesthetized animal in wavelength dependency and time course, the latter was slightly slower in the awake animal. Therefore, a longer frame duration for image acquisition was used to improve the quality of the maps. However, Shoham and Grinvald (2001) have optimized the imaging procedures, and have been able to obtain functional maps more rapidly. Moreover, Vnek et al. (1999) showed that well trained animals required considerably fewer trials in order to obtain a good signal-to–noise ratio.

Optical imaging has also contributed to the understanding of the functional architecture in association cortices, particularly the inferior parietal lobe areas, whose neurons combine visual information with eye position signals. In a recent study, Siegel et al. (2003) reported a novel topographical map of eye position in macaque monkey, which is modulated by visual responses in the inferior parietal lobule. The authors proposed that this functional architecture may serve as the scaffolding on which other sensory, attentional, and intentional maps may be embedded at finer columnar scales.

c. Studies in humans

Due to the opacity of the human skull, optical imaging of intrinsic signals, of the kind described in this review so far, in humans has been limited to intra-operative procedures. However, recent advances in optical imaging technology and methodology, reviewed by Pouratian et al. (2003), have allowed significantly improving optical imaging studies of the human cortex and even making the study of higher cognitive processes feasible.

The pioneering studies by Haglund et al. (1992), Toga et al. (1995) and Cannestra et al. (1998), using optical imaging in surgical procedures, were aimed at delineating functional borders that helped minimizing the potential damage to healthy

tissue that can occur during resection of tumors, epileptic foci or arteriovenous malformations.

One prominent area of study has been the somatosensory and motor cortex. Toga et al. (1995) analyzed the temporal and spatial evolution of optical signals combined with evoked potential in response to transcutaneous electrical stimulation of the median and ulnar nerves in patients undergoing surgical resection of brain tumors. The obtained optical signal colocalized with the largest evoked potentials in both motor and sensory regions, illustrating the relationship between neuronal firing and vascular and metabolic function. More recently, Cannestra et al. (1998) demonstrated that the peak optical responses generated after the stimulation of different fingers do not overlap but the non-peak signals do. This result could be due either to a partial overlapping of digit representations in the human cortex or to the large point-spread generally observed in somatosensory cortex (see above). In another study of human somatosensory cortex, Sato et al., (2002) identified a neuronal response area in the postcentral gyrus differentially activated depending on the finger that was stimulated. While first and fifth digit stimulation elicited optical responses in different areas near the central sulcus, their stimulation resulted in overlapping activity closer to the postcentral sulcus, suggesting a hierarchical organization of the primary somatosensory cortex.

Another application of optical imaging in humans has been the functional characterization of cortical language areas in awake patients undergoing a neurosurgical procedure (Haglund et al., 1992; Cannestra et al., 2000; Pouratian et al., 2000). The pioneering study by Haglund et al. (1992) demonstrated cognitively evoked activity in language areas. In this report, the authors correlated the optical changes with cortical stimulation mapping and observed that functional imaging yielded significant activation in both essential and secondary languages regions, in contrast with electrocortical stimulation (ESM), which only identified the essential language cortex (i.e. Wernicke's and Broca's areas). Cannestra et al. (2000) used imaging coupled with ESM and studied cortical activation in response to different language tasks in awake patients. Distinct spatial and temporal response patterns, dependent on task and performance, were characterized both within Broca´s and Wernicke´s areas, consistent with the existence of task-specific semantic and phonologic regions within these areas; the differing temporal patterns were proposed to reflect unique processing performed by receptive (Wernicke's) and productive (Broca's) language centers.

The first non-invasive optical imaging studies in humans were performed with near-infrared spectroscopy (NIRS; Villringer and Chance, 1997). Using light of 700-1000 nm wavelength for illumination, the reflectance signal in NIRS primarily represents the increase in oxy-hemoglobin (and *decrease* in deoxy-hemoglobin) associated with the delayed increase in blood flow and volume following cortical activation and is therefore of opposite polarity to the intrinsic signals that this review is concerned with. The NIRS signal has a similar time-course and spatial pattern and resolution limit as most fMRI studies. More recently, Gratton and colleagues (Gratton et al., 1997; Gratton and Fabiani, 2001) have developed an optical imaging method, in which the signal is derived primarily from activity-induced changes in light scattering and which is therefore much closer to the technique reviewed here. This "event-related optical signal" (EROS) allows a spatial resolution of better than 1 cm^3 and has a latency of around 100 msec. Illumination at wavelengths of 690-850 nm is typically provided by laser diodes, which (in contrast with halogen lamps) permit high frequency modulation (110-220 MHz) of light intensity; as light detectors, photomultiplier tubes or CCD cameras can be used. The variation of the incident light intensity allows for precise measurements of the time required by photons to travel from the source to the

detector; the different delays introduced by cortical tissues constitute a more sensitive measure of neural activity than the total number of photons absorbed. The maximum depth of penetration with this technique is currently limited to about 3 cm (Gratton and Fabiani, 2001).

d. Clinically relevant studies

Optical imaging has not only proved to be a breakthrough in the understanding of functional organization and physiology of the cerebral cortex, but has also allowed gaining insights into pathophysiological processes such as epilepsy and stroke.

i. Epilepsy

Epilepsy is a neurological condition characterized by recurrent seizures which comprise complex electrical firing of a population of neurons. Most studies in epilepsy have been done using electrophysiological recordings from surface field and extracellular single-unit electrodes. However these methodologies have significant limitations in the acute localization of the generation and spread of neuronal activity mainly due to temporal and spatial sampling limitations. Other techniques based on the focal coupling of alteration of blood flow and metabolism with neuronal activity, such as fMRI, positron emission tomography (PET), single photon emission computed tomography (SPECT), do not have the temporal or spatial resolution to resolve brief paroxysmal or interictal spikes and to localize proximal areas of early electrical activity spread.

To gain insights in the study of the epileptogenic pathophysiology, some models of epilepsy such as cortical slices (Hochman et al., 1995), isolated guinea-pig whole brain (Federico et al., 1994), penicillin-induced seizures in rat (Chen et al., 2000), induced epileptic foci in ferret cerebral cortex (Schwartz and Bonhoeffer, 2001) and even intra-operative procedures in humans (Haglund et al., 1992) have been analyzed using OI.

Schwartz and Bonhoeffer (2001) mapped spontaneous epileptic events such as interictal, ictal and secondary homotopic foci as well as a decreased neuronal activity surrounding the epileptic focus in vivo. In this study, interictal events were induced by the focal application of the $GABA_A$ receptor antagonist, bicuculline and ictal activity by injecting 4-aminopyridine into cortical layers II/III. OI allowed the generation of high-resolution maps of the spread epileptiform activity and its relation with the functional cortical architecture in real time.

Optical mapping offers the potential of being used intra-operatively during the resection of an epileptic focus in humans, where it could contribute to a much higher degree of neurosurgical precision (Haglund et al., 1992; Schwartz and Bonhoeffer, 2001).

ii. Ischemia and stroke

A number of experiments have shown that cerebrovascular disease can significantly influence the cerebral blood flow and oxygen response to functional activation. However, until recently effects on functional cortical maps of an ischemic event remained unknown. In a recent study, Zepeda et al (2003) induced a small photochemical lesion in primary visual cortex of kittens and analyzed the subsequent reorganization of cortical maps using optical imaging. Given that photochemical lesions are induced without manipulating the brain and are highly reproducible, they provide a very "clean" method for studying the consequences of a focal ischemic event.

Zepeda et al. (2003) observed an area of capillary occlusion that was co-extensive with an area void of functional activity immediately after the lesion (Fig. 5). Some revascularization started within the functionally silent area as early as two weeks

after the lesion; this process coincided in time with the reduction in size of the inactive region. Moreover, near the lesion both the retinotopic and the orientation preference maps were found to reorganize over a period of five weeks after the lesion.

IV. Conclusion

Optical imaging has emerged as a potent tool to analyze the spatial distribution of neuronal activity in vivo over large areas of the brain surface, with high spatial resolution. OI studies contribute to our understanding of the neuronal integration of different stimulus features at a population level and allow to observe the functional development of the brain and to study its plasticity under different experimental manipulations and in experimental models of neuropathology. Moreover, OI may be applied in human intra-operative procedures, providing a tool for delineating the functional borders of epileptic foci or during a tumor resection. If intrinsic signal imaging methods such as event-related optical signals (EROS), which allow imaging through the intact human skull, could be improved further in terms of spatial resolution and acquisition times, then we might even be able to study the functional architecture of the human cerebral cortex and monitor patterns of activity during the execution of different tasks.

Acknowledgements

We thank Thomas Mrsic-Flogel for helpful comments on the manuscript. A.Z. and C.A. were supported by CONACYT 36250M. F.S. was supported by the Medical Research Council and the Human Frontiers Science Program Organization.

References

Arieli A, Grinvald A. Optical imaging combined with targeted electrical recordings, microstimulation, or tracer injections. J Neurosci Methods 2002;116:15-28.

Arieli A, Grinvald A, Slovin H. Dural substitute for long-term imaging of cortical activity in behaving monkeys and its clinical implications. J Neurosci Methods 2002;114:119-133.

Attwell D, Laughlin SB. An energy budget for signaling in the grey matter of the brain. J Cereb Blood Flow Metab 2001;21:1133-1145.

Bakin JS, Kwon MC, Masino SA, Weinberger NM, Frostig RD. Suprathreshold auditory cortex activation visualized by intrinsic signal optical imaging. Cereb Cortex 1996;6:120-130.

Bartfeld E, Grinvald A. Relationships between orientation-preference pinwheels, cytochrome oxidase blobs, and ocular-dominance columns in primate striate cortex. Proc Natl Acad Sci U S A 1992;89:11905-11909.

Bell AJ, Sejnowski TJ. An information-maximization approach to blind separation and blind deconvolution. Neural Comput, 1995; 7: 1129-1159.

Belluscio L, Katz LC. Symmetry, stereotypy, and topography of odorant representations in mouse olfactory bulbs. J Neurosci 2001;21:2113-2122.

Blasdel G, Campbell D. Functional retinotopy of monkey visual cortex. J Neurosci 2001; 21:8286-8301.

Blasdel GG, Salama G. Voltage-sensitive dyes reveal a modular organization in monkey striate cortex. Nature, 1986; 321: 579-585.

Blood AJ, Narayan SM, Toga AW. Stimulus parameters influence characteristics of optical intrinsic signal responses in somatosensory cortex. J Cereb Blood Flow Metab 1995;15:1109-1121.

Bonhoeffer T, Grinvald A. Iso-orientation domains in cat visual cortex are arranged in pinwheel- like patterns. Nature 1991;353:429-431.

Bonhoeffer T, Grinvald A. The layout of iso-orientation domains in area 18 of cat visual cortex: optical imaging reveals a pinwheel-like organization. J Neurosci 1993;13:4157-4180.

Bonhoeffer T, Grinvald A. Optical imaging based on intrinsic signals. The methodology. In Toga A, Mazziota J, editors. Brain mapping: The methods. Academic Press: London, 1996;55-97.

Bonhoeffer T, Kim DS, Malonek D, Shoham D, Grinvald A. Optical imaging of the layout of functional domains in area 17 and across the area 17/18 border in cat visual cortex. Eur J Neurosci 1995;7:1973-1988.

Bosking WH, Crowley JC, Fitzpatrick D. Spatial coding of position and orientation in primary visual cortex. Nat Neurosci 2002;5:874-882.

Bosking WH, Y. Z, B. S, Fitzpatrick D. Orientation selectivity and the arrangement of horizontal connections in tree shrew striate cortex. J Neurosci 1997;17:2112-2127.

Bosking WH, Kretz R, Pucak ML, Fitzpatrick D. Functional specificity of callosal connections in tree shrew striate cortex. J Neurosci 2000;20:2346-2359.

Boynton GM, Engel SA, Glover GH, Heeger DJ. Linear systems analysis of functional magnetic resonance imaging in human V1. J Neurosci 1996;16:4207-4221.

Bozza TC, Mombaerts P. Olfactory coding: revealing intrinsic representations of odors. Curr Biol 2001;11:R687-690.

Brett-Green BA, Chen-Bee CH, Frostig RD. Comparing the functional representations of central and border whiskers in rat primary somatosensory cortex. J Neurosci 2001;21:9944-9954.

Carandini M, Sengpiel F. Contrast invariance of functional maps in cat primary visual cortex. J Vision 2004; in press.

Cannestra AF, Pouratian N, Bookheimer SY, Martin NA, Beckerand DP, Toga AW. Temporal spatial differences observed by functional MRI and human intraoperative optical imaging. Cereb Cortex 2001;11:773-782.

Cannestra AF, Black KL, Martin NA, Cloughesy T, Burton JS, Rubinstein E, Woods RP, Toga AW. Topographical and temporal specificity of human intraoperative optical intrinsic signals. Neuroreport 1998;9:2557-2563.

Cannestra AF, Bookheimer SY, Pouratian N, O'Farrell A, Sicotte N, Martin NA, Becker D, Rubino G, Toga AW. Temporal and topographical characterization of language cortices using intraoperative optical intrinsic signals. Neuroimage 2000;12:41-54.

Chapman B, Bonhoeffer T. Overrepresentation of horizontal and vertical orientation preferences in developing ferret area 17. Proc Natl Acad Sci U S A 1998;95:2609-2614.

Chapman B, Gödecke I. Cortical cell orientation selectivity fails to develop in the absence of ON-center retinal ganglion cell activity. J Neurosci 2000;20:1922-1930.

Chapman B, Stryker MP, Bonhoeffer T. Development of orientation preference maps in ferret primary visual cortex. J Neurosci 1996;16:6442-6453.

Chen JW, O'Farrell AM, Toga AW. Optical intrinsic signal imaging in a rodent seizure model. Neurology 2000;55:312-315.

Chen LM, Friedman RM, Ramsden BM, LaMotte RH, Roe AW. Fine-scale organization of SI (area 3b) in the squirrel monkey revealed with intrinsic optical imaging. J Neurophysiol 2001;86:3011-3029.

Chen LM, Heider B, Williams GV, Healy FL, Ramsden BM, Roe AW. A chamber and artificial dura method for long-term optical imaging in the monkey. J Neurosci Methods 2002;113:41-49.

Chen-Bee CH. Variability and interhemispheric asymmetry of single-whisker functional representations in rat barrel cortex. J Neurophysiol 1996;76:884-894.

Chen-Bee CH, Kwon MC, Masino SA, Frostig RD. Areal extent quantification of functional representations using intrinsic signal optical imaging. J Neurosci Methods 1996;68:27-37.

Clarke DD, Sokoloff L. Circulation and energy metabolism of the brain. In Siegel G, Agranoff B, Albers R, Fisher S, Uhler M, editors. Basic Neurochemistry: Molecular, Cellular and Medical Aspects. Lippincott-Raven: Philadelphia, 1999;637-669.

Cohen LB. Changes in neuron structure during action potential propagation and synaptic transmission. Physiol Rev 1973;53:373-418.

Crair MC, Gillespie DC, Stryker MP. The role of visual experience in the development of columns in cat visual cortex. Science 1998;279:566-570.

Crair MC, Ruthazer ES, Gillespie DC, Stryker MP. Relationship between the ocular dominance and orientation maps in visual cortex of monocularly deprived cats. Neuron 1997;19:307-318.

Das A, Gilbert CD. Long-range horizontal connections and their role in cortical reorganization revealed by optical recording of cat primary visual cortex. Nature 1995;375:780-784.

Dinse HR, Godde B, Hilger T, Reuter G, Cords SM, Lenarz T, von Seelen W. Optical imaging of cat auditory cortex cochleotopic selectivity evoked by acute electrical stimulation of a multi-channel cochlear implant. Eur J Neurosci 1997;9:113-119.

Dragoi V, Sharma J, Sur M. Adaptation-induced plasticity of orientation tuning in adult visual cortex. Neuron 2000;28:287-298.

Engel SA, Rumelhart DE, Wandell BA, Lee AT, Glover GH, Chichilnisky EJ, Shadlen MN. fMRI of human visual cortex. Nature 1994;369:525.

Engelmann R, Crook JM, Löwel S. Optical imaging of orientation and ocular dominance maps in area 17 of cats with convergent strabismus. Vis Neurosci 2002;19:39-49.

Federico P, Borg SG, Salkauskus AG, MacVicar BA. Mapping patterns of neuronal activity and seizure propagation by imaging intrinsic optical signals in the isolated whole brain of the guinea-pig. Neuroscience 1994;58:461-480.

Frostig RD, Lieke EE, Ts'o DY, Grinvald A. Cortical functional architecture and local coupling between neuronal activity and the microcirculation revealed by in vivo high-resolution optical imaging of intrinsic signals. Proc Natl Acad Sci U S A 1990;87:6082-6086.

Gabbay M, Brennan C, Kaplan E, Sirovich L. A principal components-based method for the detection of neuronal activity maps: Application to optical imaging. NeuroImage, 2000; 11: 313-325.

Ghose GM, Ts'o DY. Form processing modules in primate area V4. J Neurophysiol 1997;77:2191-2196.

Gillespie DC, Crair MC, Stryker MP. Neurotrophin-4/5 Alters Responses and Blocks the Effect of Monocular Deprivation in Cat Visual Cortex during the Critical Period. J Neurosci 2000;20:9174-9186.

Gochin PM, Bedenbaugh P, Gelfand JJ, Gross CG, Gerstein GL. Intrinsic signal optical imaging in the forepaw area of rat somatosensory cortex. Proc Natl Acad Sci USA 1992;89:8381-8383.

Godde B, Hilger T, von Seelen W, Berkefeld T, Dinse HR. Optical imaging of rat somatosensory cortex reveals representational overlap as topographic principle. Neuroreport 1995;7:24-28.

Gödecke I, Bonhoeffer T. Development of identical orientation maps for two eyes without common visual experience. Nature 1996;379:251-254.

Gödecke I, Kim DS, Bonhoeffer T, Singer W. Development of orientation preference maps in area 18 of kitten visual cortex. Eur J Neurosci 1997;9:1754-1762.

Gratton G, Fabiani M. The event-related optical signal: a new tool for studying brain function. Int J Psychophysiol, 2001; 42: 109-121.

Gratton G, Fabiani M, Corballis PM, Hood DC, Goodman-Wood MR, Hirsch J, Kim K, Friedman D, Gratton E. Fast and localized event-related optical signals (EROS) in the human occipital cortex: Comparisons with the visual evoked potential and fMRI. NeuroImage, 1997; 6: 168-180.

Grinvald A, Frostig RD, Siegel RM, Bartfeld E. High-resolution optical imaging of functional brain architecture in the awake monkey. Proc Natl Acad Sci USA 1991;88:11559-11563.

Grinvald A, Lieke E, Frostig RD, Gilbert CD, Wiesel TN. Functional architecture of cortex revealed by optical imaging of intrinsic signals. Nature 1986;324:361-364.

Grinvald A, Shoham D, Shmuel A, Glaser DE, Vanzetta I, Shtoyerman E, Slovin H, Wijnbergen C, Hildesheim R, Sterkin A, Arieli A. In-vivo optical imaging of cortical architecture and dynamics. In Windhorst U, Johansson H, editors. Modern Techniques in Neuroscience Research. Springer Verlag: Heidelberg, 1999; 893-969.

Guthrie KM, Anderson AJ, Leon M, Gall C. Odor-induced increases in c-fos mRNA expression reveal an anatomical "unit" for odor processing in olfactory bulb. Proc Natl Acad Sci USA 1993;90:3329-3333.

Haglund MM, Ojemann GA, Hochman DW. Optical imaging of epileptiform and functional activity in human cerebral cortex. Nature 1992;358:668-671.

Harel N, Mori N, Sawada S, Mount RJ, Harrison RV. Three distinct auditory areas of cortex (AI, AII, and AAF) defined by optical imaging of intrinsic signals. Neuroimage 2000;11:302-312.

Harrison RV, Harel N, Kakigi A, Raveh E, Mount RJ. Optical imaging of intrinsic signals in chinchilla auditory cortex. Audiol Neurootol 1998;3:214-223.

Hess A, Scheich H. Optical and FDG mapping of frequency-specific activity in auditory cortex. Neuroreport 1996;7:2643-2647.

Hess A, Stiller D, Kaulisch T, Heil P, Scheich H. New insights into the hemodynamic blood oxygenation level-dependent response through combination of functional magnetic resonance imaging and optical recording in gerbil barrel cortex. J Neurosci 2000;20:3328-3338.

Hildebrand JG, Shepherd GM. Mechanisms of olfactory discrimination: converging evidence for common principles across phyla. Annu Rev Neurosci 1997;20:595-631.

Hill DK, Keynes RD. Opacity changes in stimulated nerve. J Physiol 1949;108:278-281.

Hochman DW, Baraban SC, Owens JW, Schwartzkroin PA. Dissociation of synchronization and excitability in furosemide blockade of epileptiform activity. Science 1995;270:99-102.

Hubel DH, Wiesel TN. Receptive fields, binocular interaction and functional architecture in the cat's visual cortex. J Physiol 1962;160:106-154.

Hubel DH, Wiesel TN. Functional architecture of macaque monkey visual cortex. Proc R Soc Lond B 1977;198:1-59.

Hübener M, Shoham D, Grinvald A, Bonhoeffer T. Spatial relationships among three columnar systems in cat area 17. J Neurosci 1997;17:9270-9284.

Imamura K, Mataga N, Mori K. Coding of odor molecules by mitral/tufted cells in rabbit olfactory bulb. I. Aliphatic compounds. J Neurophysiol 1992;68:1986-2002.

Issa NP, Trepel C, Stryker MP. Spatial frequency maps in cat visual cortex. J Neurosci 2000;20:8504-8514.

Issa NP, Trachtenberg JT, Chapman B, Zahs KR, Stryker MP. The critical period for ocular dominance plasticity in the Ferret's visual cortex. J Neurosci 1999;19:6965-6978.

Johnson BA, Woo CC, Leon M. Spatial coding of odorant features in the glomerular layer of the rat olfactory bulb. J Comp Neurol 1998;393:457-471.

Kalatsky VA, Stryker MP. New paradigm for optical imaging: temporally encoded maps of intrinsic signal. Neuron 2003;38:529-545.

Kalatsky VA, Stryker M.P. Supratheshold organization of rat auditory cortex revealed by new method of intrinsic signal optical imaging. Soc Neurosci Abstract Viewer 2002; Program No. 354.15.

Kauer JS. Real-time imaging of evoked activity in local circuits of the salamander olfactory bulb. Nature 1988;331:166-168.

Kim DS, Bonhoeffer T. Reverse occlusion leads to a precise restoration of orientation preference maps in visual cortex. Nature 1994;370:370-372.

Kim DS, Duong TQ, Kim SG. High-resolution mapping of iso-orientation columns by fMRI. Nat Neurosci 2000;3:164-169.

Kim DS, Matsuda Y, Ohki K, Ajima A, Tanaka S. Geometrical and topological relationships between multiple functional maps in cat primary visual cortex. Neuroreport 1999;10:2515-2522.

Kisvarday ZF, Kim DS, Eysel UT, Bonhoeffer T. Relationship between lateral inhibitory connections and the topography of the orientation map in cat visual cortex. Eur J Neurosci 1994;6:1619-1632.

Kisvarday ZF, Toth E, Rausch M, Eysel UT. Orientation-specific relationship between populations of excitatory and inhibitory lateral connections in the visual cortex of the cat. Cereb Cortex 1997;7:605-618.

Krug K, Akerman CJ, Thompson ID. Responses of neurons in neonatal cortex and thalamus to patterned visual stimulation through the naturally closed lids. J Neurophysiol 2001;8:1436-1443.

Landisman CE, Ts'o DY. Color processing in macaque striate cortex: relationships to ocular dominance, cytochrome oxidase, and orientation. J Neurophysiol 2002;87:3126-3137.

Liu GB, Pettigrew JD. Orientation mosaic in barn owl's visual Wulst revealed by optical imaging: comparison with cat and monkey striate and extra-striate areas. Brain Res 2003;961:153-158.

Löwel S, Schmidt KE, Kim DS, Wolf F, Hoffsümmer F, Singer W, Bonhoeffer T. The layout of orientation and ocular dominance domains in area 17 of strabismic cats. Eur J Neurosci 1998;10:2629-2643.

Lyon DC, Xu X, Casagrande VA, Stefansic JD, Shima D, Kaas JH. Optical imaging reveals retinotopic organization of dorsal V3 in New World owl monkeys. Proc Natl Acad Sci U S A 2002;99:15735-15742.

MacVicar BA, Hochman D. Imaging of synaptically evoked intrinsic optical signals in hippocampal slices. J Neurosci 1991;11:1458-1469.

Malach R, Tootell RB, Malonek D. Relationship between orientation domains, cytochrome oxidase stripes, and intrinsic horizontal connections in squirrel monkey area V2. Cereb Cortex 1994;4:151-165.

Malach R, Amir Y, Harel M, Grinvald A. Relationship between intrinsic connections and functional architecture revealed by optical imaging and in vivo targeted biocytin injections in primate striate cortex. Proc Natl Acad Sci U S A 1993;90:10469-10473.

Malach R, Schirman TD, Harel M, Tootell RB, Malonek D. Organization of intrinsic connections in owl monkey area MT. Cereb Cortex 1997;7:386-393.

Maldonado PE, Gödecke I, Gray CM, Bonhoeffer T. Orientation selectivity in pinwheel centers in cat striate cortex. Science 1997;276:1551-1555.

Malonek D, Tootell RB, Grinvald A. Optical imaging reveals the functional architecture of neurons processing shape and motion in owl monkey area MT. Proc R Soc Lond B Biol Sci 1994;258:109-119.

Malonek D, Dirnagl U, Lindauer U, Yamada K, Kanno I, Grinvald A. Vascular imprints of neuronal activity: relationships between the dynamics of cortical blood flow, oxygenation, and volume changes following sensory stimulation. Proc Natl Acad Sci USA 1997;94:14826-14831.

Masino SA, Frostig RD. Quantitative long-term imaging of the functional representation of a whisker in rat barrel cortex. Proc Natl Acad Sci USA 1996;93:4942-4947.

Masino SA, Kwon MC, Dory Y, Frostig RD. Characterization of functional organization within rat barrel cortex using intrinsic signal optical imaging through a thinned skull. Proc Natl Acad Sci USA 1993;90:9998-10002.

Mayhew JE, Askew S, Zheng Y, Porrill J, Westby GW, Redgrave P, Rector DM, Harper R. Cerebral vasomotion: a 0.1 Hz oscillation in reflected light imaging of neural activity. NeuroImage, 1996; 4: 183-193.

McLoughlin NP, Blasdel GG. Wavelength-dependent differences between optically determined functional maps from macaque striate cortex. NeuroImage 1998;7:326-336.

Meister M, Bonhoeffer T. Tuning and topography in an odor map on the rat olfactory bulb. J Neurosci 2001;21:1351-1360.

Merzenich MM, Knight PL, Roth GL. Cochleotopic organization of primary auditory cortex in the cat. Brain Res 1973;63:343–346.

Merzenich MM, Knight PL, Roth GL. Representation of cochlea within primary auditory cortex in the cat. J Neurophysiol 1975;38:231-249.

Mombaerts P. Molecular biology of odorant receptors in vertebrates. Annu Rev Neurosci 1999;22:487-509.

Narayan SM, Santori EM, Toga AW. Mapping functional activity in rodent cortex using optical intrinsic signals. Cereb Cortex 1994a;4:195-204.

Narayan SM, Santori EM, Blood AJ, Burton JS, Toga AW. Imaging optical reflectance in rodent barrel and forelimb sensory cortex. Neuroimage 1994b;1:181-190.

Narayan SM, Esfahani P, Blood AJ, Sikkens L, Toga AW. Functional increases in cerebral blood volume over somatosensory cortex. J Cereb Blood Flow Metab 1995;15:754-765.

Nelson RJ, Sur M, Felleman DJ, Kaas JH. Representation of the body surface in postcentral parietal cortex of Macaca fascicularis. J Comp Neurol 1980;192:611-643.

Payne BR, Berman N, Murphy EH. Organization of direction preferences in cat visual cortex. Brain Res 1981;211:445-450.

Peterson BE, Goldreich D. Optical imaging and electrophysiology of rat barrel cortex. I. Responses to small single-vibrissa deflections. Cereb Cortex 1998;8:173-183.

Petersen CCH, Grinvald A, Sakmann B. Spatiotemporal dynamics of sensory responses in layer 2/3 of rat barrel cortex measured in vivo by voltage-sensitive dye imaging combined with whole-cell voltage recordings and neuron reconstructions. J Neurosci 2003;23:1298-1309.

Polley DB, Chen-Bee CH, Frostig RD. Two directions of plasticity in the sensory-deprived adult cortex. Neuron 1999;24:623-637.

Pons TP, Garraghty PE, Cusick CG, Kaas JH. A sequential representation of the occiput, arm, forearm and hand across the rostrocaudal dimension of areas 1, 2 and 5 in macaque monkeys. Brain Res 1985;335:350-353.

Pons TP, Wall JT, Garraghty PE, Cusick CG, Kaas JH. Consistent features of the representation of the hand in area 3b of macaque monkeys. Somatosens Res 1987;4:309-331.

Pouratian N, Bookheimer SY, O'Farrell AM, Sicotte NL, Cannestra AF, Becker D, Toga AW. Optical imaging of bilingual cortical representations. Case report. J Neurosurg 2000;93:676-681.

Pouratian N, Sheth SA, Martin NA, Toga AW. Shedding light on brain mapping: advances in human optical imaging. Trends Neurosci 2003;26:277-282.

Prakash N, Cohen-Cory S, Frostig RD. Rapid and opposite effects of BDNF and NGF on the functional organization of the adult cortex in vivo. Nature 1996;381:702-706.

Ratzlaff EH, Grinvald A. A tandem-lens epifluorescence macroscope: hundred-fold brightness advantage for wide-field imaging. J Neurosci Methods 1991; 36:127-137.

Rose JE. The cellular structure of the auditory cortex of the cat. J Comp Neurol 1949;91:409–440.

Rubin BD, Katz LC. Optical imaging of odorant representations in the mammalian olfactory bulb. Neuron 1999;23:499-511.

Sato K, Nariai T, Sasaki S, Yazawa I, Mochida H, Miyakawa N, Momose-Sato Y, Kamino K, Ohta Y, Hirakawa K, Ohno K. Intraoperative intrinsic optical imaging of neuronal activity from subdivisions of the human primary somatosensory cortex. Cereb Cortex 2002;12:269-280.

Schuett S, Bonhoeffer T, Hübener M. Mapping of retinotopy in rat visual cortex by combined linear extraction and principle component analysis of optical imaging data. Eur J Neurosci 2000; 12 (Suppl 11): 74.

Schuett S, Bonhoeffer T, Hübener M. Pairing-induced changes of orientation maps in cat visual cortex. Neuron 2001;32:325-337.

Schuett S, Bonhoeffer T, Hübener M. Mapping retinotopic structure in mouse visual cortex with optical imaging. J Neurosci 2002;22:6549-6559.

Schulze S, Fox K. Single whisker representation in the barrel cortex of rats visualised with optical imaging of intrinsic signals. Soc Neurosci Abstr, 2000; 26: 1687.

Schwartz TH, Bonhoeffer T. In vivo optical mapping of epileptic foci and surround inhibition in ferret cerebral cortex. Nat Med 2001;7:1063-1067.

Sengpiel F, Bonhoeffer T. Orientation specificity of contrast adaptation in visual cortical pinwheel centres and iso-orientation domains. Eur J Neurosci 2002;15:876-886.

Sengpiel F, Stawinski P, Bonhoeffer T. Influence of experience on orientation maps in cat visual cortex. Nat Neurosci 1999;2:727-732.

Sengpiel F, Gödecke I, Stawinski P, Hübener M, Lowel S, Bonhoeffer T. Intrinsic and environmental factors in the development of functional maps in cat visual cortex. Neuropharmacology 1998;37:607-621.

Sharp FR, Kauer JS, Shepherd GM. Local sites of activity-related glucose metabolism in rat olfactory bulb during olfactory stimulation. Brain Res 1975;98:596-600.

Sharp FR, Kauer JS, Shepherd GM. Laminar analysis of 2-deoxyglucose uptake in olfactory bulb and olfactory cortex of rabbit and rat. J Neurophysiol 1977; 40:800-813.

Sheth S, Nemoto M, Guiou M, Walker M, Pouratian N, Toga AW. Evaluation of coupling between optical intrinsic signals and neuronal activity in rat somatosensory cortex. Neuroimage 2003;19:884-894.

Shmuel A, Grinvald A. Functional organization for direction of motion and its relationship to orientation maps in cat area 18. J Neurosci 1996;16:6945-6964.

Shmuel A, Grinvald A. Coexistence of linear zones and pinwheels within orientation maps in cat visual cortex. Proc Natl Acad Sci U S A 2000;97:5568-5573.

Shoham D, Grinvald A. The cortical representation of the hand in macaque and human area S-I: High resolution optical imaging. J Neurosci 2001;21:6820-6835.

Shoham D, Glaser DE, Arieli A, Kenet T, Wijnbergen C, Toledo Y, Hildesheim R, Grinvald A. Imaging cortical dynamics at high spatial and temporal resolution with novel blue voltage-sensitive dyes. Neuron, 1999; 24: 791-802

Shoham D, Hübener M, Schulze S, Grinvald A, Bonhoeffer T. Spatio-temporal frequency domains and their relation to cytochrome oxidase staining in cat visual cortex. Nature 1997;385:529-533.

Shtoyerman E, Arieli A, Slovin H, Vanzetta I, Grinvald A. Long-term optical imaging and spectroscopy reveal mechanisms underlying the intrinsic signal and stability of cortical maps in V1 of behaving monkeys. J Neurosci 2000;20:8111-8121.

Siegel RM, Raffi M, Phinney RE, Turner JA, Jando G. Functional architecture of eye position gain fields in visual association cortex of behaving monkey. J Neurophysiol 2003;90:1279-1294.

Singer W. Topographic organization of orientation columns in the cat visual cortex. A deoxyglucose study. Exp Brain Res 1981;44:431-436.

Singer W, Freeman B, Rauschecker J. Restriction of visual experience to a single orientation affects the organization of orientation columns in cat visual cortex. A study with deoxyglucose. Exp Brain Res 1981;41:199-215.

Sirovich L, Everson RM. Management and analysis of large scientific data sets. Int J Supercomp Appl, 1992; 6: 50-68.

Spitzer MW, Calford MB, Clarey JC, Pettigrew JD, Roe AW. Spontaneous and stimulus-evoked intrinsic optical signals in primary audi-tory cortex of the cat. J Neurophysiol 2001;85:1283-1298.

Stetter M, Schiessl I, Otto T, Sengpiel F, Hübener M, Bonhoeffer T, Obermayer K. Principal component analysis and blind separation of sources for optical imaging of intrinsic signals. NeuroImage, 2000; 11: 482-490.

Stepnoski RA, LaPorta A, Raccuia-Behling F, Blonder GE, Slusher RE, Kleinfeld, D. Noninvasive Detection of Changes in Membrane Potential in Cultured Neurons by Light Scattering. Proc Natl Acad Sci U S A 1991;88:9382-9386.

Sur M, Nelson RJ, Kaas JH. Representations of the body surface in cortical areas 3b and 1 of squirrel monkeys: comparisons with other primates. J Comp Neurol 1982; 211:177-192.

Swindale NV. How many maps are there in visual cortex? Cereb Cortex 2000;10:633-643.

Swindale NV, Grinvald A, Shmuel A. The spatial pattern of response magnitude and selectivity for orientation and direction in cat visual cortex. Cereb Cortex, 2003; 13: 225.

Swindale NV, Shoham D, Grinvald A, Bonhoeffer T, Hübener M. Visual cortex maps are optimized for uniform coverage. Nat Neurosci 2000;3:822-826.

Takashima I, Kajiwara R, Iijima T. Voltage-sensitive dye versus intrinsic signal optical imaging: comparison of optically determined functional maps from rat barrel cortex. Neuroreport 2001;12:2888-2894.

Toga AW, Cannestra AF, Black KL. The temporal/spatial evolution of optical signals in human cortex. Cereb Cortex 1995;5:561-565.

Tolhurst DJ, Dean AF, Thompson ID. Preferred direction of movement as an element in the organization of cat visual cortex. Exp Brain Res 1981;44:340-342.

Tommerdahl M, Favorov O, Whitsel BL, Nakhle B, Gonchar YA. Minicolumnar activation patterns in cat and monkey SI cortex. Cereb Cortex 1993;3:399-411.

Tommerdahl M, Delemos KA, Vierck CJJ, Favorov OV, Whitsel BL. Anterior parietal cortical response to tactile and skin-heating stimuli applied to the same skin site. J Neurophysiol 1996;75:2662-2670.

Tommerdahl M, Delemos KA, Whitsel BL, Favorov OV, Metz CB. Response of anterior parietal cortex to cutaneous flutter versus vibration. J Neurophysiol 1999a;82:16-33.

Tommerdahl M, Whitsel BL, Favorov OV, Metz CB, O'Quinn BL. Responses of contralateral SI and SII in cat to same-site cutaneous flutter versus vibration. J Neurophysiol 1999b;82:1982-1992.

Tommerdahl M, Delemos KA, Favorov OV, Metz CB, Vierck CJJ, Whitsel BL. Response of anterior parietal cortex to different modes of same-site skin stimulation. J Neurophysiol 1998;80:3272-3283.

Tootell RB, Silverman MS, De Valois RL. Spatial frequency columns in primary visual cortex. Science 1981;214:813-815.

Ts'o DY, Gilbert CD, Wiesel TN. Relationships between horizontal interactions and functional architecture in cat striate cortex as revealed by cross-correlation analysis. J Neurosci 1986;6:1160-1170.

Ts'o DY, Roe AW, Gilbert CD. A hierarchy of the functional organization for color, form and disparity in primate visual area V2. Vision Res 2001;41:1333-1349.

Ts'o DY, Frostig RD, Lieke EE, Grinvald A. Functional organization of primate visual cortex revealed by high resolution optical imaging. Science 1990;249:417-420.

Tsunoda K, Yamane Y, Nishizaki M, Tanifuji M. Complex objects are represented in macaque inferotemporal cortex by the combination of feature columns. Nat Neurosci 2001;4:832-838.

Uchida N, Takahashi YK, Tanifuji M, Mori K. Odor maps in the mammalian olfactory bulb: domain organization and odorant structural features. Nat Neurosci 2000;3:1035-1043.

Vanzetta I, Grinvald A. Increased cortical oxidative metabolism due to sensory stimulation: implications for functional brain imaging. Science 1999;286:1555-1558.

Versnel H, Mossop JE, Mrsic-Flogel TD, Ahmed B, Moore DR. Optical imaging of intrinsic signals in ferret auditory cortex: responses to narrowband sound stimuli. J Neurophysiol 2002;88:1545-1558.

Villringer A, Chance B. Non-invasive optical spectroscopy and imaging of human brain function. Trends Neurosci, 1997; 20: 435-442.

Villringer A, Dirnagl U. Coupling of brain activity and cerebral blood flow: basis of functional neuroimaging. Cerebrovasc Brain Metab Rev 1995;7:240-276.

Vnek N, Ramsden BM, Hung CP, Goldman-Rakic PS, Roe AW. Optical imaging of functional domains in the cortex of the awake and behaving monkey. Proc Natl Acad Sci USA 1999;96:4057-4060.

Wang G, Tanaka K, Tanifuji M. Optical imaging of functional organization in the monkey inferotemporal cortex. Science 1996;272:1665-1668.

Weliky M, Bosking WH, Fitzpatrick D. A systematic map of direction preference in primary visual cortex. Nature 1996;379:725-728.

White LE, Coppola DM, Fitzpatrick D . The contribution of sensory experience to the maturation of orientation selectivity in ferret visual cortex. Nature 2001;411: 1049-1052.

Woolsey CN, Marshall WH, Bard P. Representation of cutaneous tactile sensibility in the cerebral cortex of the monkey as indicated by evoked potentials. Bull Johns Hopkins Hosp 1942;70:399–441.

Woolsey TA, Van der Loos H. The structural organization of layer IV in the somatosensory region (SI) of mouse cerebral cortex. The description of a cortical field composed of discrete cytoarchitectonic units. Brain Res 1970;17:205-242.

Xiao Y, Wang Y, Felleman DJ. A spatially organized representation of colour in macaque cortical area V2. Nature 2003;421:535-539.

Yang X, Renken R, Hyder F, Siddeek M, Greer CA, Shepherd GM, Shulman RG. Dynamic mapping at the laminar level of odor-elicited responses in rat olfactory bulb by functional MRI. Proc Natl Acad Sci USA 1998;95.

Yousef T, Bonhoeffer T, Kim DS, Eysel UT, Toth E, Kisvarday ZF. Orientation topography of layer 4 lateral networks revealed by optical imaging in cat visual cortex (area 18). Eur J Neurosci 1999;11:4291-4308.

Zepeda A, Vaca L, Arias C, Sengpiel F. Reorganization of visual cortical maps after focal ischemic lesions. J Cereb Blood Flow Metab 2003;23:811-820.

Zurita P, Villa AE, de Ribaupierre Y, de Ribaupierre F, Rouiller EM. Changes of single unit activity in the cat's auditory thalamus and cortex associated to different anesthetic conditions. Neurosci Res 1994;19:303-316.

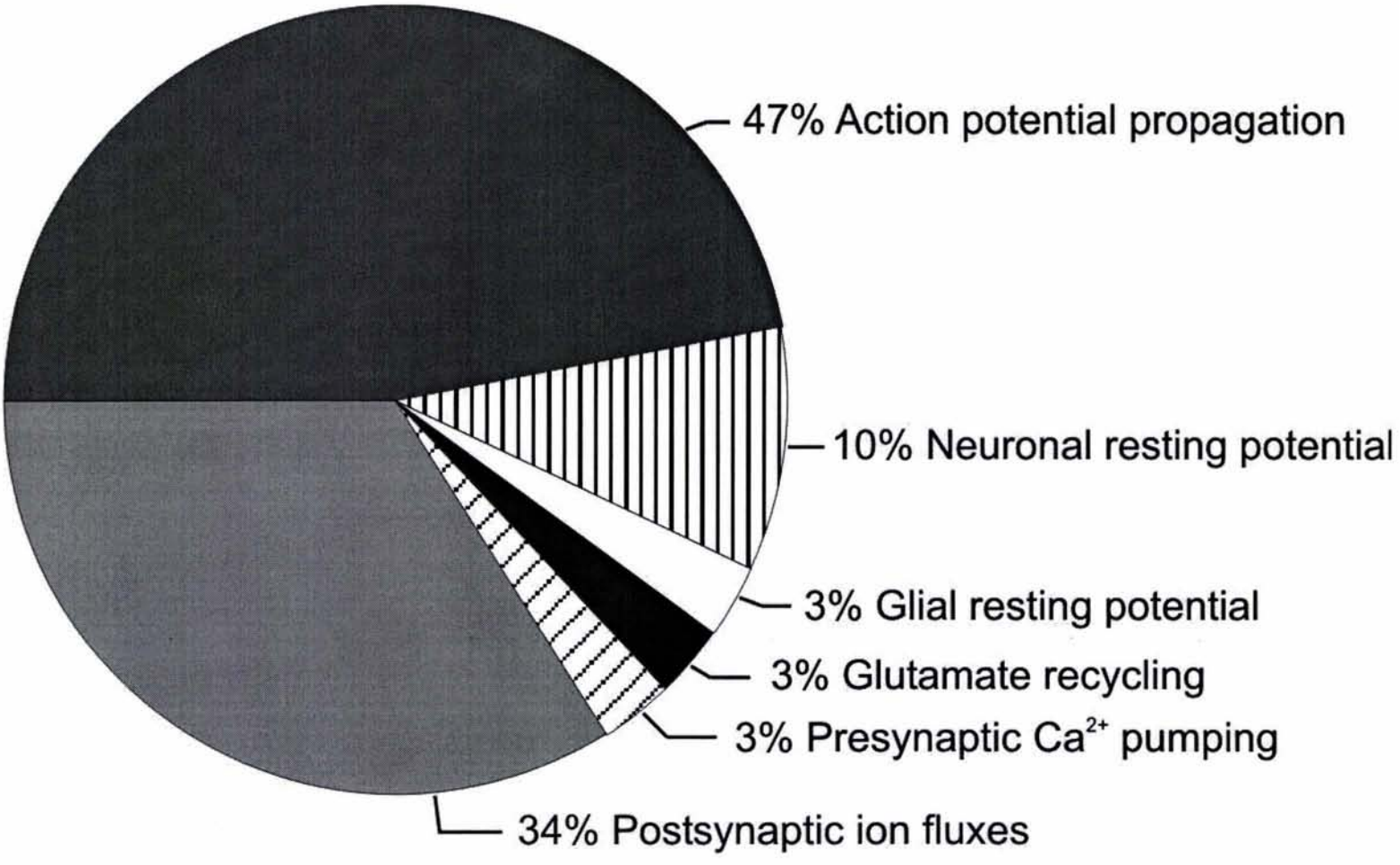

Fig. 1, Zepeda, Arias & Sengpiel

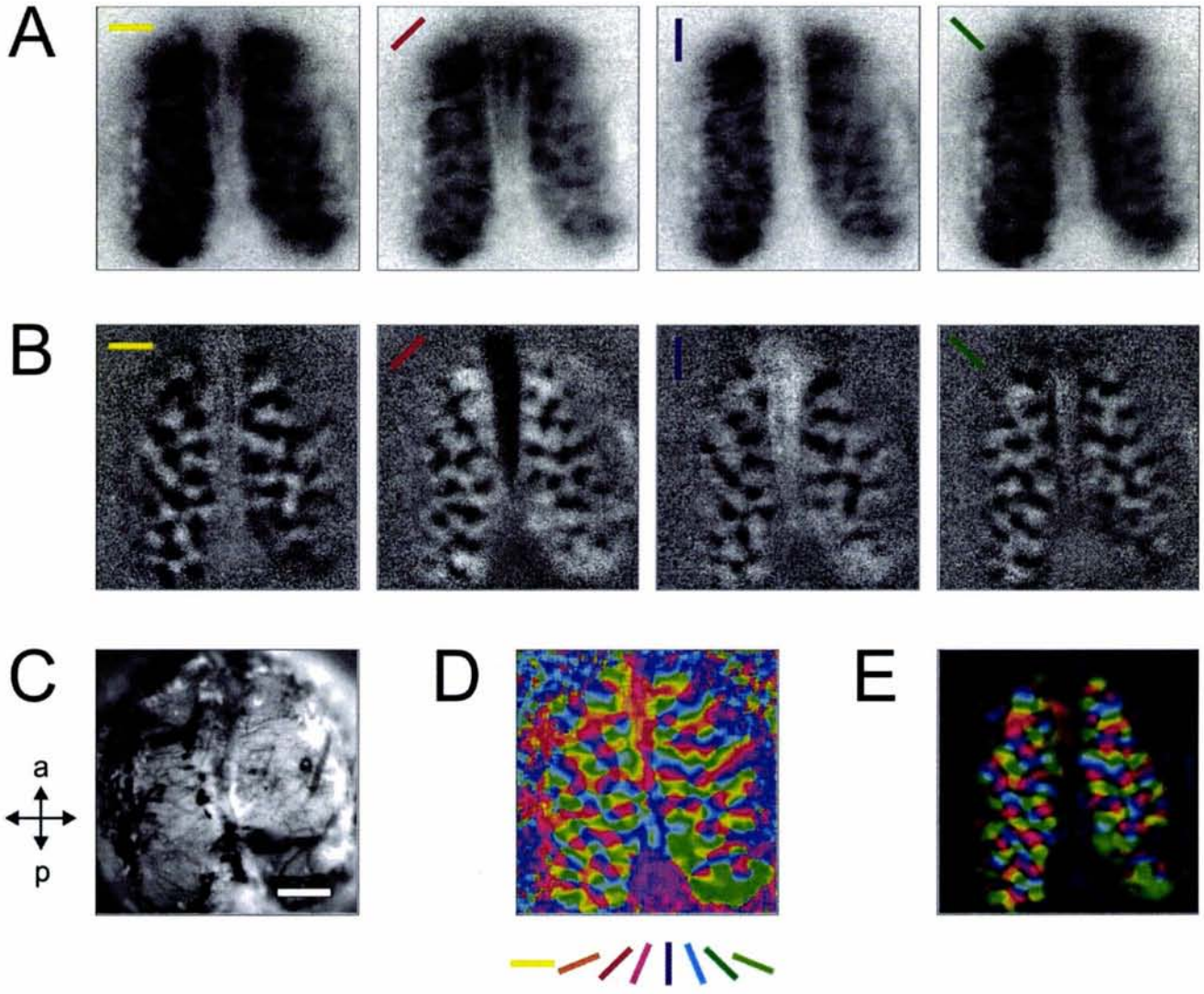

Fig. 2, Zepeda, Arias & Sengpiel

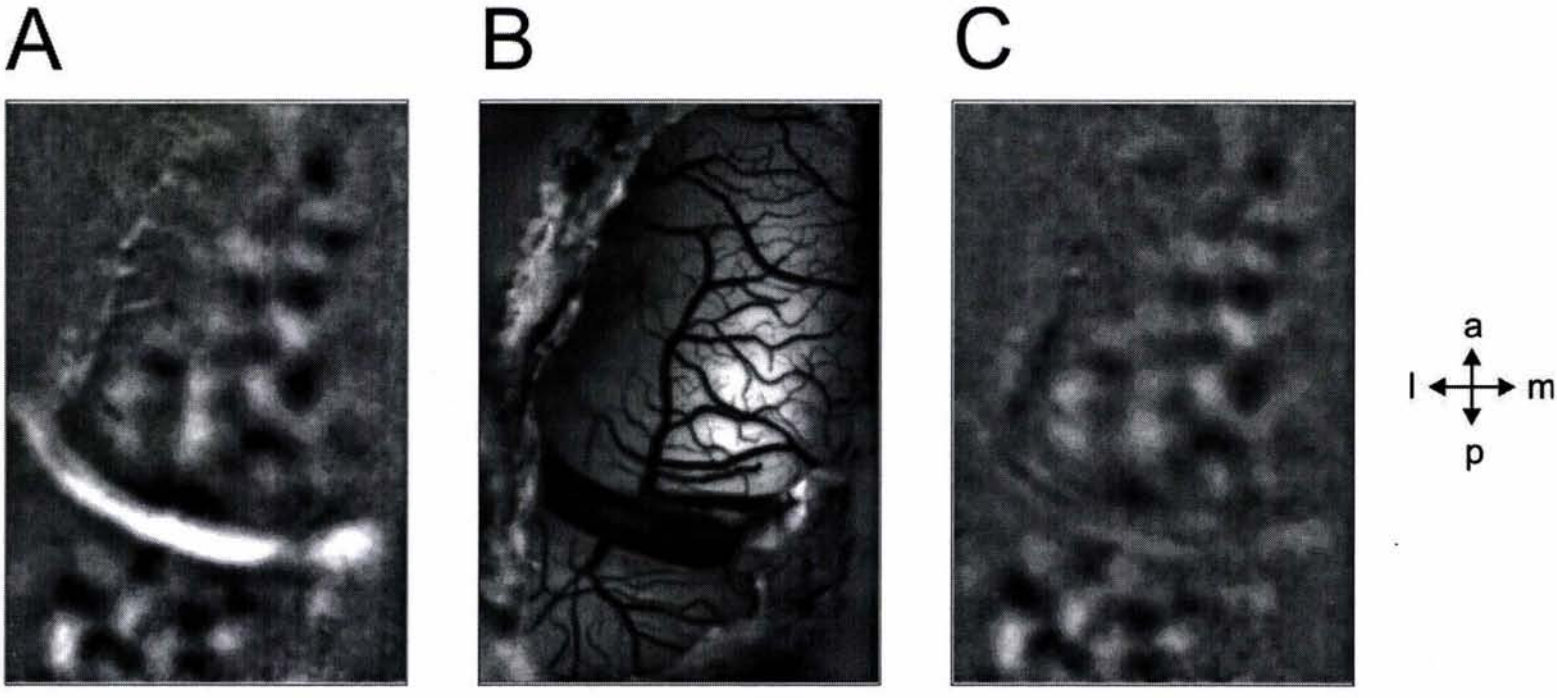

Fig. 3, Zepeda, Arias & Sengpiel

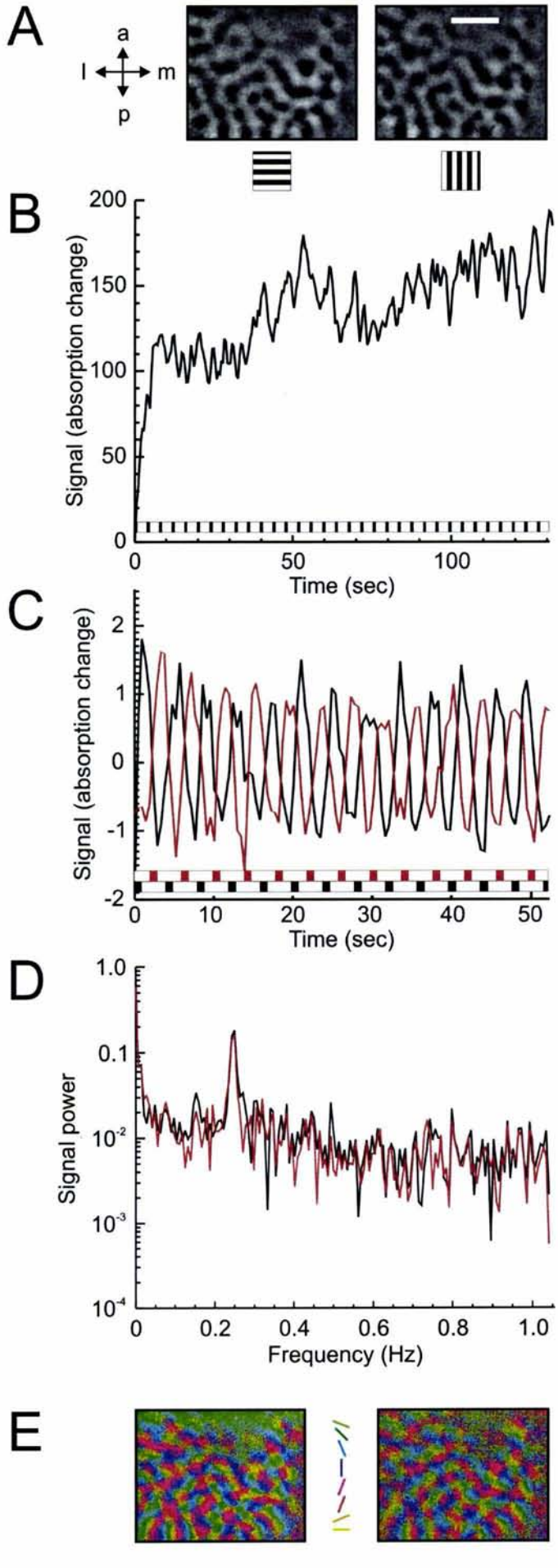

Fig. 4, Zepeda, Arias & Sengpiel

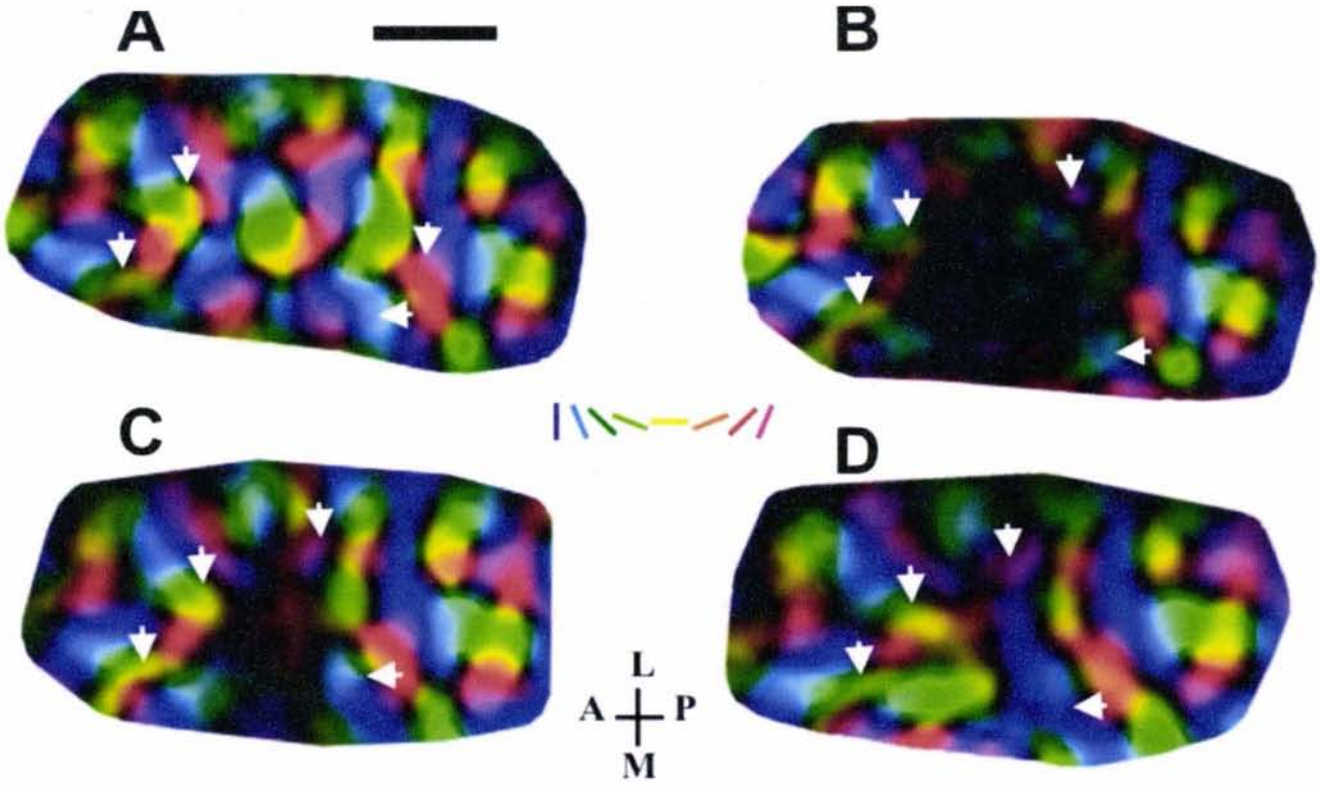

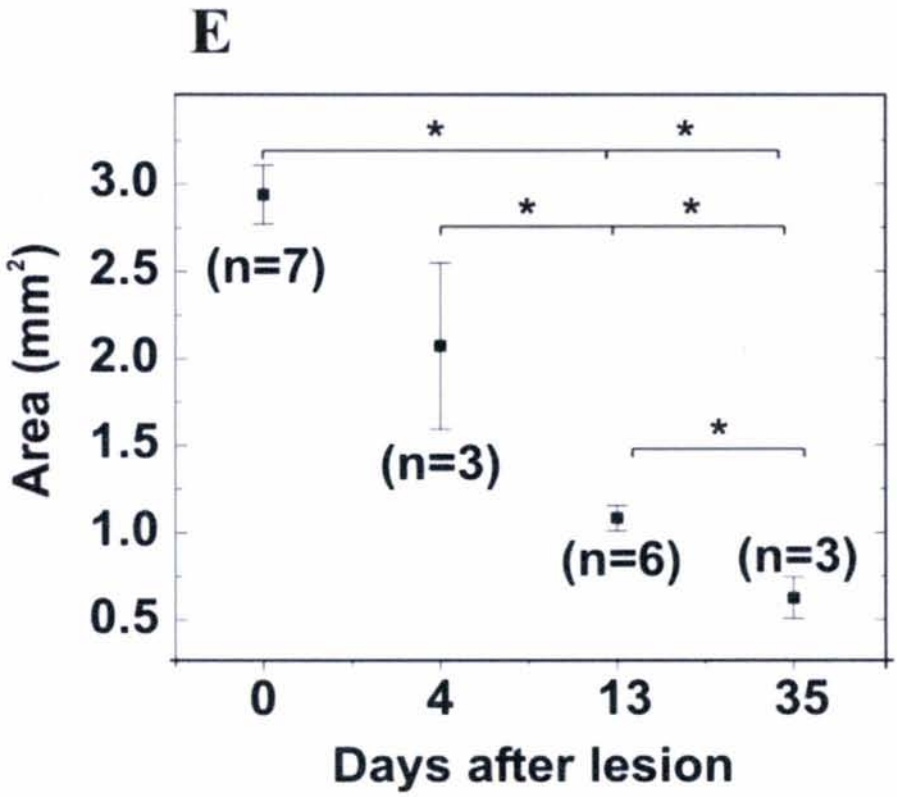

Fig. 5, Zepeda, Arias & Sengpiel

Figure legends

Figure 1
Relative energy budget of the cerebral cortex. Metabolic cost (in molecules of ATP) of resting potentials, synaptic transmission and action-potential propagation is shown (modified from Attwell and Laughlin, 2001). At a firing rate of 4 spikes/sec, just 13% of the ATP consumption of neural tissue (neurons and glial cells in approximately equal numbers) is due to maintaining resting potential, while almost half of the ATP consumption is expended on action-potential propagation. These figures refer to excitatory, glutamatergic neurons, which constitute about 80% of all neurons in the cortex.

Figure 2
Orientation preference maps obtained with event-related optical imaging.
A) Iso-orientation maps of cat area 17 obtained by dividing single-orientation responses by blank-screen responses. Stimulus orientation is indicated by the colored bar in the top left corner of each image. The images have not been filtered. They have been range-fitted identically, with a pixel value of 1.0 (response to grating equal to response to blank) represented by a gray-scale value of 255 (white) and a value of 0.988 (or lower) represented by a gray-scale value of 0 (black). The overall signal strength is therefore approx.1.2%. Note that each orientation causes a global response from the entire imaged region of visual cortex.
B) Iso-orientation maps obtained by dividing single-orientation responses by the "cocktail blank" (see text). The images have been high-pass filtered (filter width, 80 pixels = 1.7 mm) and range fitted (pixel values of 0 and 255, respectively, signify ±0.2% signal change compared with the cocktail blank).
C) Blood vessel pattern of the imaged region of cortex, imaged with green illuminating light through the intact dura. Area 17 of both hemispheres is visible; the arrows indicate the orientation (a, anterior; p, posterior). Scale bar, 1 mm.
D) Angle map of orientation preference, obtained by vectorial addition of the maps shown in (B) and subsequent low-pass filtering. The vector angle (preferred orientation) of each pixel is encoded as hue, as indicated by the color legend below.
E) Polar map of orientation preference, obtained by vectorial addition of the maps shown in (B) and subsequent low-pass filtering. The vector angle (preferred orientation) of each pixel is encoded as hue, as indicated by the color legend below (D), while the vector length is encoded as brightness.
F) Time course of reflection signal measured before and during presentation of a horizontal (0°) grating (stimulus duration = 4.2 sec, as indicated by horizontal bar below time axis). Six blocks of four trials each were recorded, using Imager 2001 (Optical Imaging Inc.) with 2x2 pixel binning. Each trial contained four stimuli of each of the four orientation, 0°, 45°, 90° and 135°. Within the activated region of cortex, we first selected those 25% of pixels responding most strongly to gratings of 0° orientation. We averaged the raw values on file for these pixels across the four 0° stimuli and then across the six data blocks; the value obtained for the first frame has been arbitrarily set to zero (black curve). The same calculation was repeated for those 25% of pixels responding most strongly to gratings of 90° (red curve). Error bars represent SEMs

across blocks. Note the magnitude of the non-orientation selective response component. (Actual signals represent reflectance and changes are negative, but for display purposes changes are shown as positive.)

Figure 3

Removal of blood vessel artifacts by means of linear extraction combined with principal component analysis

(**A**) Ocular dominance map obtained from kitten V1 by recording responses to drifting gratings of 0°, 45°, 90° and 135° through left and right eye separately and dividing the summed responses. A huge blood vessel artifact can be seen in the occipital part of the image. (**B**) Surface blood vessel pattern recorded with green (546 nm) illuminating light, showing clearly the vein that caused the large artifact in (A). (**C**) Following principal-component analysis of images obtained while the animal viewed a blank screen, components that showed the highest spatial correlation with the blood vessel pattern were selected and extracted from images obtained in the presence of grating stimuli (Schuett et al., 2000).

Figure 4

Orientation selective responses obtained with periodic stimulation.

A) Standard iso-orientation maps obtained from tree shrew area 17, using horizontal and vertical gratings respectively (see icons below maps). Scale bar, 1 mm.

B) Time course of raw signal during periodic stimulation. The stimulus was a drifting grating whose orientation advanced by 22.5° every 0.5 sec, such that a 180° cycle was completed every 4 sec. The reflectance signal was summed up over 25% of pixels that responded best to horizontal gratings in a region of interest defined on the basis of responses to standard stimulation (see **A**). The bar above the abscissa indicates when, during the continuous periodic stimulation, a horizontal grating was present.

C) Time course of temporally and spatially smoothed signal. Temporal smoothing was by subtraction of boxcar average of signal across one stimulus period, spatial smoothing by subtraction of boxcar signal average over a 200-by-200-pixel area (pixel width, 21.2 μm). Note that activity of pixels responding best to horizontal gratings (black curve) is in anti-phase with activity of those pixels responding best to vertical gratings (red curve). For greater clarity, only the first 50 sec are shown at an expanded time-scale compared with (B). The bars above the abscissa indicate when, during the periodic stimulation, a horizontal grating (black) or a vertical grating (red) was present.

D) Power spectrum of smoothed signal (black, pixels responding best to horizontal gratings; red, pixels responding best to vertical gratings). Note the peak of each spectrum at 0.25 Hz, corresponding to the stimulus cycling period of 4 sec.

E) Orientation preference maps obtained with 2 hours of standard event-related imaging (left) and 20 min of periodic stimulation (right). The standard orientation preference map is calculated by vectorial addition of iso-orientation maps in response to gratings of 0°, 45°, 90° and 135°; the resulting vector angle is plotted (see color code). The periodic stimulation map plots the phase angle of each pixel's response at the frequency of stimulation (0.25 Hz). The apparent difference in preferred orientation between the two maps of about 45° corresponds to the hemodynamic delay of cortical responses during periodic stimulation.

Figure 5

Temporal evolution of changes in orientation preference maps and lesion size following a focal ischemic lesion in kitten V1 (modified from Zepeda et al., 2003). (**A-D**) High

magnification of polar orientation maps of the imaged cortical area in one kitten (**A**) in the intact cortex (pre-lesion); (**B**) immediately post-lesion; (**C**) 13 days post-lesion (dPL) and, (**D**) 33 days post-lesion. Arrowheads point at domains which recovered after 13 dPL and enlarged by day 33 PL. Orientation of imaged cortical area is shown (a, anterior; p, posterior; m, medial; l, lateral). Scale bar: 1mm. (**E**) Reduction of functionally silent area obtained from polar maps during up to 5 weeks following the lesion. Each data point represents the mean ± SD of the silent area per time-group as assessed through imaging.

Journal of Cerebral Blood Flow & Metabolism
23:811–820 © 2003 The International Society for Cerebral Blood Flow and Metabolism
Published by Lippincott Williams & Wilkins, Inc., Baltimore

Reorganization of Visual Cortical Maps After Focal Ischemic Lesions

*†Angelica Zepeda, ‡Luis Vaca, †Clorinda Arias, and *§Frank Sengpiel

**Max-Planck-Institut für Neurobiologie, München-Martinsried, Germany; †Departamento de Biología Celular y Fisiología, Instituto de Investigaciones Biomédicas, Universidad Nacional Autónoma de México, and ‡Departamento de Biología Celular, Instituto de Fisiología Celular, Universidad Nacional Autónoma de México, México, DF, México; and §Cardiff School of Biosciences, Cardiff University, Museum Avenue, Cardiff, UK*

Summary: Plasticity after central lesions may result in the reorganization of cortical representations of the sensory input. Visual cortex reorganization has been extensively studied after peripheral (retinal) lesions, but focal cortical lesions have received less attention. In this study, we investigated the organization of retinotopic and orientation preference maps at different time points after a focal ischemic lesion in the primary visual cortex (V1). We induced a focal photochemical lesion in V1 of kittens and assessed, through optical imaging of intrinsic signals, the functional cortical layout immediately afterwards and at 4, 13, 33, and 40 days after lesion. We analyzed histologic sections and evaluated temporal changes of functional maps. Histological analysis showed a clear lesion at all time points, which shrank over time. Imaging results showed that the retinotopic and orientation preference maps reorganize to some extent after the lesion. Near the lesion, the cortical retinotopic representation of one degree of visual space expands over time, while at the same time the area of some orientation domains also increases. These results show that different cortical representations can reorganize after a lesion process and suggest a mechanism through which filling-in of a cortical scotoma can occur in cortically damaged patients. **Key Words:** Ischemia—Injury–Imaging techniques—Plasticity—Cat—Retinotopy.

Cortical maps represent numerous aspects of sensory information about the outside world in a dynamic mosaic, which has been shown to change under different circumstances. In particular, lesion studies have provided important information regarding plasticity of cortical maps and have shown that damage to the cortical body surface representation often leads to the remodeling of the spared representational zones surrounding the lesion (Doetsch et al., 1990; Nudo et al., 1996).

Responses of cortical neurons depend on the inputs that they receive from the thalamus as well as on those from neurons within their local network. Therefore, lesion-induced changes observed in cortical sensory maps may rely on remodeling of thalamic inputs (Jones and Pons, 1998) and intrinsic cortical connections (Darian-Smith and Gilbert, 1994; Jones, 2000). Modifications of motor and somatosensory maps in response to focal cortical lesions have been extensively studied (Coq and Xerri, 1999; Doetsch et al., 1990; Nudo et al., 1996), as opposed to the effects of focal visual cortex lesions, which have received little attention (Eysel and Schweigart, 1999; Schweigart and Eysel, 2002).

The primary visual cortex is characterized by a columnar functional organization and contains a number of orderly maps of visual stimulus properties (Hubel and Wiesel, 1974; Hübener et al., 1997), such as the retinotopic and the orientation preference map.

Reorganization of the cortical retinotopic representation has been extensively explored after retinal lesions (Kaas et al., 1990) and more recently after cortical lesions (Eysel and Schweigart, 1999), whereas reorganization of orientation preference maps has not been explored after either of these procedures.

Previous studies investigating the consequences of primary visual cortex (V1 or area 17) lesions have been mainly concerned with behavioral compensation and reorganization in other visual cortical areas (Illig et al., 2000; MacNeil et al., 1996; Orban et al., 1990; Payne

Received January 27, 2003; final version received April 14, 2003; accepted April 16, 2003.

F.S. was supported by the Max-Planck-Gesellschaft and the Medical Research Council. C.A. was partially supported by CONACyT (Project 36250M). A.Z. was in part supported by Deutscher Akademischer Austausch Dienst, Graduierten-Kolleg München and CONACyT, Mexico.

Address correspondence and reprint requests to Angelica Zepeda, Departmento de Biología Celular y Fisiología, Instituto de Investigaciones Biomédicas, Universidad Nacional Autónoma de México, AP 70228, 04510-México, DF, México; e-mail: azepeda@biomedicas.unam.mx

DOI: 10.1097/01.WCB.0000075010.31477.1E

and Lomber, 2002; Spear et al., 1988; Vandenbussche et al., 1991). Only one study has analyzed the effects of a focal visual cortical lesion on the damaged cortical area itself, showing changes in receptive field size of neurons outside the lesion (Eysel and Schweigart, 1999). This study provided information regarding modifications in the receptive fields of single cells in the surrounding of a cortical lesion. However, an imaging analysis evaluating the reorganization of visual cortex maps and the temporal evolution of such a process has not been performed.

The aim of the present work was to address whether the cortical retinotopic representation and the orientation preference maps reorganized with time in areas adjacent to a focal ischemic lesion and to establish a temporal correlation between functional and morphologic lesion size.

We induced a focal photochemical lesion in V1 of kittens and visualized retinotopic and orientation preference maps by optical imaging of intrinsic signals before the lesion, immediately afterwards, and after survival times of 4, 13, 33, and 40 days. At each of these time points, animals were killed and histologic analysis was performed.

SUBJECTS AND METHODS

The experiments were performed on 9 kittens (6–10 weeks old) bred in colonies; all procedures were carried out in accordance with local government rules.

Seven kittens were subjected to optical imaging experiments before lesion and at several times afterwards; two additional kittens received a lesion and were killed 4 days later, without imaging (Table 1). Thus, except for the 40 days postlesion time point, we obtained imaging and histologic data from at least 3 animals per time point.

Before and after the lesion, kittens were housed in a laboratory environment with a 12:12-hour artificial light–dark cycle. They lived within a colony of cats and did not receive any specific training or treatment at any time.

TABLE 1. *Number of kittens used in the present study*

Kitten number	Optical imaging sessions after lesion (days)	Killed (day)
01	0–13–33–40	40
02	0–13	13
10	0–13–33	33
13	0–4–13	13
17	0–4–13	13
35	0–4	4
41	0–13–33–40	40
50	—	4
51	—	4

All nine kittens received a lesion; seven were imaged prior to the lesion and at different time points postlesion (middle column, 0 means "immediately after the lesion"). The right column shows the day postlesion when the animals were killed.

Optical imaging of intrinsic signals

Surgery and optical imaging techniques have been described in detail elsewhere (Bonhoeffer and Grinvald, 1993; Bonhoeffer and Grinvald, 1996). All procedures were performed under sterile conditions. Animals were anesthetized intramuscularly with ketamine (20 to 40 mg/kg) and xylazine (Rompun, Bayer, Leverkusen, Germany, 2 to 4 mg/kg) and then intubated. They were placed in a stereotaxic frame and were artificially respired with a mixture of 60% N_2O and 40% O_2 with 0.7% to 1.5% halothane. Electrocardiogram, expired CO_2, and body temperature were monitored throughout the experiment. A 4% glucose in saline solution was infused intravenously at 3 $mL \cdot kg^{-1} \cdot h^{-1}$ throughout the experiment. To prevent eye movements, the infusion solution was supplemented with a fast-acting muscle relaxant, atracurium (Tracrium, GlaxoWellcome, Munich, Germany, 0.6 $mg \cdot kg^{-1} \cdot h^{-1}$).

In the initial imaging session, the scalp was incised and retracted. A circular craniotomy was performed above area 17 (centered on P4, Horsley-Clarke coordinates), and a titanium chamber was cemented onto the skull. The chamber was filled with silicon oil and was sealed with a glass coverslip.

Animals were fitted with contact lenses to focus their eyes on a computer screen at a distance of 33 cm. For imaging of orientation preference maps, visual stimuli (VSG Series Three, Cambridge Research Systems, Rochester, UK) consisted of high-contrast square-wave gratings of 0.15 to 0.5 cycles/degree, drifting back and forth at 2 cycles/s and presented at 4 different orientations (0, 45, 90, and 135°).

For retinotopic stimulation, we presented drifting high-contrast square-wave gratings of 1 cycle/degree oriented at 0° or 90° within a 1°-wide horizontal aperture. Stimuli were presented in random order at 11 positions separated by 1°, from an elevation of 5° above to 5° below the horizontal meridian.

For both stimulation protocols, each stimulus lasted 3 seconds (data consisted of 5 frames of 600-millisecond duration) and was followed by a 9-second interstimulus interval during which the next stimulus was displayed but remained stationary. For the analysis, the first frame (after the onset of drift) was discarded.

For intrinsic-signal imaging, the cortex was illuminated with bandpass-filtered light of 707 ± 10 nm. At this wavelength, much of the intrinsic signal derives from increased light scatter of active brain regions, as opposed to the deoxy- versus oxyhemoglobin (oximetry) signal that dominates at wavelengths just above 600 nm. The increase in light scatter is caused by ion and water movement during neural activity and is therefore correlated more closely with electrical activity both in time course and spatial extent (Bonhoeffer and Grinvald, 1996). Responses to visual stimulation were captured by a cooled slow-scan CCD camera focused 500 μm below the cortical surface (ORA 2001, Optical Imaging, Germantown, NY, U.S.A.).

A control optical imaging experiment was carried out immediately before the photochemical lesion. A second recording session was conducted immediately after the lesion ($n = 7$), and subsequent experiments were carried out 4 ($n = 3$), 13 ($n = 5$), 33 ($n = 3$), and 40 ($n = 2$) days after lesion (Table 1).

After all but the final experiment, the chamber was half-filled with agar containing antibiotic (Paraxin, Bayer); the rest of the chamber was filled with silicone oil and sealed with a glass coverslip. Anesthesia was suspended; kittens were allowed to recover and were then returned to their mother and littermates.

Photochemical lesion

We used the photochemical lesion technique initially described by Watson et al. (1985) with some variations. We found

that removal of the dura from the exposed cortical region was a requirement for the lesion to succeed. The cortical surface was carefully cleared and kept free from any traces of blood using Sugi sterile swabs (Kettenbach, Eschenburg, Germany). A krypton/argon 514-nm laser beam (Ion Laser Technology, Frankfort, IL, U.S.A.) light guide positioned 5 cm above V1 was directed towards the area of the cortex where the ischemic lesion was to be produced. Rose bengal dye, 10 mg/kg (Sigma, St. Louis, MO, U.S.A.), was injected during a 2-minute interval through the femoral vein; the cortex was illuminated simultaneously and for the next 12 minutes. The parameters ensured vascular occlusion in an area of approximately 3 mm (see Results).

Image analysis

Retinotopic and orientation preference maps

For producing retinotopic maps, signal averaging across 48 stimulus presentations was performed. Single condition maps elicited by orthogonal orientations (0° and 90°) at each of the 11 stimulus positions were divided by each other to obtain the response to the respective position.

For producing orientation preference maps, signal averaging across 128 to 192 stimulus presentations was performed. Iso-orientation maps were produced by dividing single condition maps by the "cocktail blank," which consists of the sum of the images obtained in response to all four orientations (Bonhoeffer and Grinvald, 1993; Bonhoeffer and Grinvald, 1996). Twelve-bit digitized camera images were range-fitted such that the 1.5% most responsive pixels were set to black, and the least responsive were set to white. Signal amplitude was displayed on an 8-bit gray scale. "Polar" maps resulting from vectorial addition of the four iso-orientation maps were calculated (Bonhoeffer and Grinvald, 1993). The vector angle was displayed as hue; the length of the vector was encoded additionally as the brightness of the colors.

Measures of functional lesion

The area devoid of response to all four orientations in the polar maps was selected and measured using Scion Image (Scion Corp., National Institutes of Health, U.S.A.). These measurements were repeated for every kitten at each time point after the lesion and the mean ± SD was calculated. One-way analysis of variance (ANOVA) was performed to assess differences between "time post-lesion" groups.

Measures of retinotopic representation

Analysis of retinotopic representation was performed at each time point for every kitten, using IDL software (RSI, Boulder, CO, U.S.A.). We determined the cortical area for each stimulus position where a response above a fixed threshold (identical between stimuli and experiments) was observed, and calculated the number of pixels for which an above-threshold response was obtained for neighboring stimulus positions. The extent of "overlap" in the responses to abutting stimuli was taken as a measure for the divergence in the retinocortical projection, or in other words, as an indicator of the aggregate receptive field size.

Measures of orientation domains

Response area analysis was performed at each time point for every kitten, using routines written in IDL. Measures of the area of identical iso-orientation domains were done at all time-points and only those domains appearing in all imaging sessions in each subject were compared intrasubject. One-way ANOVA followed by a *post hoc* Scheffe test was performed to evaluate changes in area of identical domains measured at different time-points. Results represent the mean area (± SD) of the pooled data. Measures were based on the gray-scale values of pixels in the image obtained after high-pass filtering.

Histology and immunohistochemistry

On completion of the final imaging session (Table 1), animals received an overdose of barbiturate and were perfused transcardially with 0.9% saline followed by chilled 2% paraformaldehyde fixative in phosphate buffer. Brains were removed and postfixed at 4°C for 4 days and were then successively transferred to sucrose solutions (up to 30%). Serial 30-μm sections were cut at the level of the lesion on a cryostat and were processed for (1) cresyl violet (Nissl) staining, (2) cytochrome oxidase histochemistry, or (3) immunohistochemically for cow anti-rabbit glial fibrillary acidic protein (Dako, Carpinteria, CA, U.S.A. 1:1,000) using Vector Elite AVE kit (Vector, Burlingame, CA, U.S.A.) and diaminobenzidine (Sigma) as the final reaction product.

Volumetric measurements and reconstruction of the lesion

All Nissl sections containing an area of photochemically damaged tissue were used to calculate the volume of the lesion. Nissl sections were 30 μm thick and were separated by 45 μm. Serial sections were placed under a transilluminator (Northern Light, Quebec, Canada), and images of the lesion were acquired through a CCD camera (NEC, Santa Clara, CA, U.S.A.) attached to a computer. The area of the lesion in each Nissl section was measured using the Scion Image Software (Scion Corp., U.S.A.) and total volume lesion (*Vol*) was calculated as follows:

$$Vol = \sum^{n} [(As)(T) + (As)(K)]_i \quad (1)$$

where As = area of lesion in one Nissl section, T = thickness of Nissl section (30 μm), K = tissue separating adjacent Nissl sections, and n = number of sections that contain the lesion.

These measurements were done for every brain, and the means ± SD were calculated. One-way ANOVA was performed to assess differences between groups killed at different time points.

All digitized images from Nissl sections were aligned using Image J (National Institutes of Health), and the three-dimensional reconstruction was rendered in two orientations (coronal and dorsal) using VolumeJ. Volumes from the reconstructed data were obtained with custom routines written with OpenDX (IBM), and were not statistically different from those obtained using Eq. 1.

RESULTS

Photochemically induced cortical lesion

The morphology of the lesion as assessed through cresyl violet staining is shown in Fig. 1a. These sections showed a well-delimited conical lesion area (extending from layer I to layer VI), composed of pyknotic nuclei and surrounded by anisomorphic astroglia (Fig. 1a, 1b, and 1d). The core and glial scar of the lesion were evident at all time points. However, the volume of the lesion decreased over time (see following paragraphs).

To compare the area of dead cells, as shown by pyknotic nuclei, with the region of metabolically inactive cells, we performed a cytochrome oxidase reaction (Fig.

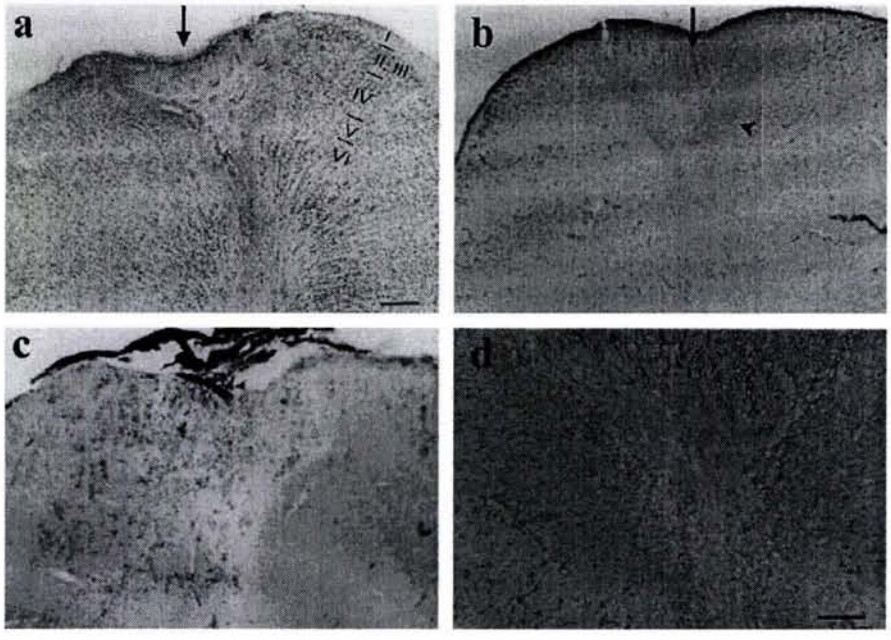

FIG 1. Histologic verification of a photochemical lesion. Coronal sections of V1 from a kitten killed 13 days after lesion. **(a)** Nissl stain delineates the area containing pyknotic nuclei (arrow). **(b)** Glial fibrillary acidic protein immunohistochemistry shows the core of the lesion devoid of glia (arrow) and the gliotic tissue surrounding the core (arrowhead). **(c)** Cytochrome oxidase reaction shows the metabolically inactive region. **(d)** High-power image of gliotic scar [square in (b)]. Scale bars (a–c) = 0.2 mm, (d) = 0.1 mm.

1c). We found a close correlation between the area occupied by pyknotic nuclei and the region devoid of metabolic activity at all time points.

The functional area of the lesion as defined by the absence of orientation domains or retinotopic activity, was not significantly different among subjects imaged at the same time points. However, it decreased significantly with time in all subjects. The average area of the lesion measured from polar orientation maps was ($mm^2 \pm SD$) 2.92 ± 0.16 immediately after the lesion ($n = 7$), 2.05 ± 0.4 at 4 days after lesion (dPL) ($n = 3$), 1.06 ± 0.07 at 13 dPL ($n = 5$), and 0.61 ± 0.11 at 33 dPL ($n = 3$) (Fig. 2 and Fig. 3a and 3c). In addition, the volume of the lesion obtained from histologic sections decreased in parallel to the functional lesion, from ($mm^3 \pm SD$) 2.87 ± 0.33 at day 4, 0.87 ± 0.08 at day 13 to 0.39 ± 0.02 at day 33 (Fig. 3b, 3d). One-way ANOVA showed statistically significant differences ($P < 0.05$) in the reduction of functional and anatomic lesion area from day 4. Although there was a reduction of functional area from day 0 to day 4, it was not significant.

Effects of the photochemical lesion on the orientation preference maps

Before inducing the lesion, orientation maps of the explored cortical area had the typical appearance of iso-orientation domains arranged around pinwheel centers (Fig. 2a). Immediately after the photochemical lesion, a circumscribed area of the functional layout of the cortex appeared disrupted, causing the disappearance of neuronal activity in an area of 3 mm^2 (Fig. 2b). Domains just outside the silenced zone showed a decrease in area, but they recovered their original prelesion area by 13 dPL, (Fig. 2a–c and Fig. 4a–c, 4e, 4f). The area of some of these domains was increased further at 33 dPL when compared to the same domains measured prelesion, immediately after lesion, and at 13 dPL (Fig. 4a–d, 4f), whereas others did not change from 13 to 33 dPL (Fig. 4a–e). In contrast, the average area of domains not affected immediately after the insult (those further away from the lesion center) did not change significantly at any time point (Fig. 4a–d, 4g). In no case could emergence of new pinwheel centers be detected. These results show that after an ischemic insult some orientation preference domains, which were in closest proximity to the original lesion, not only recovered fully but increased in size by 33 dPL.

Effects of the photochemical lesion on the retinotopic maps

Typically, we found that before the lesion, two adjacent stimuli of 1° width each were sufficient for together eliciting responses in the complete imaged cortical area (4.42×3.32 mm^2). The more dorsal ("upper") stimulus evoked responses in the more posterior part and the more ventral ("lower") stimulus responses in the more anterior part of the imaged region (Fig. 5a, c, d). In the example shown, the area of overlap between the two stimulus representations was 0.93 mm^2 prelesion (Fig. 5e and 5f). Immediately after the photochemical lesion, the "upper" stimulus elicited activity only in the most posterior part of the imaged cortex, whereas the "lower" one evoked responses only in the most anterior region. Thus, there was virtually no overlap between the two stimulus representations (Fig. 5e and 5f). At 13 dPL, the cortical area covered by each of the stimuli was enlarged: the lesion

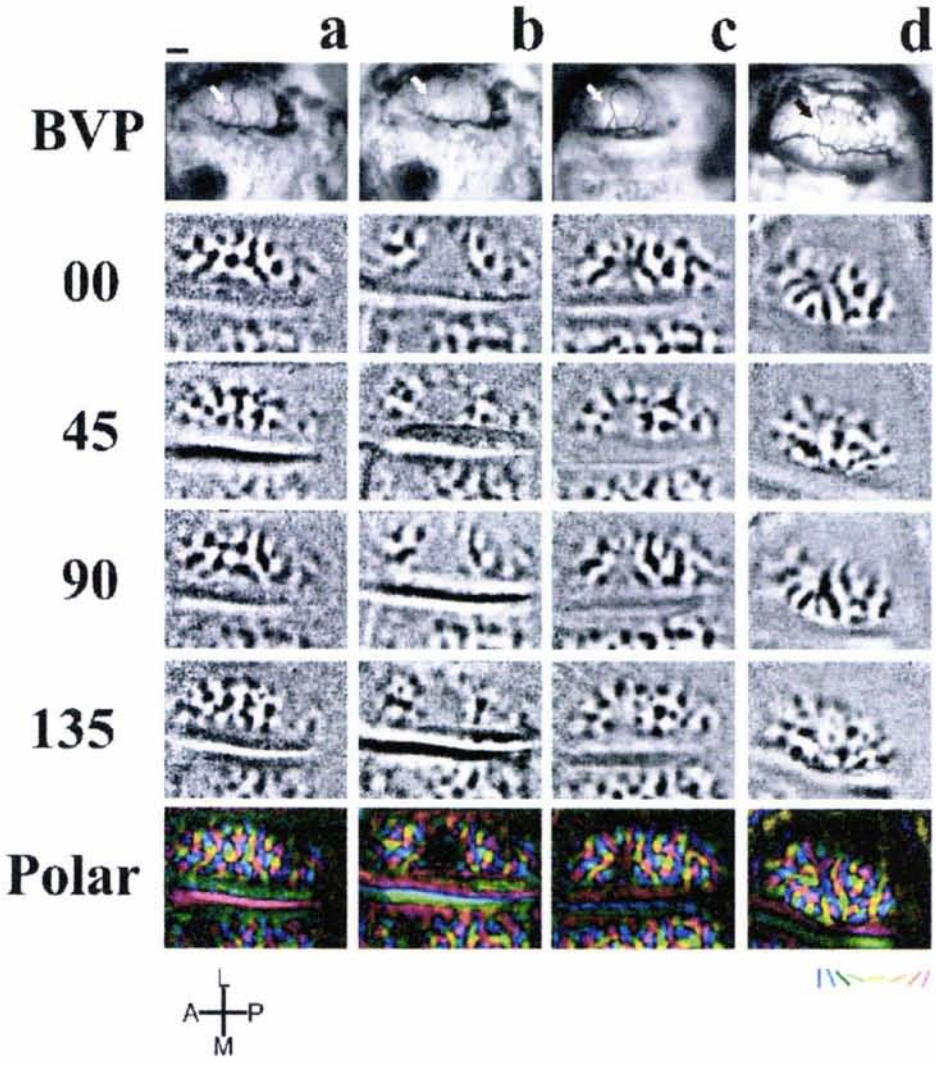

FIG 2. Temporal follow-up of blood vessel pattern (BVP) and orientation preference maps. **(a)** Before the lesion; **(b)** immediately after the lesion; **(c)** 13 days after lesion; and **(d)** 33 days after lesion. Iso-orientation maps in response to gratings of 0, 45, 90, and 135° are shown as well as polar maps (see Subjects and Methods). Orientation of imaged cortical area is shown (a, anterior; p, posterior; m, medial; l, lateral). Note the recovery of domains at 13 days after lesion, the reorganization of the blood vessel pattern (arrows) and the shrinkage of the functionally silent area. Scale bar = 1 mm.

area remained inactive, but each stimulus evoked responses in a larger cortical area, and an overlap zone of 0.24 mm^2 of common activation was observed (Fig. 5e, f). The extent of cortical response evoked by each of the stimuli continued to grow in size, such that at 33 dPL the area of overlapping activation covered 0.46 mm^2 and 0.59 mm^2 at 40dPL (Fig. 5e–f). These results show that after a focal ischemic lesion, the retinotopic map reorganizes to some extent as the area responding to a stimulus of a given size increases, overlapping with adjacent, previously unresponsive areas. In other words, clusters of neurons near the lesion will respond to stimulation in an enlarged portion of the visual field, i.e., their aggregate receptive field size will have increased.

DISCUSSION

In the present study, we report functional reorganization at the borders of a focal ischemic lesion in the cat visual cortex within 5 weeks of recovery, in the absence of any training.

The visual cortex is arranged in columns, which are spatially and functionally interrelated. Given the retinotopic organization of V1, all the features in each point of the visual world must be represented and analyzed in a defined region of cortex, the so-called "hypercolumn" (Hubel and Wiesel, 1974).

The disruption or loss of one or more hypercolumns leads to the perception of a blind spot in the visual field (cortical scotoma). It has been shown that such scotomas can diminish over time after training, or to a lesser degree without, in adult humans (Kasten et al., 1998; Zihl and von Cramon, 1985).

Our results suggest a mechanism by which the reduction of the visual scotoma may occur. The "normal" overlap in cortical activation by two adjacent points in the visual field disappears after a focal lesion. However, the cortical area involved in the processing of information from one point in the visual field enlarges with time in such a way that areas initially not involved in the processing of information of that point in space now become activated.

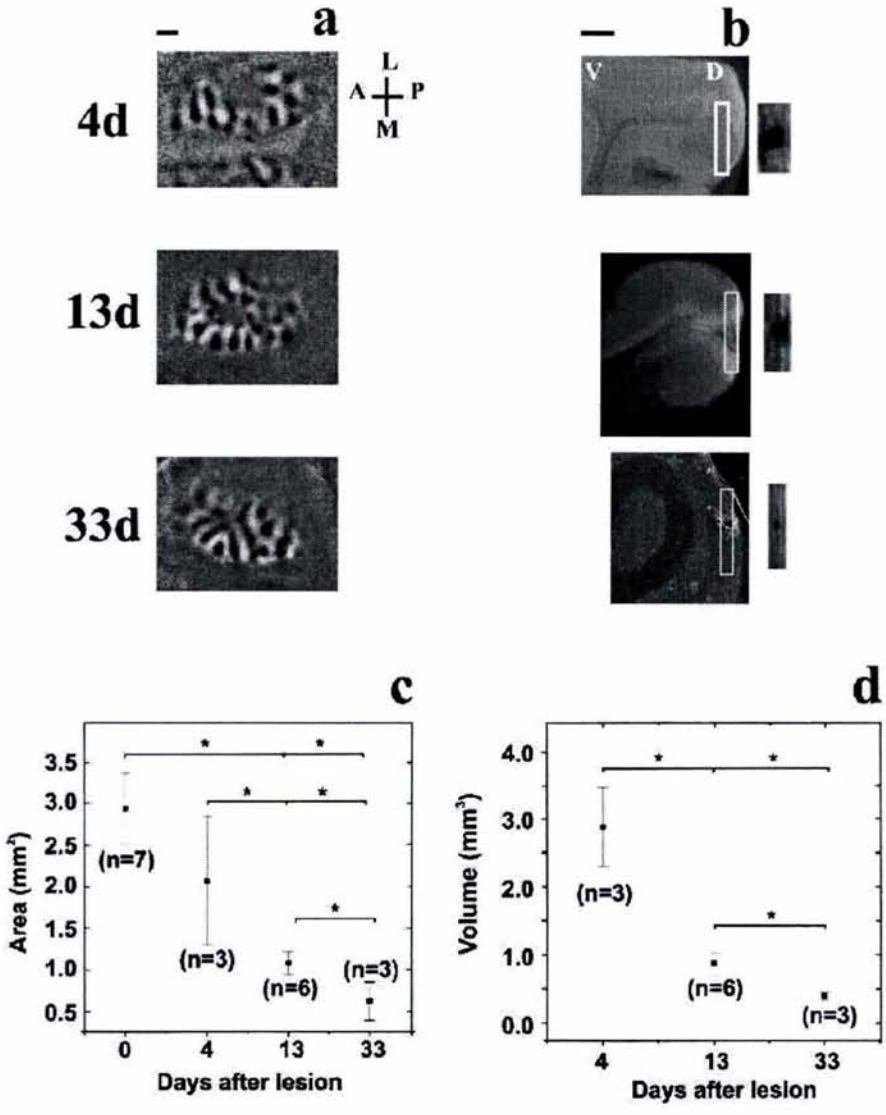

FIG 3. Functional and anatomic correlates of the decrease in size of the lesions through time. **(a)** Zero-degree iso-orientation domains obtained at 4, 13, and 33 days after lesion from three different kittens killed on the respective days. Orientation of imaged cortical area is shown (a, anterior; p, posterior; m, medial; l, lateral). **(b)** Volumetric reconstruction of the lesion from the same cats. **Left:** Projections from Nissl-stained coronal sections containing the ischemic lesion within the rectangle (V = ventral, left; D = dorsal, right); **right:** dorsal view of lesion shown on left, reconstructed from series of coronal sections. **(c)** Reduction of functionally silent area obtained from polar maps. Each data point represents the mean ± SD of the silent area per time-group as assessed through imaging. **(d)** Reduction of lesion volume obtained from serial Nissl sections. Each data point represents the mean ± SD. In (c) and (d), n is the number of kittens in each group. Asterisks denote a significant difference ($p < 0.05$). Scale bars in (a) and (b) = 1 mm

Our results are in agreement with recent results from Eysel and Schweigart (1999), who report that 55 days after an excitotoxic lesion in cat V1, the receptive fields of cells surrounding the lesion were, on average, significantly enlarged. The technique used in the present study allowed us to monitor over time the responses of much larger groups of neurons, thus painting a more representative picture than that obtained through the recording of single neurons.

We show that a focal cortical lesion may also lead to the reorganization of the orientation preference map. Analysis of individual domains in the orientation maps revealed a two-step recovery process. First, some domains, which were immediately affected by the insult, recovered after 13 dPL. As has been previously suggested, this may rely on the metabolic reactivation of surviving cells after the ischemic shock (Sharp et al., 2000). The second process, which was observed at 33 dPL, involved the enlargement of previously existing domains and reflects a partial reorganization of the orientation preference map. At this time point, we observed some revascularization of the damaged zone only in some animals. Thus, even though perfusion could contribute to the cascade of events involved in the reorganization process, it does not seem to be a necessary condition for it to occur. The enlargement of cortical retinotopic representations and orientation domains observed in this study could represent a plastic mechanism common to different cortical areas (Doetsch et al., 1990; Eysel and Schweigart, 1999; Nudo et al., 1996). Therefore, our results suggest that mechanisms of cortical plasticity not only allow the reorganization of a topographic map but also of a stimulus feature map.

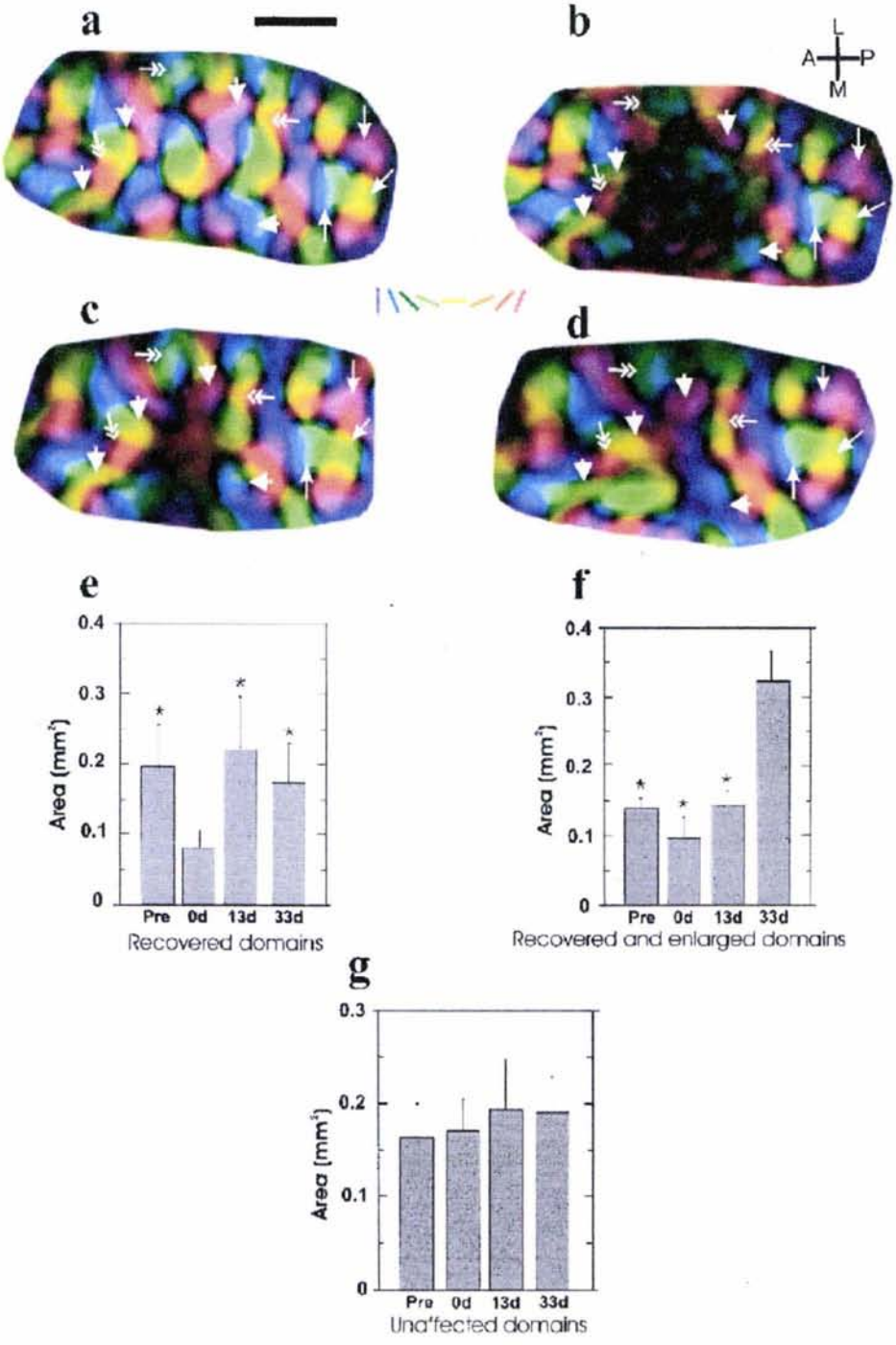

FIG 4. Temporal evolution of changes of orientation preference maps. (a-d) High magnification of polar maps of the imaged cortical area in one kitten **(a)** in the intact cortex (prelesion); **(b)** immediately after lesion; **(c)** 13 days after lesion; and **(d)** 33 days after lesion. Double arrows point at domains that recovered by 13 days after lesion (dPL), but which were not enlarged by day 33PL. Arrowheads point at domains that recovered after 13 dPL and enlarged by 33 dPL, arrows point at domains which were not affected by the lesion and whose area did not change over time. Orientation of imaged cortical area is shown (a, anterior; p, posterior; m, medial; l, lateral). **(e)** Area (mean ± SD) of domains whose area was reduced immediately after the lesion (0d) and recovered within 13 days; asterisk denotes a significant difference ($P < 0.05$) with respect to 0d. **(f)** Area (mean ± SD) of domains whose area changed by 33 dPL. Asterisk denotes a significant difference ($P < 0.05$) with respect to 33 dPL. **(g)** Area (mean ± SD) of domains that were unaffected by the lesion. Scale bar = 1 mm.

It is difficult to know why only some domains at the border of the original lesion expand, whereas others maintain their original size. It might simply reflect an anisotropy of the contraction of the scar. However, differential expansion of functional domains has been described previously in somatosensory cortex of enucleated animals (Bronchti et al., 1992; Rauschecker et al., 1992) and in subjects that had undergone whisker cauterization (Woolsey and Wann, 1976).

Plasticity of orientation preference maps has been well documented (Schuett et al., 2001; Sengpiel et al., 1999). However, despite this potential for experience-dependent modification of neuronal responses, the general layout of orientation maps seems remarkably robust. We, too, did not observe changes with respect to the number and position of pinwheel centers in the reorganizing visual cortex surrounding a focal lesion; therefore, any recovery appears to be limited to a resto-

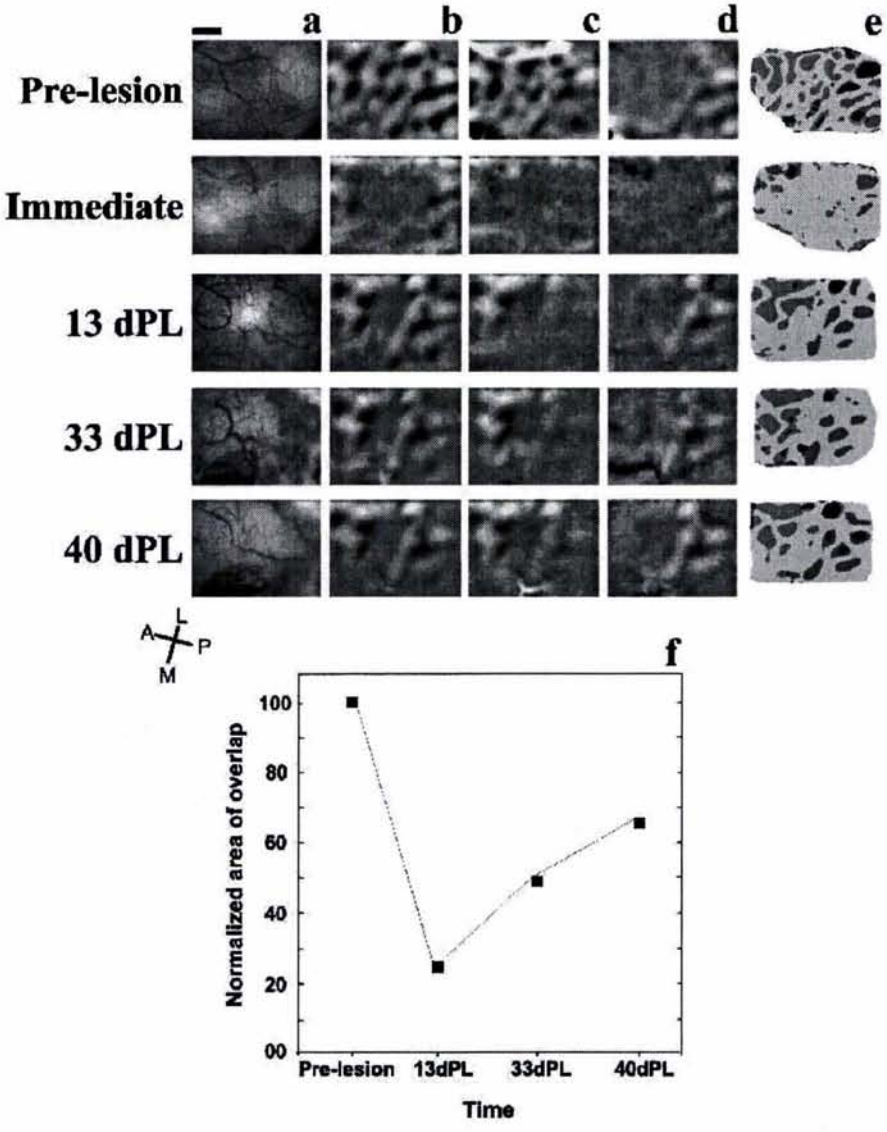

FIG 5. Longitudinal development of blood vessel patterns (BVP) and retinotopic maps in one kitten. **(a)** BVP; **(b)** iso-orientation maps in response to gratings of 0°; **(c)** retinotopic map in response to a 1°-wide stimulus oriented at 0°; **(d)** retinotopic map in response to 1°-wide stimulus oriented at 0°, adjacent to stimulus presented in (c); **(e)** overlap between responses in (c) and (d): light gray domains correspond to active zones in (c), dark gray domains correspond to active zones in (d), and black zones correspond to active areas in both (c) and (d), the "overlap." Note that the overlapping area disappears immediately after the lesion, but it gradually recovers over time. Orientation of imaged cortical area is shown (a, anterior; p, posterior; m, medial; l, lateral). **(f)** Normalized area of overlap (prelesion = 100) in the response to adjacent stimuli (dPL, days postlesion). Scale bar = 1 mm.

ration of responses that are very similar to those before the lesion.

The present work did not address the possible cellular mechanisms underlying the reorganization of the functional maps. However, plastic mechanisms involved in reorganization within the visual system are likely to depend on the level of the lesion. It has been suggested that early and long-term topographic remodeling of the visual cortex after *retinal* lesions (Gilbert and Wiesel, 1992; Kaas et al., 1990) is due to spared viable circuits providing cross-connectivity within the reorganized area (Calford et al., 1999), to functional reconnection at the level of the lateral geniculate nucleus (Eysel, 1982) and, to a greater extent, to axonal sprouting of lateral connections (Darian-Smith and Gilbert, 1994, 1995).

Several recent studies (Carmichael and Chesselet, 2002; Li et al., 1998; Stroemer et al., 1995) also describe axonal and dendritic sprouting in the border of ischemic *cortical* lesions. Axonal sprouting has been correlated with functional recovery (Stroemer et al., 1995) and has also been linked to enhanced synchronous neuronal activity in perilesion cortex (Carmichael and Chesselet, 2002). Another mechanism likely to contribute to the observed reorganization of functional maps is the increased propensity for synaptic long-term potentiation at the border of focal cortical lesions both in the somatosensory cortex (Hagemann et al., 1998) and in the visual cortex (Mittmann and Eysel, 2001). Experiments addressing modifications in cytoskeletal proteins and in the excitatory/inhibitory balance in our lesion model are currently being undertaken in our laboratory (A.Z. and C.A.).

Together with the observed functional changes, histologic results showed that the lesion, consisting of an area

of pyknotic nuclei surrounded by anisomorphic astroglia, diminished over time. The temporal evolution of the histologic lesion in this study may be the result of a very localized and reproducible stroke induced by the photochemical procedure described here. This contrasts with other studies where functional deficits recovered within the penumbra area, while the structural lesion grew (Baird et al., 1997; see Dirnagl et al., 1999). The discrepancy may be the result of the focal lesion produced by our protocol, whereas in the above-mentioned studies, the initial lesion was extensive and not well defined.

It should be borne in mind that experiments described here were performed on kittens 8 to 12 weeks of age, within the latter part of the critical period of visual cortical plasticity during which manipulations of visual experience have the greatest effect on cortical representations of the visual input. Research on the molecular correlates of this increased susceptibility and on the reasons for its termination is still ongoing (for reviews see Katz, 1999; Sengpiel and Kind, 2002). Previous studies on visual cortical reorganization after more extensive lesions have shown that the scope for functional recovery in young animals is far greater than in adults (Payne and Lomber, 2002). This would suggest that the extent of recovery we observed in kitten visual cortex might represent an upper limit, unless the ability of the cortex to compensate focal lesions is not age dependent. Indeed, some functional reorganization of receptive fields after cortical lesions has been observed in adult cats, both within the first few days after the lesion (Schweigart and Eysel, 2002) and after 2 months of recovery (Eysel and Schweigart, 1999). This reorganization appears to be due to lesion-induced increases in excitability at the border of the lesion (Schweigart and Eysel, 2002).

One can only speculate as to why cortical reorganization is not more extensive in our model. It is possible that photochemical lesions (as opposed to thermal coagulation) do not allow synchronous neuronal activity to develop in the perilesion cortex, which appears to be a prerequisite for axonal sprouting (Carmichael and Chesselet, 2002). Furthermore, repeated anesthesia, which can prevent visual cortical plasticity during the critical period (Rauschecker and Hahn, 1987), may have also interfered with synaptic modifications necessary for a more extensive cortical reorganization. Finally, the ability to reorganize after lesions may simply be lower in the visual than in the motor or somatosensory systems. This is certainly true for peripheral nerve lesions, and it might also hold for the respective cortical areas.

The present results show that functional plasticity of retinotopic and orientation preference maps occur after a focal cortical lesion in V1. Reorganization of such representations suggests a mechanism by which the "filling in" process may occur, and may be the basis of functional recovery after a cortical scotoma in patients.

Acknowledgments: We thank Tobias Bonhoeffer for generous support in the development of this project, and for providing animal and optical imaging facilities, Ulf Eysel for advice on the production of cortical lesions, Gerhard Brändle for developing image analysis software, Michael Abramoff for providing a copy of VolumeJ rendering engine, Iris Kehrer and Frank Brinkmann for technical assistance, and Gabriel Gutierrez for helpful comments on the manuscript.

REFERENCES

Baird AE, Benfield A, Schlaug G, Siewert B, Lovblad KO, Edelman RR, Warach S (1997) Enlargement of human cerebral ischemic lesion volumes measured by diffusion-weighted magnetic resonance imaging. *Ann Neurol* 41:581–589

Bonhoeffer T, Grinvald A (1993) The layout of iso-orientation domains in area 18 of cat visual cortex: optical imaging reveals a pinwheel-like organization. *J Neurosci* 13:4157–4180

Bonhoeffer T, Grinvald A (1996) Optical imaging based on intrinsic signals. The methodology. In *Brain mapping: the methods* (Toga A, Mazziota J, eds), London: Academic Press, pp 55–97

Bronchti G, Schonenberger N, Welker E, Van der Loos H (1992) Barrelfield expansion after neonatal eye removal in mice. *Neuroreport* 3:489–492

Calford MB, Schmid LM, Rosa MG (1999) Monocular focal retinal lesions induce short-term topographic plasticity in adult cat visual cortex. *Proc R Soc Lond B Biol Sci* 266:499–507

Carmichael ST, Chesselet MF (2002) Synchronous neuronal activity is a signal for axonal sprouting after cortical lesions in the adult. *J Neurosci* 22:6062–6070

Coq JO, Xerri C (1999) Acute reorganization of the forepaw representation in the rat SI cortex after focal cortical injury: neuroprotective effects of piracetam treatment. *Eur J Neurosci* 11:2597–2608

Darian-Smith C, Gilbert CD (1994) Axonal sprouting accompanies functional reorganization in adult cat striate cortex. *Nature* 368:737–740

Darian-Smith C, Gilbert CD (1995) Topographic reorganization in the striate cortex of the adult cat and monkey is cortically mediated. *J Neurosci* 15:1631–1647

Dirnagl U, Iadecola C, Moskowitz MA (1999) Pathobiology of ischemic stroke: an integrated view. *TINS* 22:391–397

Doetsch GS, Johnston KW, Hannan CJ Jr (1990) Physiological changes in the somatosensory forepaw cerebral cortex of adult raccoons following lesions of a single cortical digit representation. *Exp Neurol* 108:162–175

Eysel UT (1982) Functional reconnections without new axonal growth in a partially denervated visual relay nucleus. *Nature* 299:442–444

Eysel UT, Schweigart G (1999) Increased receptive field size in the surround of chronic lesions in the adult cat visual cortex. *Cereb Cortex* 9:101–109

Gilbert CD, Wiesel TN (1992) Receptive field dynamics in adult primary visual cortex. *Nature* 356:150–152

Hagemann G, Redecker C, Neumann-Haefelin T, Freund HJ, Witte OW (1998) Increased long-term potentiation in the surround of experimentally induced focal cortical infarction. *Ann Neurol* 44:255–258

Hubel DH, Wiesel TN (1974) Uniformity of monkey striate cortex: a parallel relationship between field size, scatter, and magnification factor. *J Comp Neurol* 158:295–305

Hübener M, Shoham D, Grinvald A, Bonhoeffer T (1997) Spatial relationships among three columnar systems in cat area 17. *J Neurosci* 17:9270–9284

Illig KR, Danilov YP, Ahmad A, Kim CB, Spear PD (2000) Functional plasticity in extrastriate visual cortex following neonatal visual cortex damage and monocular enucleation. *Brain Res* 882:241–250

Jones EG (2000) Cortical and subcortical contributions to activity-dependent plasticity in primate somatosensory cortex. *Annu Rev Neurosci* 23:1–37

Jones EG, Pons TP (1998) Thalamic and brainstem contributions to large-scale plasticity of primate somatosensory cortex. *Science* 282:1121–1125

Kaas JH, Krubitzer LA, Chino YM, Langston AL, Polley EH, Blair N

(1990) Reorganization of retinotopic cortical maps in adult mammals after lesions of the retina. *Science* 248:229–231

Kasten E, Wüst F, Behrens-Baumann W, Sabel B (1998) Computer-based training for the treatment of partial blindness. *Nature Med* 4:1083–1087

Katz LC (1999) What's critical for the critical period in visual cortex? *Cell* 99:673–676

Li Y, Jiang N, Powers C, Chopp M (1998) Neuronal damage and plasticity identified by microtubule-associated protein 2, growth associated protein 43, and cyclin D1 immunoreactivity after focal cerebral ischemia in rats. *Stroke* 29:1972–1980

MacNeil MA, Lomber SG, Payne BR (1996) Rewiring of transcortical projections to middle suprasylvian cortex following early removal of cat areas 17 and 18. *Cereb Cortex* 6:362–376

Mittmann T, Eysel UT (2001) Increased synaptic plasticity in the surround of visual cortex lesions in rats. *Neuroreport* 12:3341–3347

Nudo RJ, Wise BM, SiFuentes F, Milliken GW (1996) Neural substrates for the effects of rehabilitative training on motor recovery after ischemic infarct. *Science* 272:1791–1794

Orban GA, Vandenbussche E, Sprague JM, De Weerd P (1990) Orientation discrimination in the cat: a distributed function. *Proc Natl Acad Sci U S A* 87:1134–1138

Payne BR, Lomber SG (2002) Plasticity of the visual cortex after injury: what's different about the young brain? *Neuroscientist* 8:174–185

Rauschecker JP, Hahn S (1987) Ketamine-xylazine anesthesia blocks consolidation of ocular dominance changes in kitten visual cortex. *Nature* 326:183–185

Rauschecker JP, Tian B, Korte M, Egert U (1992) Crossmodal changes in the somatosensory vibrissa/barrel system of visually deprived animals. *Proc Natl Acad Sci U S A* 89:5063–5067

Schuett S, Bonhoeffer T, Hubener M (2001) Pairing-induced changes of orientation maps in cat visual cortex. *Neuron* 32:325–337

Schweigart G, Eysel UT (2002) Activity-dependent receptive field changes in the surround of adult cat visual cortex lesions. *Eur J Neurosci* 15:1585–1596

Sengpiel F, Stawinski P, Bonhoeffer T (1999) Influence of experience on orientation maps in cat visual cortex. *Nat Neurosci* 2:727–732

Sengpiel F, Kind PC (2002) The role of activity in development of the visual system. *Curr Biol* 12:R818–R826

Sharp FR, Lu A, Tang Y, Millhorn DE (2000) Multiple molecular penumbras after cerebral ischemia. *J Cereb Blood Flow Metab* 20:1011–1032

Spear PD, Tong L, McCall MA (1988) Functional influence of areas 17, 18, and 19 on lateral suprasylvian cortex in kittens and adult cats: implications for compensation following early visual cortex damage. *Brain Res* 447:79–91

Stroemer RP, Kent TA, Hulsebosch CE (1995) Neocortical neural sprouting, synaptogenesis, and behavioral recovery after neocortical infarction in rats. *Stroke* 26:2135–2144

Vandenbussche E, Sprague JM, de Weerd P, Orban GA (1991) Orientation discrimination in the cat: its cortical locus. I. Areas 17 and 18. *J Comp Neurol* 305:632–658

Watson BD, Dietrich WD, Busto R, Wachtel MS, Ginsberg MD (1985) Induction of reproducible brain infarction by photochemically initiated thrombosis. *Ann Neurol* 17:497–504

Woolsey TA, Wann JR (1976) Areal changes in mouse cortical barrels following vibrissal damage at different postnatal ages. *J Comp Neurol* 170:53–66

Zihl J, von Cramon D (1985) Visual field recovery from scotoma in patients with postgeniculate damage. *Brain Behav Evol* 108:335–365

Development/Plasticity/Repair

Functional Reorganization of Visual Cortex Maps after Ischemic Lesions Is Accompanied by Changes in Expression of Cytoskeletal Proteins and NMDA and $GABA_A$ Receptor Subunits

Angelica Zepeda,[1,3] Frank Sengpiel,[3,4] Miguel Angel Guagnelli,[1] Luis Vaca,[2] and Clorinda Arias[1]

[1]Departamento de Biología Celular y Fisiología, Instituto de Investigaciones Biomédicas, [2]Departamento de Biología Celular, Instituto de Fisiología Celular, Universidad Nacional Autónoma de México, 04510-México, Distrito Federal, México, [3]Max-Planck-Institut für Neurobiologie, 82152 München-Martinsried, Germany, and [4]Cardiff School of Biosciences, Cardiff University, Cardiff CF10 3US, United Kingdom

Reorganization of cortical representations after focal visual cortex lesions has been documented. It has been suggested that functional reorganization may rely on cellular mechanisms involving modifications in the excitatory/inhibitory neurotransmission balance and on morphological changes of neurons peripheral to the lesion. We explored functional reorganization of cortical retinotopic maps after a focal ischemic lesion in primary visual cortex of kittens using optical imaging of intrinsic signals. After 1, 2, and 5 weeks postlesion (wPL), we addressed whether functional reorganization correlated in time with changes in the expression of MAP-2, GAP-43, GFAP, $GABA_A$ receptor subunit $\alpha 1$ ($GABA_A\alpha 1$), subunit 1 of the NMDA receptor (NMDAR1), and in neurotransmitter levels at the border of the lesion. Our results show that: (1) retinotopic maps reorganize with time after an ischemic lesion; (2) MAP-2 levels increase gradually from 1wPL to 5wPL; (3) MAP-2 upregulation is associated with an increase in dendritic-like structures surrounding the lesion and a decrease in GFAP-positive cells; (4) GAP-43 levels reach the highest point at 2wPL; (5) NMDAR1 and glutamate contents increase in parallel from 1wPL to 5wPL; (6) $GABA_A\alpha 1$ levels increase from 1wPL to 2wPL but do not change after this time point; and (7) GABA contents remain low from 1wPL to 5wPL. This is a comprehensive study showing for the first time that functional reorganization correlates in time with dendritic sprouting and with changes in the excitatory/inhibitory neurotransmission systems previously proposed to participate in cortical remodeling and suggests mechanisms by which plasticity of cortical representations may occur.

Key words: **plasticity; visual cortex; sprouting; maps; ischemia; injury; imaging techniques; cat; retinotopy; receptors; photochemical lesion; unmasking**

Introduction

CNS as well as PNS lesions lead to functional deficits, yet recovery of the lost functions may occur over time. It has been proposed that restoration of functions after focal somatosensory and motor cortical damage (Nudo et al., 1996a; Rouiller et al., 1998a; Coq and Xerri, 1999; Rijntjes and Weiller, 2002) may rely, to some degree, on the reorganization of cortical maps. Cortical reorganization has been observed to involve either zones surrounding the lesion area (Castro and Borrell, 1995; Nudo et al., 1996a; Rouiller et al., 1998a; Zepeda et al., 1999, 2003) or regions within the homologous contralateral cortex (Jones and Schallert, 1992; Jones et al., 1996; Nudo et al., 1996b; Dijkhuizen et al., 2003).

Reorganization of the visual cortex after focal lesions has been studied less until recently despite its clinical relevance. We have previously shown that visual cortex maps reorganize to a certain extent with time after an ischemic lesion (Zepeda et al., 2003), while Eysel and Schweigart (1999) have reported that single cells in the surrounding area of the lesion exhibit enlarged receptive fields. However, neurorepair mechanisms associated with such visual reorganization remain unknown.

Functional reorganization after central and peripheral lesions may rely on plasticity mechanisms involving modifications in the excitatory/inhibitory neurotransmission balance (Jones, 1993; Das and Gilbert, 1995a; Hagemann et al., 1998; Eysel and Schweigart, 1999; Arckens et al., 2000; Mittmann and Eysel, 2001) as well as in dendritic and axonal sprouting (Darian-Smith and Gilbert, 1994, 1995; Florence and Kaas, 1995; Stroemer et al., 1995; Li et al., 1998; Carmichael, 2003).

Dendritic and axonal regrowth have been associated with the expression of molecules such as MAP-2 and GAP-43, respec-

Received July 7, 2003; revised Nov. 25, 2003; accepted Nov. 25, 2003.

This work was supported by Consejo Nacional de Ciencia y Tecnologia (CONACYT) 36250M. F.S. was supported by the Max-Planck-Gesellschaft and the Medical Research Council. A.Z. was supported in part by Deutscher Akademischer Austausch Dienst, Graduierten-Kolleg München, and CONACYT, Mexico. We thank Tobias Bonhoeffer for support in the development of this project and for providing animal and optical imaging facilities, Gerhard Brändle for developing image analysis software, Beatriz Jimenez for assistance with confocal microscopy, and Patricia Ferrera, Iris Kehrer, and Frank Brinkmann for technical assistance. We are grateful to Federico Bermudez-Rattoni, Ricardo Tapia, and Ranulfo Romo for helpful comments on this manuscript.

Correspondence should be addressed to Dr. Clorinda Arias, Departamento de Biología Celular y Fisiología, Instituto de Investigaciones Biomédicas, Universidad Nacional Autónoma de México, Apartado Postal 70228, 04510-México, Distrito Federal, México. E-mail: carias@servidor.unam.mx.

DOI:10.1523/JNEUROSCI.3213-03.2004

 0270-6474/04/241812-10$15.00/0

tively. MAP-2 is a protein mainly found in soma and dendrites that plays a key role in maintaining neuronal architecture, in cellular differentiation, and in structural and functional plasticity (Sanchez et al., 2000). GAP-43 is mainly localized in growth cones. It is synthesized after cortical stroke, and its expression after nervous injury has been correlated with axonal regeneration (Stroemer et al., 1995; Li et al., 1998; Carmichael and Chesselet, 2002).

Studies addressing reorganization in the surrounding area of focal visual cortex lesions have also suggested neurochemical modifications involving a reduction in GABAergic inhibition and an increased glutamatergic response mediated by the NMDA receptor (Mittmann et al., 1994; Schiene et al., 1996; Eysel and Schweigart, 1999; Que et al., 1999a; Mittmann and Eysel, 2001). However, to our knowledge, a comprehensive temporal study exploring cortical reorganization after focal visual cortex lesions and its related morphological and biochemical modifications has not been performed. The goal of the current study was to induce a photochemical ischemic lesion in the primary visual cortex of kittens and correlate in time the observed functional reorganization with expression of MAP-2, GAP-43, neurotransmitter levels, and expression of subunit 1 of the NMDA receptor (NMDAR1) and $GABA_A$ receptor subunit $\alpha 1$ ($GABA_A\alpha 1$) at the border of the lesion.

Materials and Methods

The experiments were performed on 22 kittens (8–10 weeks old); all procedures were performed in accordance with local government rules and the Society for Neuroscience Guide for the Care and Use of Laboratory Animals. Efforts were made to minimize animal suffering and to reduce the number of subjects used.

Before and after the lesion, kittens were housed in a laboratory environment with a 12 hr artificial light/dark cycle. They lived within a colony of cats and did not receive any specific training or treatment at any time.

Optical imaging of intrinsic signals. Surgery and optical imaging techniques have been described in detail previously (Bonhoeffer and Grinvald, 1993, 1996). Animals ($n = 2$) were anesthetized intramuscularly with ketamine (20–40 mg/kg) and xylazine (Rompun; 2–4 mg/kg; Bayer, Leverkusen, Germany) and then intubated. They were placed in a stereotaxic frame and artificially respired with a mixture of 60% N_2O and 40% O_2 with 0.7–1.5% halothane. Electrocardiogram, expired CO_2, and body temperature were monitored throughout the experiment. A solution of 4% glucose in saline was infused intravenously at 3 ml/kg/hr throughout the experiment. To prevent eye movements, the infusion solution was supplemented with the fast-acting muscle relaxant atracurium (Tracrium; 0.6 mg/kg/hr; GlaxoWellcome, Munich, Germany).

In the initial imaging session, the scalp was incised and retracted. A circular craniotomy was performed above area 17 (centered on P4, Horsley–Clarke coordinates), and a titanium chamber was cemented onto the skull. The chamber was filled with silicon oil and was sealed with a glass coverslip.

As described previously (Zepeda et al., 2003), animals were fitted with contact lenses to focus their eyes on a computer screen at a distance of 33 cm. Retinotopic stimuli (VSG Series Three; Cambridge Research Systems, Rochester, UK) consisted of drifting high-contrast square wave gratings of 1 cycle/degree oriented at 0° or 90° within a 1° wide horizontal aperture. Stimuli were presented in random order at 11 positions separated by 1°, from an elevation of 5° above to 5° below the horizontal meridian. In addition to retinotopic maps, orientation preference maps were obtained; visual stimuli consisted of high-contrast square wave gratings of 0.15–0.5 cycles/degree, drifting back and forth at 2 cycles/sec and presented at 0 and 90°.

Each stimulus lasted 3 sec (data consisted of five frames of 600 msec duration) and was followed by a 9 sec interstimulus interval during which the next stimulus was displayed but remained stationary. For the analysis, the first frame (after the onset of drift) was discarded.

For intrinsic signal imaging, the cortex was illuminated with bandpass-filtered light of 707 ± 10 nm. Responses to visual stimulation were captured by a cooled slow-scan CCD camera focused 500 μm below the cortical surface (ORA 2001; Optical Imaging, Germantown, NY).

A control optical imaging experiment was performed immediately before the photochemical lesion. A second recording session was conducted immediately after the lesion, and subsequent experiments were performed at 2 and 5 weeks postlesion (wPL).

After each but the final experiment, the chamber was half-filled with agar containing antibiotic (Paraxin; Bayer), and the rest of the chamber was filled with silicone oil and sealed with a glass coverslip. Anesthesia was suspended; kittens were allowed to recover and were then returned to their mother and littermates.

Retinotopic and orientation map analyses. Analysis of retinotopic representation was performed for two kittens, using Interactive Data Language software (Research Systems, Boulder, CO). We determined the cortical area for each stimulus position where a response above a fixed threshold (identical between stimuli and experiments) was observed and calculated the number of pixels for which an above-threshold response was obtained for neighboring stimulus positions. The extent of "overlap" in the responses to abutting stimuli was taken as a measure for the divergence in the retinocortical projection or, in other words, as an indicator of the aggregate receptive field size.

Analysis of orientation preference maps has been described in detail previously (Zepeda et al., 2003). Briefly, orientation maps were produced by dividing cortical responses to 0 and 90° grating stimuli. Twelve-bit digitized camera images were range-fitted such that the 1.5% most responsive pixels were set to black and the least responsive to white. Signal amplitude was displayed on an eight-bit gray scale.

Photochemical lesion. For inducing the lesion, we used the photochemical lesion technique initially described by Watson et al. (1985), with some variations. Animals were anesthetized as described above. The scalp was incised and retracted, a circular craniotomy was performed above area 17 (centered on P4, Horsley–Clarke coordinates), and the dura was removed from the area to be lesioned. The cortical surface was carefully cleared of any traces of blood using Sugi sterile swabs (Kettenbach, Eschenburg, Germany). A krypton/argon 514 nm laser beam (Ion Laser Technology, Salt Lake City, UT) light guide positioned ~5 cm above V1 was directed toward the area of the cortex where the ischemic lesion was to be produced. Rose Bengal dye (10 mg/kg; Sigma, St. Louis, MO) was injected over a 2 min interval through the femoral vein; the cortex was illuminated simultaneously and for the next 12 min. The parameters ensured vascular occlusion in an area of ~3 mm. In those animals not used for optical imaging, the titanium chamber was replaced by a glass coverslip that fitted in the craniotomy. The coverslip was cemented onto the skull, and a plastic ring (1 cm height) was cemented on top of it. The skin was sutured, leaving a window in which the coverslip and the plastic ring had been placed. This enabled us to monitor the lesion area at all time points. After different survival times postlesion (1, 2, and 5 weeks), animals were killed.

Histology and immunohistochemistry. Animals ($n = 10$; three lesioned per time point and one nonlesioned) received an overdose of barbiturate and were perfused transcardially with 0.9% saline, followed by chilled 2% paraformaldehyde fixative and 0.18% picric acid in phosphate buffer. Brains were removed, postfixed at 4°C for 4 d, and then successively transferred to sucrose solutions (up to 30%). Sequential 14 and 30 μm coronal sections were cut at the level of the lesion on a cryostat. Thirty-micrometer sections were mounted on gelatin-covered slides and processed for cresyl violet (Nissl) staining. Fourteen-micrometer sections were mounted on silane (g-methacryloxypropyltrimethoxysilane; Sigma)-covered slides and processed for double immunofluorescence. Briefly, slides containing 14 μm sections were placed in a vacuum chamber for 20 min before and after mounting the sections. A layer of Glyco (artwork glue; Distribuidora Rodin, Mexico City, Mexico) surrounding the sections was applied. This would act as a barrier for the solutions bathing the sections. Once the glue was dry, sections were washed three times for 10 min in PBS–Triton (0.3%) and incubated in normal horse serum (1:25; Vector Laboratories, Burlingame, CA) in PBS–Triton (0.3%) for 2 hr. Afterward, they were incubated in rabbit anti-cow GFAP

(1:1000; DAKO, Carpinteria, CA) and monoclonal anti-MAP2 (1:250; Chemicon, Temecula, CA) for 12 hr in a humid chamber. Sections were washed three times for 10 min in PBS–Triton (0.3%) and then incubated in fluorescein-conjugated goat anti-rabbit (1:250; Zymed, San Francisco, CA) (excitation, 494 nm; emission, 519 nm; green fluorescence) and Cy5 goat anti-mouse (1:40; Jackson ImmunoResearch, West Grove, PA) (excitation, 650 nm; emission, 670 nm; blue fluorescence) secondary antibodies for 2 hr in a humid chamber. Sections were washed three times for 10 min in PBS–Triton (0.3%) and then incubated in Radiant Red (1:100; Bio-Rad, Hercules, CA) (excitation 596 nm, emission, 615 nm; red fluorescence) for 10 min in a humid chamber. Afterward, they were washed three times for 10 min in PBS and covered with fluorescent mounting medium (DAKO). Cross-reactivity was excluded by appropriate controls: control sections were incubated in the same solutions as experimental sections but without primary antibodies. Incubation with secondary antibodies was performed as described for experimental sections. Tissue processed in the absence of primary antibodies showed no immunostaining.

Confocal microscopy reconstructions and density measurements. Sections were analyzed with a confocal laserscan microscope (Bio-Rad). For each subject ($n = 3$ per time point), we analyzed six sections of tissue corresponding to the beginning, middle, and end of the lesion. Individual images (~80) from the lesion zone were acquired; 10 optical sections from each image were acquired. Confocal images were imported into the Confocal Assistant Program version 4.02 (designed by Todd Clark Brelje, University of Minnesota, Minneapolis, MN); each image was projected in the z plane (10 optical sections), and maximal values of pixels were integrated to produce single images containing the information of the 10 optical sections. Projected images were then imported to Corel Photopaint 10 (Corel, Ottawa, Ontario, Canada), and the center and surrounding area of the lesions were reconstructed.

Measurements of optical density of MAP-2 from confocal images. Areas of 1.5 mm in height and 2 mm width immediately adjacent to the pyknotic area were extracted from the reconstructed lesion area (see Fig. 3) at all postlesion times. The images corresponding to the blue channel (MAP-2) were used to measure the number of pixels in the 1.5 × 2 mm area for cortical layers IV–VI. Measurements were done using Igor Pro 4.02 (Wavemetrics, Lake Oswego, OR); values (pixels/micrometer) are reported for all postlesion times. Cortical layers were identified following the criteria reported by Peters and Yilmaz (1993).

Measurements of MAP-2-positive somata from confocal images. Immunopositive MAP-2 somata were counted in an area of 2 mm in height and 1 mm width immediately adjacent to the pyknotic area from all animals using Igor Pro 4.02 (Wavemetrics).

Volumetric measurements and reconstruction of the lesion. All Nissl sections containing an area of photochemically damaged tissue were used to calculate the volume of the lesion. Nissl sections were 30 μm thick and were separated by 45 μm. Serial sections were placed under a transilluminator (Northern Light, Quebec, Canada), and images of the lesion were acquired through a CCD camera (NEC, Santa Clara, CA) attached to a computer. The area of the lesion in each Nissl section was measured using NIH Image software (Scion, Frederick, MD), and total lesion volume (Vol) was calculated as:

$$Vol = \Sigma^{n}[(As)(T) + (As)(K)]_{i},$$

where, As is the area of lesion in one Nissl section, T is the thickness of the Nissl section (30 μm), K is the tissue separating adjacent Nissl sections, and n is the number of sections that contain the lesion.

These measurements were done for every brain, and the means ± SEM were calculated. One-way ANOVA was performed to assess differences between groups sacrificed at different time points.

Electrophoresis and immunoblotting. Animals ($n = 10$; three lesioned per time point and one nonlesioned) were decapitated, and brains were removed, submerged in chilled phosphate buffer (0.1 M for 1 min), transferred to liquid nitrogen, and stored at −70°C. Guided by the visible lesion area (pale region) on the surface of the brain, coronal sections (120 μm) were cut in a cryostat at −20°C. The lesion area from each section was then extracted using a suction pipette. In every case, the extracted tissue contained the center of the lesion and 2 mm of surrounding tissue (see Fig. 4*A*). Alternate sections were used for immunoblotting and HPLC (see below). Tissue samples were homogenized in lysis buffer containing Tris-HCl (0.05 M, pH 7.5), NaCl (0.15 M), NP-40 (1%), and sodium deoxycholate (0.5%) supplemented with a protease inhibitor mixture (Complete; EDTA free; Roche, Mannheim, Germany). Tissue extracts were analyzed by using SDS-PAGE. Samples (50 μg of protein/well) diluted in Laemmli's (1970) solution were run under reducing conditions (5% β-mercaptoethanol) through 0.75 mm thick, 10% gels (Miniprotean II; Bio-Rad) at 50 mA constant current for 2 hr. Prestained molecular weight markers (Amersham Biosciences, Piscataway, NJ) were used to determine the relative mobility of proteins. After the electrophoresis, the gels were equilibrated in transferring buffer (25 mM Tris, 192 mM glycine, and 20% methanol) for 15 min, and the proteins were electro-transferred to nitrocellulose sheets (Bio-Rad) at 200 mA for 1 hr at 4°C. The membranes were blocked with nonfat milk (5%) in TBS (20 mM Tris and 135 mM NaCl) for 2 hr at room temperature, washed three times for 5 min in TBS containing Tween 20 (0.05%) (TTBS), and then incubated with one of the following monoclonal antibodies: anti-NMDAR1 (1:400; PharMingen, San Diego, CA), anti-$GABA_A\alpha 1$ (1:600; Santa Cruz Biotechnology, Santa Cruz, CA), anti-MAP2 (1:400; Chemicon), anti-NeuN (1:500; Chemicon), or a polyclonal anti-GAP43 (1:500; Chemicon) overnight at 4°C. Membranes were washed three times in TTBS and incubated with a goat anti-mouse secondary antibody conjugated with biotin (1:1000; Vector Laboratories) for 2 hr at room temperature, washed three times in TTBS, and then incubated in avidin–biotin (1:200; Vector Laboratories) for 30 min at room temperature. Finally, after washing the membranes with TTBS four times for 5 min each, immunolabeled bands were identified by using a chemiluminescence-based detection kit according to the protocol suggested by the manufacturer (ECL; Amersham Biosciences, Buckinghamshire, UK). Densitometric analysis of bands was performed using NIH Image for Windows 2000 (Scion). One-way ANOVA was performed to establish differences in contents of proteins evaluated at different time points after the lesion.

HPLC. To determine total contents of amino acids in the lesion area and its surrounding area, 120 μm coronal sections were obtained as described above and processed for HPLC. Two to three sections per animal were weighed (~4 mg wet weight/section). Sections containing the center of the lesion and 2 mm of surrounding tissue were homogenized in 0.2 ml of 0.7% perchloric acid (see Fig. 4*A*). After the precipitated protein was sedimented by centrifugation, the extracts were neutralized with 1 M KOH, and potassium perchlorate was spun down. Aliquots of the extracts were derivatized automatically with o-phthalaldehyde (Geddes and Wood, 1984) in an automatic sampler (Waters, Milford, MA). Twenty microliters of the sample were injected automatically into a HPLC system. An ODS column (25 × 4 mm internal diameter; Supelco, Bellefonte, PA) was used, and the column effluent was monitored with a fluorescence detector, at 340 nm excitation wavelength and 418 nm emission wavelength. The mobile phase was phosphate buffer (60 mM), pH 6.65, in one line and 46% phosphate buffer, 18% methanol, 22% acetonitrile, and 14% isopropanol in the other line and was run at 1 ml/min. Obtained results were compared with standard samples processed similarly. Results were expressed as picomoles of wet tissue per milligram, and differences between groups were evaluated with one-way ANOVA.

Results

Photochemically induced cortical lesion

Using the photochemical procedure described previously (Zepeda et al., 2003), we obtained reproducible lesions in the visual cortex of anesthetized animals. The lesion area was easily identified in the blood vessel pattern immediately after the lesion procedure was completed and was characterized macroscopically by a pale area (~3 mm^2) containing occluded blood vessels (Fig. 1*A*).

Retinotopic cortical maps reorganize in time after the photochemical lesion

Immediately after the lesion, optical imaging of intrinsic signals revealed an area of cortex devoid of visually driven activity, which

was very similar in size (~3 mm^2) to the area identified macroscopically as ischemic. To evaluate overall responsiveness to visual stimulation in the exposed cortical area, orientation preference maps were first obtained (Fig. 1*B*) as reported previously (Zepeda et al., 2003). To assess retinotopic representation of visual space of the cortical surface before and after the lesion, grating stimuli oriented at 0 or 90° were presented within a 1° wide horizontal aperture, the position of which was varied in 1° steps. Typically, two such stimuli presented in adjacent positions (covering a total of 2° of visual space) elicited responses from almost the entire exposed visual cortex (Fig. 1*C*,*D*). Before the lesion, the overlap in cortical surface area responding to two adjacent retinotopic stimuli was, on average, 0.755 mm^2 (Fig. 1*C–E*, top row, *F*). Because most of this overlap was within the lesion zone, it was lost almost completely immediately after lesion (data not shown). However, in the course of 5 weeks after the lesion, the area of representational overlap recovered considerably, to 0.285 mm^2 at 2wPL (Fig. 1*C–E*, third row, *F*) and 0.65 mm^2 at 5wPL (Fig. 1*C–E*, bottom row, *F*). We observed a statistically significant ($p < 0.05$; *t* test) reduction in representational overlap from prelesion to 2wPL and then a significant increase from 2 to 5wPL. Prelesion and 5wPL data, however, were not significantly different. This increased overlap indicates that the area of visual space represented in the surrounding area of the ischemic lesion expanded over time, thus compensating, at least in part, for the representational loss at the lesion site itself.

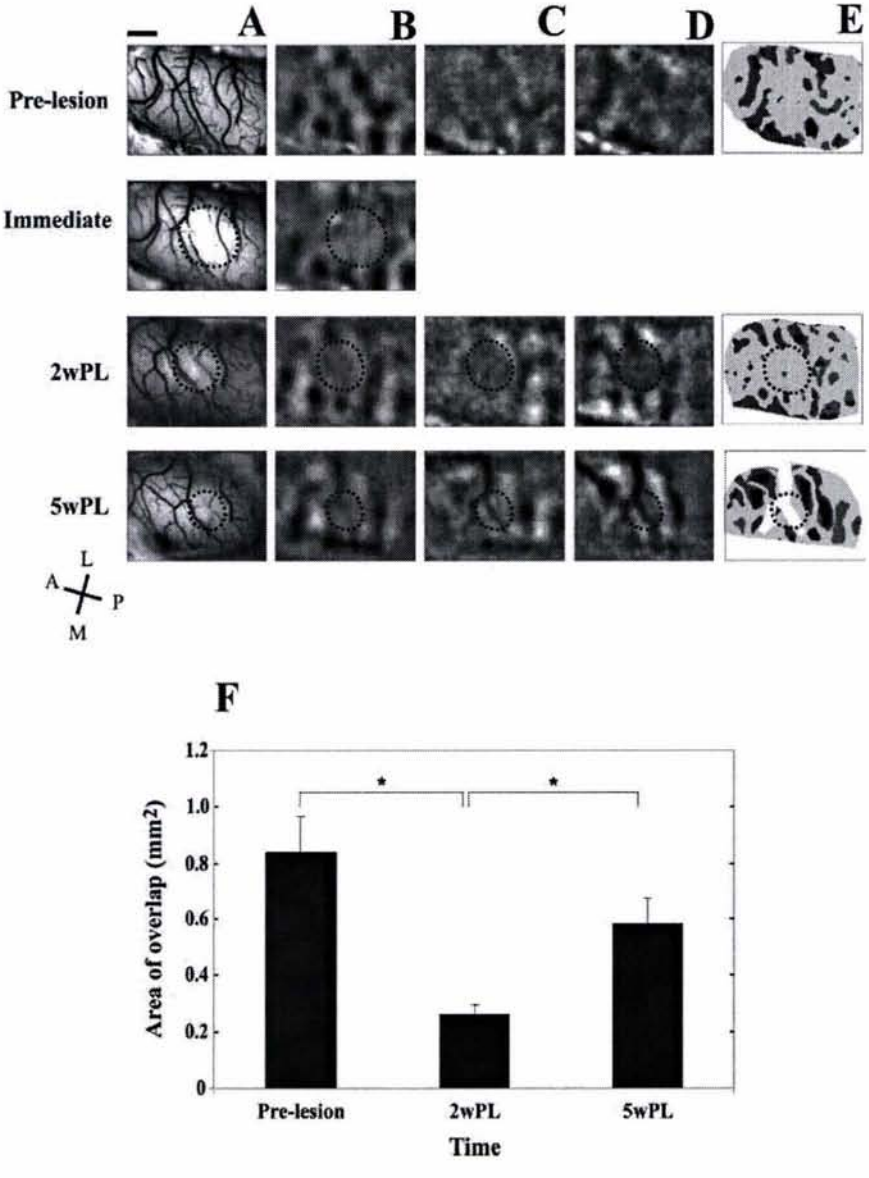

Figure 1. Retinotopic map reorganization after an ischemic lesion. *A*, Blood vessel pattern. *B*, Iso-orientation maps in response to gratings of 0°. *C*, Retinotopic map in response to a 1° wide stimulus oriented at 0°. *D*, Retinotopic map in response to 1° wide stimulus oriented at 0°, adjacent to the stimulus presented in *C*. *E*, Overlap between responses in *C* and *D*: light gray domains correspond to active zones in *C*, dark gray domains correspond to active zones in *D*, and black zones correspond to active areas in both *C* and *D*, the "overlap." Note that the overlapping area fully recovers after 5wPL. Orientation of the imaged cortical area is shown (A, anterior; P, posterior; M, medial; L, lateral). *F*, Area of overlap (mm^2) in response to adjacent stimuli. Values represent the mean ± SEM. Asterisks denote significant differences (*t* test; $p < 0.05$) between groups. Scale bar, 1 mm.

Functional reorganization is associated with modifications in cellular markers of morphological plasticity

To study morphological modifications of the ischemic lesion and its surrounding area over time, we performed a triple labeling of MAP-2, GFAP, and nuclei. This allowed us to establish a correlation between neuronal death, the gliotic scar process, and the presence of dendritic structures in the surrounding area of the ischemic lesion. Figure 2*A* shows the reconstruction of layers I–VI from a control animal. Control tissue showed the following characteristics: (1) GFAP immunoreactivity was exclusively seen for astrocyte-like cells; (2) GFAP-immunopositive cortical astrocytes were mainly protoplasmic, whereas white matter astrocytes were fibrous; (3) the glial density was more or less uniform across all cortical layers, except for layers I and II, where the glia limitans is found; (4) MAP-2 was found surrounding exclusively the soma of neurons and in dendritic-like processes; (5) no colocalization of GFAP and MAP-2 was observed; and (6) MAP-2-immunopositive fibers were differentially distributed along cortical layers (Peters and Yilmaz, 1993). Given that MAP-2 is abundant in layers I and II but very scarce in white matter, we used the presence of MAP-2 in layers I and II as a positive control and the absence of MAP-2 in white matter as a negative control of immunoreactivity in all experiments.

Figure 2, *B–D*, shows reconstructions of ~80 confocal images obtained at 1, 2, and 5wPL. Morphology of the lesion shows that in all cases the lesion was successfully induced in cortical area 17. Triple labeling histochemistry revealed at all time points a well delimited conical-shaped lesion extending from layers I to VI characterized by a body of pyknotic nuclei surrounded mainly by anisomorphic fibrous astrocytes. MAP-2-immunopositive fibers were clearly observed in control sections (Figs. 2*A*, 3*A*) but were absent in the surrounding area of the lesion center in sec-

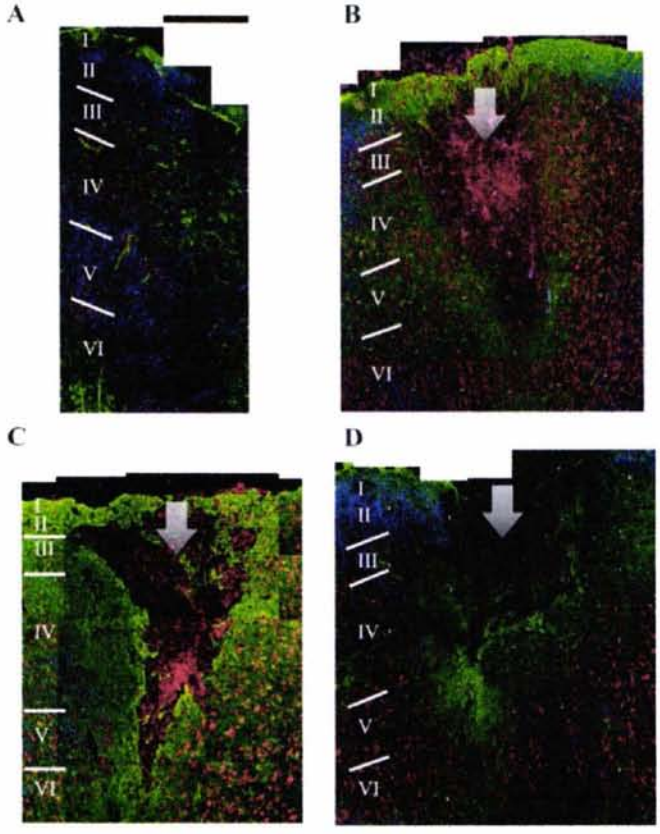

Figure 2. Triple inmunohistochemistry and confocal microscopy reconstructions of the lesion area from a coronal section. The section belongs, in every case, to the largest area of the lesion in the anteroposterior coordinate. Each image (~86 per section) was projected in the z plane (10 optical sections), and maximal values of pixels were integrated to produce single images containing the information of the 10 optical sections; images were then assembled to reconstruct the coronal section. Red, Nuclei; green, GFAP; blue, MAP-2. A section from a control cat (*A*) and sections from cats killed at 1wPL (*B*), 2wPL (*C*), and 5wPL (*D*) are shown. Each image is representative of three different animals per time point. Cortical layers are indicated to the left. The arrow points at the center of the lesion. Scale bar, 500 μm.

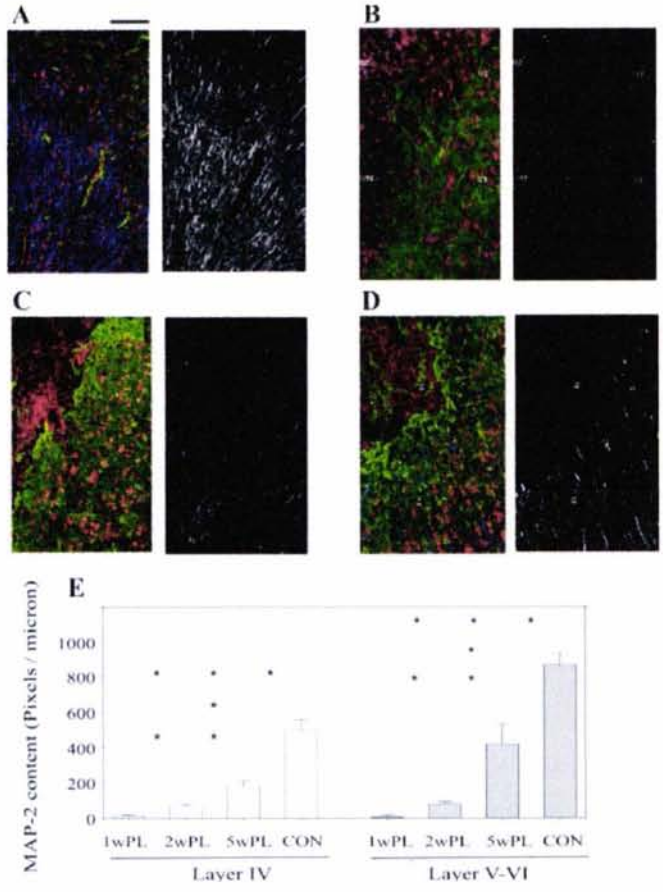

Figure 3. Increase in time of MAP-2-IR fibers within the gliotic area surrounding the lesion center. Red, Nuclei; green, GFAP; blue, MAP-2. In black and white images to the right of each color image, the corresponding blue channel was isolated and coded in gray scale for clarity. *A*, Control; *B*, 1wPL; *C*, 2wPL; *D*, 5wPL. Notice the absence of MAP-2 after 2wPL (*B*, right) and the presence of dendritic structures at 5wPL (*D*, right). *E*, Optical density of MAP-2 contents in cortical layers IV (□) and V and VI (▨). Each bar represents the mean ± SD from six sections containing the beginning, middle, and end of the lesion from three different animals, measured in an area adjacent to the lesion as described in Materials and Methods. The asterisk denotes a significant difference ($p < 0.05$) between groups. CON, Control. Scale bar, 500 μm.

tions obtained at 1wPL (Figs. 2*B*, 3*B*). After 2 and 5wPL, MAP-2 density of immunopositive fibers gradually increased (Figs. 2*C*,*D*, 3*C*,*D*). The figure clearly shows that the size of lesion diminishes over time; this observation was corroborated by the volumetric analysis from serial Nissl-stained sections (data not shown) that revealed a lesion volume of (mm^3 ± SEM) 2.65 ± 0.21 at 1wPL, 0.90 ± 0.12 at 2wPL, and 0.40 ± 0.08 at 5wPL (Redecker et al., 2002; Zepeda et al., 2003).

Figure 3*A* shows the magnification of layers IV–VI from a control subject (area 17) and from areas immediately adjacent to the lesion center in animals killed at 1, 2, and 5wPL (Fig. 3*B–D*). In sections from lesion animals, pyknotic nuclei were found to aggregate in a region devoid of GFAP- or MAP-2-immunopositive cells (center of the lesion) and were also found in the dense glial scar surrounding the center (Fig. 3*B–D*). The area occupied by pyknotic nuclei diminished over time in all subjects. At no time point did we detect the presence of fragmented nuclei that have been associated with apoptotic processes.

Reconstructions from the lesion area show that both density and distribution of GFAP and MAP-2 changed with time. After 1wPL, a dense region of anisomorphic astroglia was found around the center of pyknotic nuclei. In areas adjacent to the dense glial scar, scattered isomorphic protoplasmic astrocytes were found. No MAP-2-immunopositive structures could be detected in the center of the lesion or within the glial scar in any cortical layer (Figs. 2*B*, 3*B*,*E*). Only at a distance of 1 mm from the center of the lesion, MAP-2 could be found surrounding intact somata and forming dendrite-like structures.

After 2wPL, the glial scar still looked dense, but few dendritic structures were found within the scar at a distance of 340 ± 117 μm from the center of the lesion (Figs. 2*C*, 3*C*,*E*). At 5wPL, the density of GFAP-immunopositive cells was considerably decreased in comparison with 1 and 2wPL, and the lesion area was obviously smaller (Figs. 2*D*, 3*D*,*E*). At this time point, a higher density of dendritic structures in comparison with 2wPL was found within the gliotic scar in all cortical layers (Fig. 3*D*,*E*). Dendritic structures were found as close as 60 ± 5 μm from the lesion center (the area of pyknotic nuclei). In no case were MAP-2-immunopositive structures found within the center of the lesion. In parallel with the occurrence of MAP-2, functional maps also reappeared closer to the lesion with time. At 2 and 5wPL, functional maps were found at 516 ± 140 μm and 317 ± 54 μm from the lesion center, respectively.

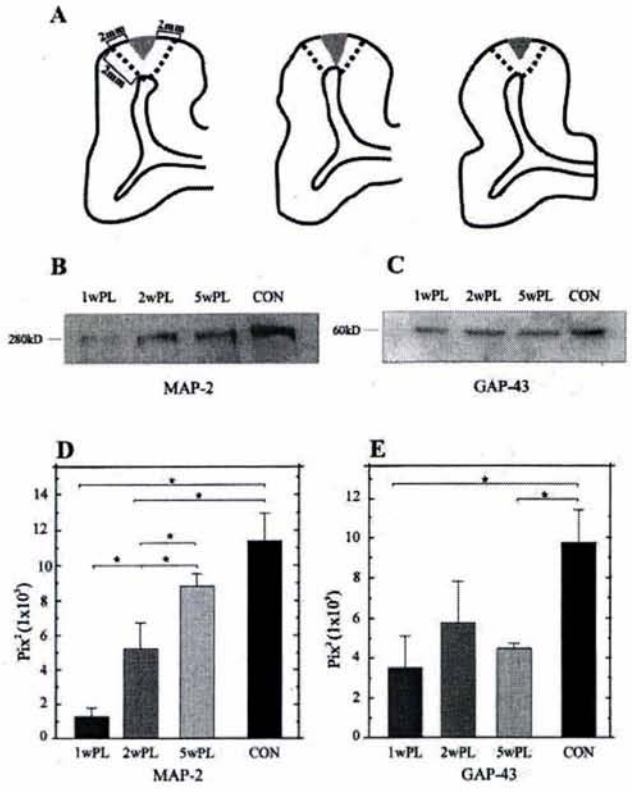

Figure 4. Time-dependent modifications in MAP-2 and GAP-43 contents in the center and surrounding area of the lesion. *A*, Schematics of V1 coronal sections from near the anterior border, the center, and the posterior border of the lesion (gray triangles). The dotted lines show the limits of tissue extracted with the suction pipette. Extracted tissue included the lesion center and 2 mm lateral and ventral to the borders of the lesion. Representative Western blots of MAP-2 (*B*) and GAP-43 (*C*) obtained from homogenates of the lesion tissue depicted in *A* are shown. Each Western blot was performed two times on three different animals. The histograms show a densitometric quantitative analysis from MAP-2 (*D*) and GAP-43 (*E*). Data are the mean ± SEM of three animals per time point. The asterisk denotes a significant difference ($p < 0.05$) between groups.

Differential modifications in time in the contents of MAP-2 and GAP-43

Western blots of MAP-2 show that at 1wPL the protein level in areas adjacent to the lesion dropped by 89% with respect to control levels (Fig. 4*B*,*D*). However, a clear recovery of protein levels toward control values was observed at 2 and 5wPL. Thus, by 2 and 5wPL, protein levels had recovered by 46 and 77%, respectively, with respect to control (Fig. 4*B*,*D*). One-way ANOVA showed significant differences between control and 1wPL ($p < 0.01$) and control and 2wPL ($p < 0.05$) but not between control and 5wPL (Fig. 4*D*). This recovery parallels the observed increase in the occurrence and density of MAP-2-positive structures in the area surrounding the lesion.

At 1wPL, GAP-43 levels were also reduced to 35% of control levels. By 2wPL, protein levels recovered to 59% with respect to the control (Fig. 4*C*,*E*). However, in contrast to MAP-2, GAP-43 levels did not continue to increase toward control values. Thus, by 5wPL, protein levels were at just 46% with respect to the control, 13% less than 2wPL levels (Fig. 4*C*,*E*). One-way ANOVA showed that GAP-43 levels were significantly reduced at 1wPL ($p < 0.05$), but at 2wPL no differences were detected when compared with control values. By 5wPL, GAP-43 levels had dropped again, and a significant difference was found when compared with control ($p < 0.05$) (Fig. 4*E*).

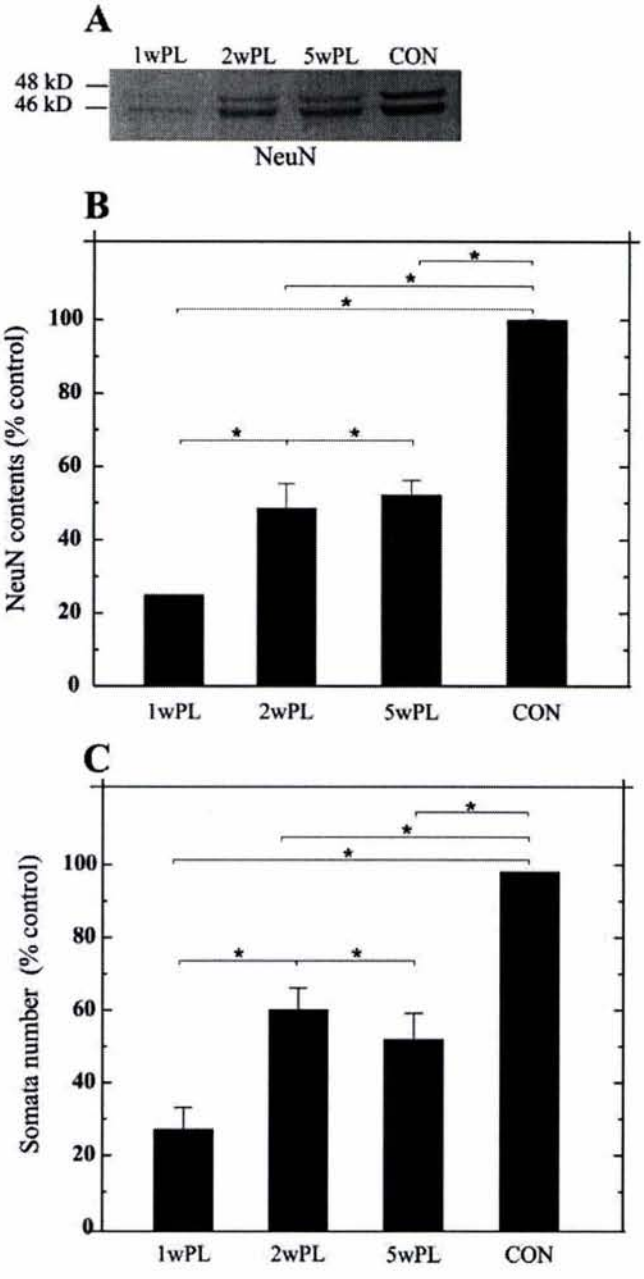

Figure 5. NeuN contents in the center and surrounding area of the lesion. *A*, Representative Western blots of NeuN obtained from homogenates of the lesion tissue as indicated in Figure 4*A* ($n = 3$). *B*, Histogram showing results of the densitometric analysis of NeuN blots. *C*, Density of neuronal somata in a 2 mm zone surrounding the lesion core. The asterisk denotes a significant difference ($p < 0.05$) between groups.

Contents of the neuronal-specific nuclear protein NeuN and MAP-2-positive somata through time

To evaluate the density of neuronal cells in the surrounding area of the lesion core through time, we analyzed the expression of the neuronal-specific nuclear antigen (NeuN) by Western blot (Mullen et al., 1992) (Fig. 5*A*,*B*) and additionally counted MAP-2-positive somata in the surrounding area of the lesion. We found that NeuN diminishes substantially after 1wPL and increases after 2wPL (Fig. 5*B*). Importantly, the values obtained after 2 and 5wPL are not significantly different and they do not reach control levels (nonlesion subjects) (Fig. 5*B*). The NeuN results show a strong correlation with the density of MAP-2-positive somata (Fig. 5*C*). Together, these two independent measures demonstrate that the num-

ber of neurons in the surrounding area of the lesion does not increase significantly between 2 and 5wPL, when significant increases in the density of MAP-2-positive fibers occur.

Functional reorganization is differentially associated with changes in NMDAR1, $GABA_A\alpha1$, glutamate, and GABA levels

Immunoblotting analysis of receptor proteins show that at 1wPL NMDAR1 subunit was 84% below control. However, protein levels increased subsequently, such that by 2 and 5wPL NMDAR1 subunit levels had recovered to 46 and 77%, respectively, of the control (Fig. 6*A*,*C*). One-way ANOVA showed significant differences ($p < 0.01$) between control and all time points including 5wPL, despite the clear recovery in NMDAR1 levels observed by that point (Fig. 6*C*).

Total contents of different amino acids as measured from HPLC from control animals and animals killed after 1, 2, and 5wPL are shown in Table 1. Significant changes between 1 and 5wPL were only detected for the excitatory amino acids, aspartate, and glutamate. Glutamate levels were diminished by 74% at 1wPL with respect to control (Fig. 6*E*; Table 1). This value was not significantly different from the value of 75% obtained at 2wPL. However, total contents of glutamate continued to increase toward control values such that at 5wPL a statistically significant rise of 90% ($p < 0.05$) was observed when compared with 1wPL (Fig. 6*E*).

Contents of $GABA_A\alpha1$ subunit showed a highly significant ($p < 0.01$) decrease of 66% at 1wPL with respect to control values. At 2 and 5wPL, protein levels almost reached control values, being 90 and 78%, respectively, when compared with control (Fig. 6*B*,*D*); these two values were not statistically different from each other or from control values.

Total contents of GABA as measured from HPLC were diminished by 74, 72, and 35% at 1, 2, and 5wPL, respectively, when compared with control values (Fig. 6*F*; Table 1). One-way ANOVA showed that GABA levels were significantly reduced ($p < 0.05$) at all time points when compared with control values and that a slight increase in amino acid contents from 1 to 5wPL was not significant (Fig. 6*F*).

Our data demonstrate that NMDAR1 and glutamate levels upregulate strongly and in parallel over time after the photochemical lesion, whereas the $GABA_A\alpha1$ receptor subunit exhibits an upregulation and GABA levels remain low throughout the explored period of time.

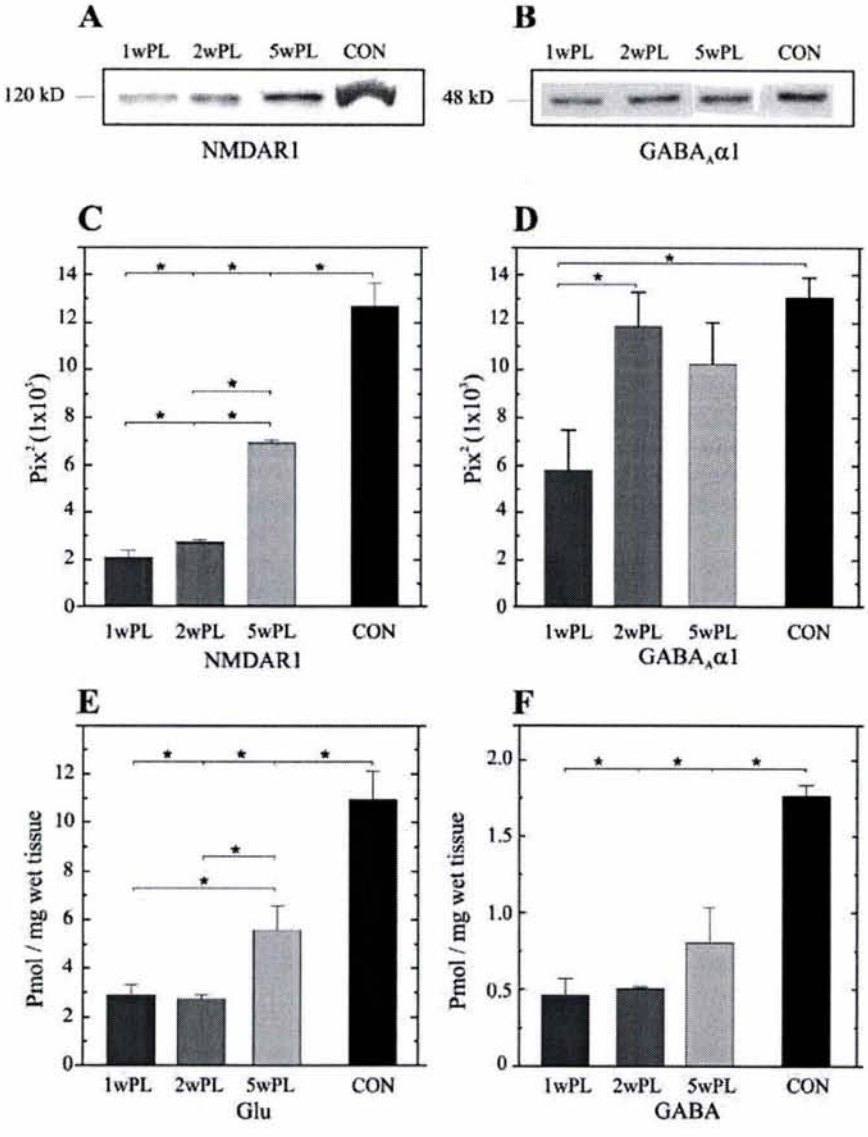

Figure 6. Time-dependent modifications in NMDAR1 and $GABA_A\alpha1$ contents and in glutamate and GABA levels in the center and surrounding area of the lesion. Representative Western blots of NMDAR1 (*A*) and $GABA_A\alpha1$ (*B*) obtained from homogenates of the lesion tissue depicted in Figure 4*A* ($n = 3$) are shown. Densitometric analysis of NMDAR1 (*C*) and $GABA_A\alpha1$ (*D*) Western blots from three different animals is shown. Each Western blot was performed two times per animal. Density is expressed as the mean ± SEM. Glutamate (*E*) and GABA (*F*) levels measured with HPLC from homogenates of the lesion tissue depicted in Figure 4*A* are shown. The asterisk denotes a significant difference ($p < 0.05$) between groups.

Discussion

In the present study, we report that cortical retinotopic maps reorganize after an ischemic lesion. Plasticity of functional maps is accompanied over time by morphological and biochemical modifications in the surrounding area of the lesion. Over a 5 week period of recovery, sprouting of MAP-2-positive dendrite-like structures in the surround of a visual cortex ischemic lesion corresponds with an upregulation of MAP-2. Concomitant with morphological modifications, an increase in NMDAR1 protein content parallels an increase in glutamate levels in the area surrounding the lesion (after a pronounced decrease immediately after the lesion).

The enlargement of the area of cortex responding to a stimulus of a given size, as evidenced by our retinotopic mapping procedure, constitutes a mechanism by which the representation of the retinal input in the visual cortex is reorganized after a focal lesion. At the single-cell level, this corresponds to an increase in receptive field size such that parts of the visual field originally represented in the lesion area of cortex are encompassed (Eysel

Table 1. Temporal course of amino acid levels from the lesion area

Amino acid	Control	1wPL	2wPL	5wPL
Asp	3.65 ± 0.44	0.96 ± 0.12	0.98 ± 0.019	1.66 ± 0.14*
Glu	10.95 ± 1.1	2.93 ± 0.40	2.76 ± 0.14	5.60 ± 0.95*
Gln	4.84 ± 0.27	1.60 ± 0.26	1.70 ± 0.20	2.86 ± 0.53
Gly	3.27 ± 0.15	2.58 ± 1.56	2.20 ± 1.35	2.06 ± 0.08
Tau	3.28 ± 1.23	0.29 ± 0.04	0.31 ± 0.02	0.96 ± 0.41
Ala	1.10 ± 0.94	1.24 ± 0.23	0.98 ± 0.06	1.96 ± 0.33
GABA	1.76 ± 0.06	0.46 ± 0.10	0.50 ± 0.008	0.81 ± 0.22

Control refers to homogenates of area 17 from a nonlesioned animal. The mean group data ± SE ($n = 3$) are shown. *$p < 0.03$ (comparisons were made between 1 and 5wPL).

and Schweigart, 1999; Schweigart and Eysel, 2002). A similar expansion of cortical receptive fields after focal retinal lesions is well documented (Kaas et al., 1990; Das and Gilbert, 1995a,b) and has been attributed to axonal sprouting of horizontal connections within the visual cortex (Gilbert and Wiesel, 1985; Darian-Smith and Gilbert, 1994, 1995).

Here, we correlated in time the reorganization of the visual cortical maps after cortical lesions with changes in cellular markers of plasticity that have been associated with mechanisms underlying functional reorganization after injury. Some of these mechanisms include dendritic and axonal sprouting, synaptogenesis, and altered synaptic efficacy (Kaas, 1991; Buonomano and Merzenich, 1998).

Cytoskeletal modifications require MAPs, such as MAP-2. Suppression of MAP-2 expression in cultured neurons inhibits neurite outgrowth and reduces neurite number (Caceres et al.,1992; Sharma et al., 1994), suggesting that MAP-2-mediated regulation of microtubules is important for dendrogenesis. MAP-2 immunoreactivity (MAP-2-IR) has been considered a suitable marker for dendrites based on experimental evidence that closely correlates dendritic growth with an increase in MAP-2-IR (Philpot et al., 1997; Sanchez et al., 2000; Bury and Jones; 2002). MAP-2 has been shown to be absent in injured neurons (Arias et al., 1997). Our data also show that at 1wPL MAP-2-immunopositive structures have disappeared from the core of the lesion. The amount of MAP-2 immunolabeling changed gradually over time and correlated with modifications in the contents of GFAP-immunopositive astrocytes. After 5wPL, MAP-2-immunopositive fibers were not only found in the boundary zone of the ischemic center but in closest proximity to the lesion core, where the glial scar (which lines the wall of the lesion) was predominant. At every time point studied, astrocytes surrounding the lesion core were anisomorphic. However, the density of the gliotic scar diminished over time, which may be partially related to the decrease in astrocytic division and migration toward the lesion area (Bignami and Dahl, 1995). Previous studies have shown that MAP-2-IR increases after cortical damage with a similar time course as that reported here (Bidmon et al., 1998; Li et al., 1998). However, to our knowledge, this is the first study showing localization of reactive astroglia mixed with dendritic-like structures, as morphological evidence of sprouting, as early as 2 weeks after an ischemic lesion.

In agreement with immunohistochemical data, immunoblot results show a time-dependent increase of MAP-2 content in the area surrounding the lesion. Because Western blot analysis was performed from total protein contents, MAP-2 upregulation reflects an increase in protein synthesis over time and discards the possibility that MAP-2 was redistributed in areas other than dendrites. The gradual upregulation in protein contents correlates with the presence of dendritic-like structures and with the observed functional plasticity reported here and in a previous study (Zepeda et al., 2003) and suggests MAP-2 synthesis, leading to dendritic sprouting, as a possible mechanism by which cortical reorganization may occur. Supporting this conclusion, NeuN immuolabeling indicated that the number of neurons did not change between 2 and 5wPL, whereas an increase in the density of MAP2-positive fibers was observed.

The role of axonal sprouting in CNS regeneration is still controversial; however, some studies have correlated axonal elongation with an upregulation of GAP-43. Recent reports (Stroemer et al., 1995; Li et al., 1998; Carmichael et al., 2001; Carmichael and Chesselet, 2002) describe an increase in GAP-43 immunoreactivity from day 3 until day 14 postlesion. Our results also show an increase in GAP-43 contents at 2wPL, but this is followed by a decline in protein levels toward 5wPL (Stroemer et al., 1995). As suggested previously, GAP-43 may be involved in the initiation of axonal growth, whereas the full regenerative program is accomplished by another set of proteins (Strata et al., 1999). In contrast, axonal sprouting cannot solely be determined on GAP-43 levels alone, because GAP-43 is not a rigid marker of axonal sprouting (Szele et al., 1995). After cortical and peripheral lesions, axonal sprouting has been shown to occur in local circuit connections, but no axonal remodeling was detected at the thalamocortical level (Darian-Smith and Gilbert, 1994; Carmichael et al., 2001). Thus, although the gradual increase in MAP-2 expression in our model correlates more evidently in time with functional reorganization than GAP-43 expression, we cannot rule out the possibility that axonal sprouting may take place at some point in the recovery process.

In addition to morphological modifications occurring in the surrounding area of the lesion, neurochemical transmission changes have been proposed to play a role in reorganization of cortical maps. A variety of studies have suggested that the balance between excitation and inhibition modulate plastic responses in the CNS after peripheral or central injuries (Schiene et al., 1996; Neumann-Haefelin et al., 1998; Que et al., 1999a,b; Arckens et al., 2000; Redecker et al., 2002), but only few studies (Qu et al., 2003) correlate time-dependent changes in neurotransmitter systems with functional recovery, which may reflect biochemical adjustments involved in shaping neuronal receptive fields during functional reorganization. Reduction of cortical inhibitory tone through a decrease in the availability of GABA or an increase in glutamate transmission have been suggested as possible mechanisms underlying functional reorganization (Garraghty et al., 1991). Changes at the amino acid level could reflect the activation of adaptive presynaptic mechanisms, whereas modifications in the receptor subunits explored in this study could be related to postsynaptic responses that lead to changes in the excitatory/inhibitory neurotransmission balance. These changes differed not only with regard to their time course but also in magnitude. The upregulation of NR1, the mandatory subunit of the NMDA receptor, between 1wPL and 5wPL was paralleled by a substantial

recovery in glutamate levels. Our results extend previously existing data that have shown increased excitability during functional recovery in the vicinity of cortical lesions (Schiene et al., 1996; Hagemann et al., 1998). We observed that the lowest levels in NR1 coincide in time with the largest functionally silent region produced by the lesion (1wPL) and that the increase in NR1 at 2wPL and the additional rise by 5wPL correlate well in time with the functional reorganization process (Zepeda et al., 2003). Thus, as shown previously for peripheral lesions (Myers et al., 2000), it is likely that the NMDA receptor participates in the synaptic changes that contribute to functional reorganization after focal cortical lesions. An increase in NMDA receptor activation could, on the one hand, mediate an increase in neuronal excitability but could also contribute to morphological modifications particularly associated with cytoskeletal changes (Montoro et al., 1993). Furthermore, the parallel increase in glutamate levels probably reflects excitatory adaptive changes at the presynaptic and postsynaptic levels. The increase of excitatory amino acid levels seems to be specific because contents of other nontransmitter amino acids, which were measured in parallel, did not change in a similar magnitude. There is evidence that changes in the GABAergic system occur after ischemic and other lesion protocols (Domann et al., 1993; Mittmann et al., 1994; Schiene et al., 1996; Neumann-Haefelin et al., 1998). Interestingly, in our model, GABA levels diminished and remained reduced after 1, 2, and 5wPL in agreement with previous reports (Domann et al., 1993; Mittmann et al., 1994; Neumann-Haefelin et al., 1998), whereas $GABA_A\alpha1$ receptor subunit contents recovered almost to control levels after 2 and 5wPL. Taken together, our results show that during reorganization of retinotopic maps after an ischemic lesion, content of GABA is reduced and that although the density of postsynaptic $GABA_A\alpha1$ increases, the $GABA_A$ receptor may not be saturated, resulting in reduced GABAergic inhibition. Reduced GABA levels in visual cortex after several peripheral manipulations have been reported previously (Jones, 1993). It has also been suggested that GABA metabolism can determine inhibitory synaptic strength and that presynaptic GABA content is a regulated mechanism for synaptic plasticity (Engel et al., 2001).

In conclusion, our results suggest that during functional recovery between 2 and 5wPL differential changes between GABAergic and glutamatergic transmission occur. In addition, modifications in the dendritic structure in the surrounding area of the lesion may contribute synergistically to biochemical adjustments, thus providing the basis for the reorganization of the cortical maps after focal ischemic damage. Our results also provide valuable information about "windows of opportunity" in which therapeutic interventions may affect the physiological process underlying functional reorganization.

References

Arckens L, Schweigart G, Qu Y, Wouters G, Pow DV, Vandesande F, Eysel UT, Orban GA (2000) Cooperative changes in GABA, glutamate and activity levels: the missing link in cortical plasticity. Eur J Neurosci 12:4222–4232.

Arias C, Arrieta I, Massieu L, Tapia R (1997) Neuronal damage and MAP2 changes induced by the glutamate transport inhibitor dihydrokainate and by kainate in rat hippocampus in vivo. Exp Brain Res 116:467–476.

Bidmon HJ, Jancsik V, Schleicher A, Hagemann G, Witte OW, Woodhams P, Zilles K (1998) Structural alterations and changes in cytoskeletal proteins and proteoglycans after cortical ischemia. Neuroscience 82:397–420.

Bignami A, Dahl D (1995) Gliosis. In: Neuroglia (Kettenmann H, Ransom BR, eds), pp 843–858. New York: Oxford UP.

Bonhoeffer T, Grinvald A (1993) The layout of iso-orientation domains in area 18 of cat visual cortex: optical imaging reveals a pinwheel-like organization. J Neurosci 13:4157–4180.

Bonhoeffer T, Grinvald A (1996) Optical imaging based on intrinsic signals. The methodology. In: Brain mapping: the methods (Toga A, Mazziota J, eds), pp 55–97. London: Academic.

Buonomano DV, Merzenich MM (1998) Cortical plasticity: from synapses to maps. Annu Rev Neurosci 21:149–186.

Bury SD, Jones TA (2002) Unilateral sensorimotor cortex lesions in adult rats facilitate motor skill learning with the "unaffected" forelimb and training-induced dendritic structural plasticity in the motor cortex. J Neurosci 22:8597–8606.

Caceres A, Mautino J, Kosik KD (1992) Suppression of MAP2 in cultured cerebellar macroneurons inhibits minor neurite formation. Neuron 9:607–618.

Carmichael ST (2003) Plasticity of cortical projections after stroke. Neuroscientist 9:64–75.

Carmichael ST, Chesselet MF (2002) Synchronous neuronal activity is a signal for axonal sprouting after cortical lesions in the adult. J Neurosci 22:6062–6070.

Carmichael ST, Wei L, Rovainen CM, Woolsey TA (2001) New patterns of intracortical projections after focal cortical stroke. Neurobiol Dis 8:910–922.

Castro MA, Borrell J (1995) Functional recovery of forelimb response capacity after forelimb primary motor cortex damage in the rat is due to the reorganization of adjacent areas of the cortex. Neuroscience 68:793–805.

Coq JO, Xerri C (1999) Acute reorganization of the forepaw representation in the rat SI cortex after focal cortical injury: neuroprotective effects of piracetam treatment. Eur J Neurosci 11:2597–2608.

Darian-Smith C, Gilbert CD (1994) Axonal sprouting accompanies functional reorganization in adult cat striate cortex. Nature 368:737–740.

Darian-Smith C, Gilbert CD (1995) Topographic reorganization in the striate cortex of the adult cat and monkey is cortically mediated. J Neurosci 15:1631–1647.

Das A, Gilbert CD (1995a) Receptive field expansion in adult visual cortex is linked to dynamic changes in strength of cortical connections. J Neurophysiol 74:779–792.

Das A, Gilbert CD (1995b) Long-range horizontal connections and their role in cortical reorganization revealed by optical recording of cat primary visual cortex. Nature 375:780–784.

Dijkhuizen RM, Singhal AB, Mandevill JB, Wu O, Halpern EF, Finklestein SP, Rosen BR, Lo EH (2003) Correlation between brain reorganization, ischemic damage, and neurologic status after transient focal cerebral ischemia in rats: a functional magnetic resonance imaging study. J Neurosci 23:510–517.

Domann R, Hagemann G, Kraemer M, Freund HJ, Witte OW (1993) Electrophysiological changes in the surrounding brain tissue of photochemically induced cortical infarcts in the rat. Neurosci Lett 155:69–72.

Engel D, Pahner I, Schulze K, Frahm C, Jarry H, Ahnert-Hilger G, Draguhn A (2001) Plasticity of rat central inhibitory synapses through GABA metabolism. J Physiol (Lond) 535:473–482.

Eysel UT, Schweigart G (1999) Increased receptive field size in the surround of chronic lesions in the adult cat visual cortex. Cereb Cortex 9:101–109.

Florence SL, Kaas JH (1995) Large-scale reorganization at multiple levels of the somatosensory pathway follows therapeutic amputation of the hand in monkeys. J Neurosci 15:8083–8095.

Garraghty PE, LaChica EA, Kaas JH (1991) Injury-induced reorganization of somatosensory cortex is accompanied by reductions in GABA staining. Somatosens Mot Res 8:347–354.

Geddes JW, Wood JD (1984) Changes in the amino acid content of nerve endings (synaptosomes) induced by drugs that alter the metabolism of glutamate and G-aminobutyric acid. J Neurochem 42:16–24.

Gilbert CD, Wiesel TN (1985) Intrinsic connectivity and receptive field properties in visual cortex. Vision Res 25:365–374.

Hagemann G, Redecker C, Neumann-Haefelin T, Freund HJ, Witte OW (1998) Increased long-term potentiation in the surround of experimentally induced focal cortical infarction. Ann Neurol 44:255–258.

Jones EG (1993) GABAergic neurons and their role in cortical plasticity in primates. Cereb Cortex 3:361–372.

Jones TA, Schallert T (1992) Overgrowth and prunning of dendrites in adult rats recovery from neocortical damage. Brain Res 581:156–160.

Jones TA, Kleim JA, Greenough WT (1996) Synaptogenesis and dendritic growth in the cortex opposite unilateral sensoriomotor cortex damage in

adult rats: a quantitative electron microscopic examination. Brain Res 733:142–148.

Kaas JH (1991) Plasticity of sensory and motor maps in adult mammals. Annu Rev Neurosci 14:137–167.

Kaas JH, Krubitzer LA, Chino YM, Langston AL, Polley EH, Blair N (1990) Reorganization of retinotopic cortical maps in adult mammals after lesions of the retina. Science 248:229–231.

Laemmli UK (1970) Cleavage of structural proteins during the assembly of the head of bacteriophage T4. Nature 227:680–685.

Li Y, Jiang N, Powers C, Chopp M (1998) Neuronal damage and plasticity identified by microtubule-associated protein 2, growth associated protein 43, and cyclin D1 immunoreactivityafter focal cerebral ischemia in rats. Stroke 29:1972–1980.

Mittmann T, Eysel UT (2001) Increased synaptic plasticity in the surround of visual cortex lesions in rats. NeuroReport 12:3341–3347.

Mittmann T, Luhmann H, Schmidt-Kastner R, Eysel U, Weigel H, Heinemann U (1994) Lesion-induced transient supression of inhibitory function in rat neocortex in vitro. Neuroscience 60:891–906.

Montoro RJ, Diaz-Nido J, Avila J, Lopez-Barneo J (1993) *N*-methyl-D-aspartate stimulates the dephosphorylation of the microtubule-associated protein 2 and potentiates excitatory synaptic pathways in the rat hippocampus. Neuroscience 54:859–871.

Mullen RJ, Buck CR, Smith AM (1992) NeuN, a neuronal specific nuclear protein in vertebrates. Development 116:201–211.

Myers WA, Churchill JD, Muja N, Garraghty PE (2000) Role of NMDA receptors in adult primate cortical somatosensory plasticity. J Comp Neurol 418:373–382.

Neumann-Haefelin T, Staiger JF, Redecker C, Zilles K, Fritschy JM, Mohler H, Witte OW (1998) Immunohistochemical evidence for dysregulation of the GABAergic system ipsilateral to photochemically induced cortical infarcts in rats. Neuroscience 87:871–879.

Nudo RJ, Wise BM, SiFuentes F, Milliken GW (1996a) Neural substrates for the effects of rehabilitative training on motor recovery after ischemic infarct. Science 272:1791–1794.

Nudo RJ, Milliken GW, Jenkins WM, Merzenich MM (1996b) Use-dependent alterations of movement representations in primary motor cortex of adult squirrel monkeys. J Neurosci 16:785–807.

Peters A, Yilmaz E (1993) Neuronal organization in area 17 of cat visual cortex. Cereb Cortex 3:49–68.

Philpot BD, Lim JH, Halpain S, Brunjes PC (1997) Experience-dependent modifications in MAP2 phosphorylation in rat olfactory bulb. J Neurosci 17:9596–9604.

Qu Y, Massie A, Van der Gucht E, Cnops L, Vandenbussche E, Eysel UT, Vandesande F, Arckens L (2003) Retinal lesions affect extracellular glutamate levels in sensory-deprived and remote non-deprived regions of cat area 17 as revealed by in vivo microdialysis. Brain Res 962:199–206.

Que M, Schiene K, Witte OW, Zilles K (1999a) Widespread up-regulation of N-methyl-D-aspartate receptors after focal photothrombotic lesion in rat brain. Neurosci Lett 273:77–80.

Que M, Witte OW, Neumann-Haefelin T, Schiene K, Schroeter M, Zilles K (1999b) Changes in GABA(A) and GABA(B) receptor binding following cortical photothrombosis: a quantitative receptor autoradiographic study. Neuroscience 93:1233–1240.

Redecker C, Wang W, Fritschy JM, Witte OW (2002) Widespread and long-lasting alterations in GABAA-receptor subtypes after focal cortical infarcts in rats: mediation by NMDA-dependent processes. J Cereb Blood Flow Metab 22:1463–1475.

Rijntjes M, Weiller C (2002) Recovery of motor and language abilities after stroke: the contribution of functional imaging. Prog Neurobiol 66:109–122.

Rouiller EM, Yu XH, Moret V, Tempini A, Wiesendanger M, Liang F (1998a) Dexterity in adult monkeys following early lesion of the motor cortical hand area: the role of cortex adjacent to the lesion. Eur J Neurosci 10:729–740.

Sanchez C, Diaz-Nido J, Avila J (2000) Phosphorylation of microtubule-associated protein 2 (MAP-2) and its relevance for the regulation of the neuronal cytoskeleton function. Prog Neurobiol 61:133–168.

Schiene K, Bruehl C, Zilles K, Qu M, Hagemann G, Kraemer M, Witte OW (1996) Neuronal hyperexcitability and reduction of GABAA-receptor expression in the surround of cerebral photothrombosis. J Cereb Blood Flow Metab 16:906–914.

Schweigart G, Eysel UT (2002) Activity-dependent receptive field changes in the surround of adult cat visual cortex lesions. Eur J Neurosci 15:1585–1596.

Sharma N, Kress Y, Shafit-Zagardo B (1994) Antisense MAP-2 oligonucleotides induce changes in microtubule assembly and neuritic elongation in pre-existing neurites of rat cortical neurons. Cell Motil Cytoskeleton 27:234–247.

Strata P, Buffo A, Rossi F (1999) Mechanisms of axonal plasticity. Arch Ital Biol 137:181–192.

Stroemer RP, Kent TA, Hulsebosch CE (1995) Neocortical neural sprouting, synaptogenesis, and behavioral recovery after neocortical infarction in rats. Stroke 26:2135–2144.

Szele FG, Alexander C, Chesselet MF (1995) Expression of molecules associated with neuronal plasticity in the striatum after aspiration and thermocoagulatory lesions of the cerebral cortex in adult rats. J Neurosci 15:4429–4448.

Watson BD, Dietrich WD, Busto R, Wachtel MS, Ginsberg MD (1985) Induction of reproducible brain infarction by photochemically initiated thrombosis. Ann Neurol 17:497–504.

Zepeda A, Montiel T, Brailowsky S (1999) Functional recovery from cortical hemiplegia in the rat: Effects of a callosotomy. J Neurotrauma 16:267–271.

Zepeda A, Vaca L, Arias C, Sengpiel F (2003) Reorganization of visual cortical maps after focal ischemic lesions. J Cereb Blood Flow Metab 23:811–820.

DISCUSIÓN

La corteza visual está organizada en columnas que se encuentran espacial y funcionalmente interrelacionadas. Debido a la organización retinotópica en V1, todos los elementos que componen un punto en el espacio visual, se representan y analizan en una región delimitada de la corteza denominada "hipercolumna" (Hubel y Wiesel, 1974). La destrucción de una o más hipercolumnas conlleva a la generación de un escotoma cortical, el cual se traduce en la percepción de un punto ciego en el espacio visual. Se ha demostrado que el escotoma visual puede disminuir a través del tiempo, ya sea de forma natural o como resultado de entrenamiento visual (Zihl y von Cramon, 1985; Kasten et al., 1998).

En el presente trabajo se presentan dos tipos de hallazgos importantes: i) que los mapas corticales de orientación preferente y retinotópicos son susceptibles de reorganizarse en un periodo de 2 a 5 semanas posteriores a la inducción de una lesión isquémica en la corteza visual del gato; y ii), que la plasticidad de los mapas funcionales se acompaña a lo largo del tiempo de cambios morfológicos y bioquímicos en el tejido que rodea a la lesión.

Funcionalmente se observó que inmediatamente después de producida la lesión se generaba un área silente de respuesta correspondiente al diámetro (aprox. 3mm) del layo laser empleado para inducir la lesión. Sin embargo entre las semanas 1 y 5PL se observó un proceso de reorganización funcional tanto en los mapas de orientación, como en los retinotópicos. En los mapas de orientación, dicha reorganización se manifestó a las 2sPL como la reaparición de dominios de orientación inicialmente silentes y hacia las 5sPL como el crecimiento de algunos dominios inmediatamente aledaños al centro isquémico. Mientras que la reorganización retinotópica se manifestó como el crecimiento del área de activación celular que produce un estímulo visual y el concomitante sobrelapamiento entre la representación cortical de 2^0 del espacio visual.

El análisis histológico mostró que inmediatamente después de producida la lesión hubo un decremento en el contenido de todas las proteínas evaluadas. Sin embrago, posterior a 2sPL se observó un incremento en el contenido de la proteína GAP-43, el cual volvió a niveles control después de este periodo. Así mismo,

después de 5 semanas de recuperación, se observó rebrote de estructuras dendríticas positivas a MAP-2 y la correspondiente regulación a la alta de la proteína. Concomitante a estas modificaciones morfológicas, se observó un incremento en el contenido de las proteínas NMDAR1 y $GABA_A\alpha 1$ en paralelo a un incremento en los niveles de glutamato, pero no de GABA en el área que rodea a la lesión.

Reorganización de los mapas de orientación preferente

La plasticidad de las representaciones funcionales, principalmente del mapa de orientación preferente, ha sido principalmente abordada con relación a manipulaciones sistema visual periférico (Sengpiel et al., 1998; Schuett et al., 2001). Sin embargo, aún cuando se ha demostrado el potencial de las neuronas visuales de la corteza cerebral, de modificar sus respuestas como consecuencia de un proceso dependiente de la experiencia, la disposición general del mapa de orientación parece ser muy estable. Esto es, en apoyo a resultados previos (Schuett et al., 2001), en este trabajo no se detectaron cambios con respecto al número y posición de los centros de rehilete en el área de la corteza visual reorganizada, lo que sugiere que los eventos de reorganización están limitados a la restauración de una arquitectura funcional similar a la previa a la lesión.

Los resultados funcionales presentados en este trabajo muestran que si bien la preferencia de su orientación no se modifica en las áreas aledañas a una lesión focal de V1, los circuitos neuronales, si sufren modificaciones que dan lugar a la reorganización del mapa cortical de orientación.

Recientemente se han empezado a evaluar algunos eventos fisiológicos que suceden ante una lesión focal de V1. Eysel y Schweigart (1999) mostraron que 55 días después de la inducción de una lesión focal en V1 de gatos, los campos receptivos de las células aledañas a la lesión se encontraban aumentados de tamaño con respecto al registro control. Sin embargo, reportan no haber encontrado diferencias en la preferencia de orientación de dichas células. Los resultados del trabajo de esta tesis tampoco muestran cambios en la preferencia de orientación de

grupos neuronales, pero si una reorganización de tamaño de los dominios preexistentes.

El análisis individual de los dominios de orientación sugiere que dicho proceso de reorganización ocurre en dos fases: Primero, algunos dominios, que desaparecieron inmediatamente post-lesión, se recuperaron a las 2sPL. Esto, como se ha sugerido, podría deberse a la reactivación metabólica de las células que sobrevivieron al evento isquémico (Sharp et al., 2000). El segundo proceso, el cual se observó a las 5sPL, involucra el crecimiento de dominios preexistentes y refleja la reorganización funcional del mapa de orientación. Aún cuando durante el proceso de reorganización se observó revascularización de la zona dañada en algunos animales, ésta no ocurrió en toda la muestra. Así, aunque la perfusión pudiera contribuir a la cascada de eventos involucrada en el proceso de reorganización, esta no parece ser una condición necesaria para su ocurrencia. Debido a ello, es posible que el fenómeno de reorganización observado en este trabajo represente un mecanismo de plasticidad común a diferentes áreas corticales que han sufrido una lesión focal (Doetsch et al., 1990; Nudo et al., 1996b; Eysel y Schweigart, 1999). Más aún, los resultados que se presentan en esta tesis sugieren que los mecanismos de plasticidad cortical no sólo permiten la reorganización de un mapa topográfico, sino también de un mapa que representa una característica particular de los estímulos visuales.

Resulta difícil determinar por qué sólo algunos de los dominios en el borde original de la lesión se expanden mientras que otros mantienen su tamaño original. Este fenómeno podría reflejar la anisotropía en la contracción de la cicatriz del tejido. Sin embargo, en trabajos previos se ha descrito la expansión diferencial de dominios funcionales localizados en la corteza somatosensorial de animales ennucleados (Bronchti et al., 1992; Rauschecker et al., 1992) y de ratas a las que se les han cauterizado los bigotes como un procedimiento de desaferentación sensorial (Woolsey y Wann, 1976).

Reorganización de los mapas retinotópicos

Los resultados de este trabajo muestran que en un periodo de 5 semanas posterior a una lesión isquémica focal de la corteza visual, el área funcional cortical que responde a un estímulo visual de un tamaño determinado, crece. Este fenómeno podría constituir un mecanismo por medio del cual la representación de la entrada de la información visual se reorganiza como consecuencia de una lesión focal cortical.

Los resultados obtenidos en el presente trabajo sugieren un mecanismo de readaptación funcional que subyace a la reducción del escotoma visual. El sobrelapamiento natural en la activación cortical por dos puntos adyacentes en el campo visual desaparece después de una lesión focal cortical. Sin embargo, el área cortical implicada en el procesamiento de la información de un punto en el campo visual crece con el tiempo, de forma tal, que áreas inicialmente no involucradas en el procesamiento de información de ese punto en el espacio, se activan. Este resultado sugiere que grupos de neuronas cercanos a la lesión responderán a estimulación visual en un área más grande del campo visual, esto es, su campo receptivo habrá incrementado.

Nuestros resultados concuerdan con un estudio reciente (Eysel y Schweigart, 1999) en el que se reporta que 55 días después de que se indujera una lesión excitotóxica en la corteza visual primaria del gato adulto, hubo un crecimiento significativo de los campos receptivos visuales de las células inmediatamente adyacentes a la lesión. La técnica empleada en el trabajo que aquí se presenta, posibilitó el monitorear en el tiempo la respuesta de grupos neuronales mucho más grandes que los evaluados por Eysel y Schweigart (1999). De esta manera, a partir del análisis por imagenología óptica se obtienen resultados más representativos de lo que ocurre en poblaciones neuronales durante el proceso de reorganización, en comparación de los que se obtienen por medio del registro de neuronas únicas.

Resultados recientes de este mismo grupo sugieren que el crecimiento de los campos receptivos se debe al incremento en la excitabilidad neuronal en los bordes de la lesión (Schweigart y Eysel, 2002). Sin embargo, una expansión similar de los campos receptivos se ha observado después de lesiones focales retineanas (Kaas

et al., 1990; Das y Gilbert, 1995a, b), y ello se ha atribuido a un fenómeno de rebrote axónico de conexiones horizontales de la corteza visual (Gilbert y Wiesel, 1985; Darian-Smith y Gilbert, 1994, 1995).

Existe evidencia electrofisiológica y anatómica que demuestra que células con preferencia por una orientación particular están conectadas por fibras intracorticales largas que permiten la sincronización de disparo de células que se encuentran hasta a 2 mm de distancia (Ts'o et al., 1986; Gilbert y Wiesel, 1989; Kisvarday et al., 1994).

Se ha sugerido que las conexiones horizontales de la corteza visual primaria pudieran ser importantes para la integración de información de puntos distantes en el campo visual y para modificaciones contexto-dependientes de las respuestas neuronales. Dado lo anterior, algunos autores han postulado que las conexiones intrínsecas largas pudieran mediar el proceso perceptual de "filling-in" de escotomas reales y artificiales (Ramachandran y Gregory, 1991).

Nuestros resultados sugieren que en el proceso de reorganización cortical visual pudieran estar ocurriendo fenómenos de plasticidad tanto funcional, como estructural. Así, por un lado, el aumento y disminución en algunos elementos de la neurotransmisión excitadora e inhibidora respectivamente pudieran dar lugar al crecimiento de campos receptivos visuales de grupos celulares cercanos a la lesión, mientras que la reorganización dendrítica podría ayudar a establecer o reestablecer circuitos neuronales perdidos o alterados a consecuencia de la lesión.

Modificaciones bioquímicas y anatómicas asociadas a la reorganización funcional visual

Un aspecto relevante que subyace a la reorganización funcional, se refiere a los mecanismos celulares y moleculares que se activan y permiten la reestructuración de campos receptivos visuales posterior a un daño en el SNC. Este aspecto fue abordado en el presente trabajo correlacionando en el tiempo la reorganización de los mapas corticales visuales con cambios en algunos marcadores moleculares de plasticidad sináptica. Algunos de estos marcadores se relacionan con la activación

de mecanismos que incluyen el rebrote dendrítico y axónico, la sinaptogénesis y alteraciones en la eficacia sináptica (Kaas, 1991; Buonomano y Merzenich, 1998).

En el caso de los sistemas motor, somatosensorial y visual, los mecanismos plásticos implicados en la reorganización dependen en gran medida del nivel de la lesión y por tanto, pueden involucrar diferentes mecanismos. Así por ejemplo, se ha sugerido que la remodelación topográfica temprana y tardía que ocurre después de lesiones a la retina (Kaas et al., 1990; Gilbert y Wiesel, 1992), depende de circuitos remanentes que proveen conectividad cruzada en el área lesionada (Calford et al., 1999), aunque también se ha propuesto que la reorganización depende de la reconexión funcional a nivel del núcleo geniculado lateral (Eysel, 1982) y en mayor medida, del rebrote de colaterales axónicas provenientes del tálamo y de circuitos locales corticales (Darian-Smith y Gilbert, 1994, 1995; Das y Gilbert, 1995b).

Las modificaciones del citoesqueleto neuronal requieren de la participación concertada de diferentes tipos de proteínas. En el caso de la remodelación dendrítica, hay evidencia importante que muestra la participación de proteínas asociadas a los microtúbulos, como MAP-2 (Sanchez et al., 2000). La supresión de MAP-2 en neuronas en cultivo inhibe el crecimiento y reduce el número de neuritas (Caceres et al., 1992; Sharma et al., 1994), lo que sugiere que la regulación de los microtúbulos mediada por MAP-2 es importante para la dendritogénesis.

Las modificaciones temporales en el contenido de MAP-2 se observaron de manera distinta dependiendo de la presencia de elementos inmunoreactivos a GFAP. Así, hacia las 2sPL en que se observa una malla densa de fibras y células GFAP-positivas, hay una presencia escasa de fibras inmunoreactivas para MAP-2 alrededor de la lesión, mientras que para la semana 5PL, en que el contenido de glia anisomórfica disminuye, aumenta el contenido de fibras MAP-2-positivas, no sólo en el área que rodea a la lesión, sino en los bordes mismos del centro de la lesión. En todo momento, la glia que rodea al tejido lesionado es de tipo anisomórfico. Sin embrago, la cicatriz glial aparece menos densa a la semana 5PL en comparación con las semanas 1 y 2 PL. Esto puede deberse parcialmente al decremento en la división y migración de astrocitos al área de lesión (Bignami y Dahl, 1995). Existe evidencia de que los astrocitos reactivos secretan factores

neurotróficos y pueden participar en la formación de la lámina basal a través de la síntesis de diferentes proteínas de matriz. Así, es posible que la presencia de neurotrofinas y la reestructuración parcial de la matriz extracelular por parte de los astrocitos, genere un ambiente más permisivo para la elongación y rebrote neurítico (Gage et al., 1988; Bignami y Dahl, 1995; Le Roux y Reh, 1996).

Los resultados preeliminares de este trabajo, en conjunto con otros estudios, apoyan la posibilidad de que la presencia de astrocitos es compatible con el rebrote axónico y dendrítico aledaño a una lesión central (Gage et al., 1988; Anders y Johnson, 1990). Aunque un aspecto que resulta de la afirmación anterior y que es muy importante explorar a futuro, es el del cambio a lo largo del tiempo, del microambiente que rodea a la lesión isquémica, particularmente relacionado con el contenido de proteínas de matriz extracelular posiblemente secretadas por la glía durante el proceso de evolución de la lesión.

En concordancia con los resultados de la inmunohistoquímica, los datos obtenidos de la cuantificación de proteína muestran un incremento dependiente del tiempo en el contenido de MAP-2 en el área que rodea a la lesión. Dado que el análisis por Western blot se realizó a partir del contenido total de proteína, la regulación al alta de MAP-2 refleja un incremento a lo largo del tiempo en la síntesis de proteína y descarta la posibilidad de que la proteína estuviera redistribuida en otras áreas celulares que no fueran las dendritas. La regulación gradual al alta del contenido de proteína correlaciona con la presencia de estructuras tipo dendrítico y con la plasticidad funcional visual, lo que sugiere que este fenómeno de aumento en el contenido de MAP-2 es concomitante con el rebrote dendrítico, y se postula como un posible mecanismo que subyace a la reorganización funcional cortical. Esta conclusión se fortalece a partir del resultado que muestra que el contenido total de NeuN, una proteína exclusiva de núcleos neuronales no cambia entre las semanas 2 y 5 post-lesión, cuando se observan cambios en la densidad de fibras inmuopositivas para MAP-2. Así, un posible mecanismo de plasticidad estructural asociado a las modificaciones funcionales pudiera resultar del establecimiento o reestablecimiento de circuitos neuronales nuevos o preestablecidos por medio del rebrote dendrítico.

El papel del rebrote axónico en la regeneración del sistema nervioso central es aún un tema controvertido. Sin embargo, algunos estudios han establecido una correlación entre la elongación axónica y la regulación a la alta de proteínas como la GAP-43 debido a que esta proteína sólo se encuentra en los conos de axones en crecimiento (Stroemer et al., 1995; Li et al., 1998; Carmichael et al., 2001; Carmichael y Chesselet, 2002). Más aún, algunos de estos estudios (Stroemer et al., 1995; Li et al., 1998) describen un aumento en la inmunoreactivdad de GAP-43 entre los días 3 y 14 posteriores a una lesión cortical, lo cual correlaciona temporalmente con fenómenos de recuperación funcional (Stroemer et al., 1995).

Los resultados de esta tesis, coincidentes con estudios previos (Stroemer et al., 1995), también muestran un incremento en el contenido de GAP-43 a las 2sPL, seguida de un decremento en los niveles de la proteína hacia las 5 semanas post-lesión. Como se ha sugerido, GAP-43 podría estar implicada en la iniciación del proceso de crecimiento axónico, mientras que el programa completo de regeneración lo lleva a cabo otro grupo de proteínas (Strata et al., 1999). Aunado a ello, se debe considerar que el proceso de rebrote axónico no puede estar exclusivamente determinado por los niveles de GAP-43, dado que éste no es el único marcador de rebrote axónico (Szele et al., 1995). Debido a que GAP-43 evalúa la presencia de conos de crecimiento, y en este modelo se exploró el rebrote regenerativo, no se puede descartar que hubiera rebrote colateral en donde no necesariamente hay presencia de GAP-43.

Se ha demostrado que el fenómeno de rebrote axónico ocurre en circuitos locales, no a nivel tálamocortical después de lesiones tanto periféricas, como centrales (Darian-Smith y Gilbert, 1994; Carmichael et al., 2001). Así, aun cuando el incremento gradual de MAP-2 en el modelo empleado en esta tesis correlaciona más evidentemente con la reorganización funcional que la expresión de GAP-43, no se puede descartar la posibilidad de que el rebrote axónico pudiera estar jugando un papel en algún momento del proceso de reorganización.

Junto con las modificaciones morfológicas que ocurren alrededor de una lesión central, también se ha postulado que cambios a nivel de la transmisión neuroquímica pudieran jugar un papel en la reorganización de los mapas corticales.

Diversos estudios han sugerido que el balance entre la excitación y la inhibición de circuitos neuronales, modulan respuestas plásticas en el sistema nervioso central después de lesiones tanto centrales como periféricas (Schiene et al., 1996; Que et al., 1999a; Que et al., 1999b; Neumann-Haefelin y Witte, 2000; Que et al., 2000; Redecker et al., 2000), pero sólo pocos estudios (Massie et al., 2003; Qu et al., 2003) correlacionan cambios a lo largo del tiempo en el contenido de neurotransmisores particulares con la recuperación funcional. Lo anterior podría reflejar ajustes bioquímicos implicados en el moldeamiento de campos receptivos visuales neuronales durante un proceso de reorganización funcional.

El desenmascaramiento de vías preexistentes, pero funcionalmente inactivas, puede deberse a diversos mecanismos, que incluyen el incremento en el contenido y liberación del neurotransmisor excitador, cambios en la conductancia iónica a través de la membrana que aumenten los efectos de "inputs" débiles o distantes el incremento de receptores excitadores en la densidad post-sináptica y/o la regulación a la baja de la transmisión inhibidora (Kaas, 1991; Chen et al., 2002).

En el presente trabajo, evaluamos tres parámetros de lo mencionado anteriormente estudiando el contenido total de neurotransmisores y de dos proteínas esenciales de los sistemas inhibidor y excitador, las subunidades a1 del receptor $GABA_A$ ($GABA_A\alpha1$) y NMDAR1 respectivamente.

Diversos estudios farmacológicos han demostrado que la inhibición GABAérgica es crucial para el mantenimiento de las representaciones corticales y que el antagonismo de ésta resulta en el crecimiento de los campos receptivos de células corticales (Sillito, 1974a, b, 1975a, b) y también en la desaparición de los límites de mapas o representaciones corticales completas (Jacobs y Donoghue, 1991). Ambos fenómenos se han detectado en los bordes de lesiones focales (Nudo et al., 1996a; Eysel y Schweigart, 1999) y se han correlacionado con la recuperación funcional del sistema afectado. Por ello, se ha planteado que modificaciones del sistema GABAérgico pudieran jugar un papel importante en el fenómeno de reorganización funcional cortical post-lesión.

La reducción del tono inhibidor cortical mediante el decremento en la disponibilidad de GABA o del incremento en la trasmisión de glutamato han sido

sugeridos como posibles mecanismos que subyacen a la reorganización funcional (Garraghty et al., 1991). Cambios en los niveles de GABA o glutamato pudieran reflejar la activación de mecanismos presinápticos adaptativos, mientras que las modificaciones en las subunidades de los receptores evaluados en este estudio pudieran relacionarse con cambios en respuestas postsinápticas que conlleven a cambios en el balance de la neurotransmisión inhibidora/excitadora. En el presente trabajo los cambios en elementos de la neurotransmisión pre y postsináptica difirieron no sólo con respecto al curso temporal, sino también en magnitud. La regulación a la alta entre 1 y 5sPL de NR1, la subunidad que permite el anclaje del receptor funcional de tipo NMDA, se acompañó de una recuperación sustancial de los niveles de glutamato. Nuestros resultados amplían así datos previos en los que se muestra un incremento en la excitabilidad neuronal durante un proceso de recuperación funcional en la vecindad de lesiones corticales (Schiene et al., 1996; Hagemann et al., 1998). En el presente trabajo se observó que los niveles más bajos de NR1 coincidían en el tiempo (1sPL) con la región de silencio funcional producto de la lesión, y que el incremento de NR1 a las 2sPL y el incremento subsecuente a las 5sPL correlacionaban en el tiempo con el proceso de reorganización. Así, como se ha mostrado previamente con respecto a lesiones periféricas (Myers et al., 2000), es posible que el receptor NMDA participe en los cambios sinápticos que contribuyen en la reorganización funcional posterior a lesiones focales corticales. El incremento en la activación del receptor NMDA pudiera por un lado mediar un aumento en la excitabilidad neuronal, pero también pudiera contribuir a las modificaciones morfológicas asociadas particularmente con cambios del citoesqueleto neuronal (Montoro et al., 1993). Más aún, el incremento paralelo en los niveles de glutamato probablemente reflejen cambios adaptativos en la neurotransmisión excitadora tanto a nivel pre como postsináptico. El incremento en los niveles de aminoácidos excitadores parece ser un fenómeno específico, ya que no se observó un incremento de la misma magnitud en el contenido de aminoácidos no transmisores evaluados en paralelo. Existe evidencia que después de una lesión isquémica y de otros tipos (Domann et al., 1993; Mittmann et al., 1994; Schiene et al., 1996; Neumann-Haefelin et al., 1998) se observan cambios en

el sistema GABAérgico. De acuerdo con reportes previos, en el modelo empleado en esta tesis, los niveles de GABA disminuyeron y permanecieron reducidos después de 1 2 y 5sPL (Domann et al., 1993; Mittmann et al., 1994; Neumann-Haefelin et al., 1998), mientras que el contenido de la subunidad $GABA_{A\alpha}1$ se recuperó a nivel casi control después de 2 y 5sPL.

En conjunto estos resultados muestran que durante un proceso de reorganización de mapas visuales corticales como resultado de una lesión isquémica, el contenido de GABA se reduce y que aunque el contenido postsináptico de $GABA_A\alpha1$ incrementa, el receptor $GABA_A$ puede no estar saturado dando así lugar a una reducción de la inhibición GABAérgica. Este aspecto podría ser relevante desde el punto de vista que se describiría que la regulación de la transmisión inhibidora ocurre preferentemente a nivel del contenido y disponibilidad del transmisor. Los niveles reducidos de GABA en la corteza visual como consecuencia de manipulaciones periféricas diversas ha sido previamente reportado (Jones, 1993). También se ha sugerido que el metabolismo de GABA puede determinar la fuerza sináptica inhibidora y que el contenido presináptico de GABA es un mecanismo regulado de plasticidad sináptica (Engel et al., 2001).

Lo anterior sugiere que un proceso relacionado al desenmascaramiento de vías podría estar teniendo lugar durante el proceso de reorganización funcional visual cortical aunque el abordaje de este trabajo no permite determinar si los cambios en el contenido de las subunidades implica la formación de receptores funcionales. Sin embargo, cambios en la expresión de una subunidad podría afectar la composición de los receptores sinápticos e influir en la respuesta del receptor.

Los resultados de este trabajo sugieren que en paralelo a las modificaciones en el contenido de glutamato, NMDAR1 y $GABAA\alpha1$, también hay un aumento dependiente del tiempo del contenido tanto de GAP-43, como de MAP-2. Sin embargo, cabe resaltar que tanto la manifestación, como la temporalidad de estos eventos se deben circunscribir al área y modelo de lesión empleado, ya que se ha observado que las respuestas nerviosas ante un proceso de daño pueden diferir de forma importante dependiendo del tipo de este último (Mir et al., 2004).

El papel de neurotransmisores como agentes neurotróficos y como moduladores de plasticidad estructural está bien documentado (Leslie, 1993). Así, se ha demostrado que los aminoácidos excitadores, como el glutamato, incrementan el rebrote dendrítico de células en cultivo derivadas del hipocampo, cerebelo y médula (Brewer y Cotman, 1989; Montoro et al., 1993), mientras que altos niveles de GABA en combinación con diazepam en cultivos de hipocampo inhiben el crecimiento neurítico hipocampal (Leslie, 1993). Esto es, las modificaciones diferenciales en el contenido de subunidades de receptores y neurotransmisores en el presente trabajo pudieran estar relacionadas con la mediación de procesos plásticos no sólo funcionales, sino también morfológicos si se tiene en cuenta el papel neurotrófico que pueden jugar dichas moléculas.

Tanto los resultados histológicos, como los funcionales, muestran que el área de lesión disminuye a lo largo del tiempo. Este resultado contrasta con otros estudios en los que se ha descrito la disminución del déficit funcional concomitante al crecimiento estructural de la lesión (Baird et al., 1997; Dirnagl et al., 1999). Esta discrepancia podría resultar del hecho de que la lesión fotoquímica genera una isquemia focal y reproducible, mientras que en los estudios mencionados, la lesión inicial era extensa y difusa.

Es importante mencionar que los resultados de este trabajo están basados en experimentos realizados en gatos de 8 a 12 semanas de edad, es decir, dentro del llamado periodo crítico de la plasticidad cortical visual. El periodo crítico se refiere al lapso en el que las manipulaciones de la experiencia visual tienen un mayor efecto en las representaciones corticales establecidas por la entrada de información visual. El correlato molecular de esta incrementada susceptibilidad a las manipulaciones periféricas y las razones por las cuales dicho periodo finaliza, aún están siendo investigadas (para una revisión ver (Katz, 1999).

Estudios previos sobre la reorganización cortical posterior a lesiones extensas han mostrado que la posibilidad de recuperar funciones es mayor en animales jóvenes que en adultos (Payne y Lomber, 2002). Sin embargo, la capacidad de la corteza de compensar lesiones focales pudiera no depender de la edad de los sujetos, ya que en estudios recientes se han observado modificaciones celulares en

etapas tempranas (Schweigart y Eysel, 2002) y tardías (Eysel y Schweigart, 1999) de un proceso de reorganización en gatos adultos.

En conclusión, los resultados de este trabajo muestran que la plasticidad funcional de los mapas de orientación y retinotópico ocurre en consecuencia a una lesión isquémica focal cortical de corteza visual primaria. Más aún la correlación espacio temporal que se estableció entre algunas modificaciones celulares y moleculares y la reorganización de las representaciones corticales visuales, permite sugerir posibles mecanismos anátomo-funcionales por medio de los que ocurre el fenómeno de "relleno" en pacientes que presentan un escotoma cortical. Esto a su vez, abre la posibilidad de conocer algunas de las ventanas de tiempo en las que se pudiera incidir farmacológicamente para inducir o incrementar las respuestas de plasticidad nerviosa que resulten en una recuperación funcional más eficiente en pacientes que han sufrido lesiones focales de tipo isquémico trombótico en el área cortical visual primaria.

CONCLUSIONES

1. La representación cortical de los mapas corticales visuales de orientación y retinotópico se reorganiza como resultado de un evento isquémico en corteza visual

2. El incremento en el tiempo de estructuras inmunopositivas a MAP-2 sugiere la reestructuración de procesos dendríticos; dicha reorganización es espacio-dependiente y coincide temporalmente con la reorganización del mapa funcional visual.

3. Las modificaciones cuantitativas en el contenido de proteínas del citoesqueleto y subunidades de receptores, que coinciden espacio-temporalmente con la reorganización del mapa funcional sugieren la coexistencia de diferentes fenómenos asociados a la neuroplasticidad:

a) El incremento en el tiempo del contenido de MAP-2 en las áreas inmediatas al centro isquémico sugiere un proceso de síntesis de la proteína espacio-dependiente. Debido a que no se observa incremento en el contenido de NeuN se apoya la hipótesis de que la síntesis de MAP-2 depende de las células aledañas a la lesión que sobrevivieron al daño.

b) El incremento de GAP-43 a los 7 y 14 días post-lesión sugiere la presencia de axones en crecimiento. Su posterior regulación a la baja se ha correlacionado con el inicio de un proceso de sinaptogénesis.

c) La regulación a la alta de la subunidad NMDAR1, pero no de la subunidad GABAAα1, sugiere una modulación diferencial en el balance de elementos de la transmisión excitadora e inhibidora en respuesta a la lesión isquémica.

d) Aún cuando el contenido postsináptico de $GABA_A\alpha1$ incrementa, el contenido de GABA permanece reducido, lo que sugiere que el receptor $GABA_A$ pudiera no estar saturado dando así lugar a una reducción de la inhibición GABAérgica.

e) El incremento paralelo en los niveles de NMDAR1 y glutamato sugiere cambios adaptativos asociados a la neurotransmisión excitadora tanto a nivel pre como postsináptico que correlacionan espacio-temporalmente con la reorganización funcional visual.

PERSPECTIVAS

El campo de estudio de la recuperación funcional como consecuencia de la plasticidad nerviosa requiere aún de un importante trabajo de investigación que permita ahondar en la forma en la que las células nerviosas modifican su estructura y función para dar lugar a la reorganización funcional posterior a una lesión focal. Los cambios que permiten modificaciones celulares durante eventos de regeneración están influidos por factores diversos tales como las neurotrofinas y la producción de moléculas de matriz extracelular entre otros, por lo que resulta interesante profundizar en la interacción de estas moléculas en un proceso de neuroreparación. Así mismo, en vista de los hallazgos recientes que sugieren neruogénesis en el mamífero adulto, resulta interesante explorar el posible papel de este fenómeno en eventos de plasticidad regenerativa.

El estudio de la cinética de los eventos que suceden al daño isquémico y el correlacionar la expresión de los diversos factores neurotóxicos y neurotróficos con la evolución temporal del daño, permitirá tener un mejor conocimiento acerca de las moléculas que promueven y limitan la recuperación. Con ello, se abre la posibilidad de proponer terapias farmacológicas que den lugar a la pronta recuperación del paciente teniendo así mismo en cuenta las ventanas de tiempo en las que el tratamiento pudiera resultar más eficaz.

Referencias

Aigner L, Caroni P (1995) Absence of persistent spreading, branching, and adhesion in GAP-43- depleted growth cones. J Cell Biol 128:647-660.

Aigner L, Arber S, Kapfhammer JP, Laux T, Schneider C, Botteri F, Brenner HR, Caroni P (1995) Overexpression of the neural growth-associated protein GAP-43 induces nerve sprouting in the adult nervous system of transgenic mice. Cell 83:269-278.

Albus K, Sieber B (1984) On the spatial arrangement of iso-orientation bands in the cats visual cortical areas 17 and 18: a 14C-deoxyglucose study. Exp Brain Res 56:384-388.

Anders J, Johnson JA (1990) Transection of the rat olfactory nerve increases glial fibrillary acidic protein immunoreactivity from the olfactory bulb to the piriform cortex. Glia 3:17-25.

Baird AE, Benfield A, Schlaug G, Siewert B, Lovblad KO, Edelman RR, Warach S (1997) Enlargement of human cerebral ischemic lesion volumes measured by diffusion-weigthed magnetic resonance imaging. Ann Neurol 41:581-589.

Bergado-Rosado JA, Almaguer-Melian W (2000) Mecanismos celulares de la neuroplasticidad. Rev Neurol 31:1074-1095.

Bidmon HJ, Jancsik V, Schleicher A, Hagemann G, Witte OW, Woodhams P, Zilles K (1998) Structural alterations and changes in cytoskeletal proteins and proteoglycans after focal cortical ischemia. Neuroscience 82:397-420.

Bignami A, Dahl D (1995) Gliosis. In: Neuroglia (Kettenman HR, BR, ed). pp 843–858. New York: Oxford UP.

Blakemore C, Cooper GF (1970) Development of the brain depends on the visual environment. Nature 228:477-478.

Bliss TV, Lomo T (1973) Long-lasting potentiation of synaptic transmission in the dentate area of the anaesthetized rabbit following stimulation of the perforant path. J Physiol 232:331-356.

Bonhoeffer T, Grinvald A (1991) Iso-orientation domains in cat visual cortex are arranged in pinwheel- like patterns. Nature 353:429-431.

Bonhoeffer T, Grinvald A (1996) Optical imaging based on intrinsic signals. The methodology. In: Brain mapping: The methods (Toga A, Mazziota J, eds), pp 55-97. London: Academic Press.

Bonhoeffer T, Kim DS, Malonek D, Shoham D, Grinvald A (1995) Optical imaging of the layout of functional domains in area 17 and across the area 17/18 border in cat visual cortex. Eur J Neurosci 7:1973-1988.

Bosking WH, Crowley JC, Fitzpatrick D (2002) Spatial coding of position and orientation in primary visual cortex. Nat Neurosci 5:874-882.

Bovolenta P, Wandosell F, Nieto-Sampedro M (1993) Characterization of a neurite outgrowth inhibitor expressed after CNS injury. Eur J Neurosci 5:454-465.

Brewer GJ, Cotman CW (1989) NMDA receptor regulation of neuronal morphology in cultured hippocampal neurons. Neurosci Lett 99:268-273.

Bronchti G, Schonenberger N, Welker E, Van der Loos H (1992) Barrelfield expansion after neonatal eye removal in mice. Neuroreport 3:489-492.

Buonomano DV, Merzenich MM (1998) Cortical plasticity: from synapses to maps. Annu Rev Neurosci 21:149-186.

Caceres A, Mautino J, Kosik KD (1992) Suppression of MAP2 in cultured cerebellar macroneurons inhibits minor neurite formation. Neuron 9:607-618.

Calford MB, Schmid LM, Rosa MG (1999) Monocular focal retinal lesions induce short-term topographic plasticity in adult cat visual cortex. Proc R Soc Lond B Biol Sci 266:499-507.

Carmichael ST, Chesselet MF (2002) Synchronous neuronal activity is a signal for axonal sprouting after cortical lesions in the adult. J Neurosci 22:6062-6070.

Carmichael ST, Wei L, Rovainen CM, Woolsey TA (2001) New patterns of intracortical projections after focal cortical stroke. Neurobiol Dis 8:910-922.

Castillo J (2000) Fisiopatologia de la isquemia cerebral. Rev Neurol 30:459-464.

Chen R, Cohen LG, Hallett M (2002) Nervous system reorganization following injury. Neurosci Lett 111:761-773.

Chino YM, Kaas JH, Smith EL, Langston AL, Cheng H (1992) Rapid reorganization of cortical maps in adult cats following restricted deafferentation in retina. Vis Res 32:789-796.

Daniel M, Whitteridge D (1961) The representation of the visual field on the cerebral cortex in monkeys. J Physiol 159:203-221.

Darian-Smith C, Gilbert CD (1994) Axonal sprouting accompanies functional reorganization in adult cat striate cortex. Nature 368:737-740.

Darian-Smith C, Gilbert CD (1995) Topographic reorganization in the striate cortex of the adult cat and monkey is cortically mediated. J Neurosci 15:1631-1647.

Das A, Gilbert CD (1995a) Receptive field expansion in adult visual cortex is linked to dynamic changes in strength of cortical connections. J Neurophysiol 74:779-792.

Das A, Gilbert CD (1995b) Long-range horizontal connections and their role in cortical reorganization revealed by optical recording of cat primary visual cortex. Nature 375:780-784.

Dirnagl U, Iadecola C, Moskowitz MA (1999) Pathobiology of ischaemic stroke: an integrated view. TINS 22:391-397.

Doetsch GS, Johnston KW, Hannan CJ, Jr. (1990) Physiological changes in the somatosensory forepaw cerebral cortex of adult raccoons following lesions of a single cortical digit representation. Exp Neurol 108:162-175.

Domann R, Hagemann G, Kraemer M, Freund HJ, Witte OW (1993) Electrophysiological changes in the surrounding brain tissue of photochemically induced cortical infarcts in the rat. Neurosci Lett 155:69-72.

Donoghue JP, Hess G, Sanes JN (1996) Substrates and mechanisms for learn-ing in motor cortex. In: Acquisition of motor behavior in vertebrates (Bloedel J, Ebner T, Wise SP, eds), pp 363-386. Cambridge: MIT Press.

Engel D, Pahner I, Schulze K, Frahm C, Jarry H, Ahnert-Hilger G, Draguhn A (2001) Plasticity of rat central inhibitory synapses through GABA metabolism. J Physiol 535:473-482.

Everson RM, Prashanth AK, Gabbay M, Knight BW, Sirovich L, Kaplan E (1998) Representation of spatial frequency and orientation in the visual cortex. Nature 95:8334-8338.

Eysel UT (1982) Functional reconnections without new axonal growth in a partially denervated visual relay nucleus. Nature 299:442-444.

Eysel UT (2002) Pharmacological studies on receptive field architecture. In: The cat primary visual cortex (Payne BR, Peters A, eds), pp 427-470. San Diego, CA.: Academic Press.

Eysel UT, Schweigart G (1999) Increased receptive field size in the surround of chronic lesions in the adult cat visual cortex. Cereb Cortex 9:101-109.

Eysel UT, Schweigart G, Mittmann T, Eyding D, Qu Y, Vandesande F, Orban GA, Arckens L (1999) Reorganization in the visual cortex after retinal and cortical damage. Restor Neurol Neurosci 15:153-164.

Farinas I, DeFelipe J (1991) Patterns of synaptic input on corticocortical and corticothalamic cells in the cat visual cortex. II The axon initial segment. J Comp Neurol 304:70-77.

Fawcett JW, Rosser AE, Dunnett SB (2001a) Metabolic damage. In: Brain damage, brain repair (Fawcett JW, Rosser AE, Dunnett SB, eds), pp 27-44. New York: Oxford University Press.

Fawcett JW, Rosser AE, Dunnett SB (2001b) Anatomicl plasticity. In: Brain damage, brain repair (Fawcett JW, Rosser AE, Dunnett SB, eds), pp 171-195. New york: Oxford University Press.

Florence SL, Taub HB, Kaas JH (1998) Large-scale sprouting of cortical connections after peripheral injury in adult macaque monkeys. Science 282:1117-1121.

Fregnac Y, Shulz D, Thorpe S, Bienenstock E (1988) A cellular analogue of visual cortical plasticity. Nature 333:367-370.

Gabbott PLA, Somogyi P (1986) Quantitative distribution of GABA immunoreactive neurons in the visual cortex (area 17) of the cat. Exp Brain Res 61:323-331.

Gage FH, Olejniczak P, Amstrong DM (1988) Astrocytes are important for sprouting in the septohippocampal circuit. Exp Neurol 102:2-13.

Garraghty PE, LaChica EA, Kaas JH (1991) Injury-induced reorganization of somatosensory cortex is accompanied by reductions in GABA staining. Somatosens Mot Res 8:347-354.

Gilbert CD, Wiesel TN (1985) Intrinsic connectivity and receptive field properties in visual cortex. Vision Res 25:365-374.

Gilbert CD, Wiesel TN (1989) Columnar specificity of intrinsic horizontal and corticocortical connections in cat visual cortex. J Neurosci 9:2432-2442.

Gilbert CD, Wiesel TN (1992) Receptive field dynamics in adult primary visual cortex. Nature 356:150-152.

Ginsberg MD (1997) Injury mechanisms in the ischemic penumbra. Approaches to neuroprotection in acutae ischemic stroke. Cerebrovascular Disease 7:S7-12.

Ginsberg MD, Pulsinelli WA (1994) The ischemic penumbra, injury, thresholds, and therapeuric window for acute stroke. Annals of Neurology 36:553-XXXX.

Godde B, Leonhardt R, Cords SM, Dinse HR (2002) Plasticity of orientation preference maps in the visual cortex of adult cats. Proc Natl Acad Sci U S A 99:6352-6357.

Godecke I, Bonhoeffer T (1996) Development of identical orientation maps for two eyes without common visual experience. Nature 379:251-254.

Godecke I, Kim DS, Bonhoeffer T, Singer W (1997) Development of orientation preference maps in area 18 of kitten visual cortex. Eur J Neurosci 9:1754-1762.

Hagemann G, Redecker C, Neumann-Haefelin T, Freund HJ, Witte OW (1998) Increased long-term potentiation in the surround of experimentally induced focal cortical infarction. Ann Neurol 44:255-258.

Hubel D, Wiesel T (1962) Receptive fields, binocular interactions, and functional architecture in the cat's visual cortex. J Physiol 160:106-154.

Hubel DH, Wiesel TN (1959) Receptive fields of single neurones in the cat's striate cortex. J Physiol (Lond) 148:574-591.

Hubel DH, Wiesel TN (1963) Shape and arrangement of columns in the cat's striate cortex. J Physiol (Lond) 165:559-568.

Hubel DH, Wiesel TN (1965) Receptive fields and functional architecture in two non striate visual areas (18 and 19) of the cat. J Neurophysiol 28:229-289.

Hubel DH, Wiesel TN (1974) Uniformity of monkey striate cortex: a parallel relationship between field size, scatter, and magnification factor. J Comp Neurol 158:295-305.

Hubener M, Shoham D, Grinvald A, Bonhoeffer T (1997) Spatial relationships among three columnar systems in cat area 17. J Neurosci 17:9270-9284.

Illig KR, Danilov YP, Ahmad A, B. KC, Spear PD (2000) Functional plasticity in extrastriate visual cortex following neonatal visual cortex damage and monocular enucleation. Brain Res 882:241-250.

Issa NP, Trepel C, Stryker MP (2000) Spatial frequency maps in cat visual cortex. J Neurosci 20:8504-8514.

Jacobs KM, Donoghue JP (1991) Reshaping the cortical motor map by unmasking latent intracortical connections. Science 251:944-947.

Jones EG (1993) GABAergic neurons and their role in cortical plasticity in primates. Cereb Cortex 3:361-372.

Jones EG, Pons TP (1998) Thalamic and brainstem contributions to large-scale plasticity of primate somatosensory cortex. Science 282:1121-1125.

Jones TA, Schallert T (1992) Overgrowth and pruning of dendrites in adult rats recovering from neocortical damage. Brain Res 581:156-160.

Jones TA, Schallert T (1994) Use-dependent growth of pyramidal neurons after neocortical damage. J Neurosci 14:2140-2152.

Kaas JH (1991) Plasticity of sensory and motor maps in adult mammals. Annu Rev Neurosci 14:137-167.

Kaas JH, Krubitzer LA, Chino YM, Langston AL, Polley EH, Blair N (1990) Reorganization of retinotopic cortical maps in adult mammals after lesions of the retina. Science 248:229-231.

Kasten E, Wust S, Behrens-Baumann W, Sabel BA (1998) Computer-based training for the treatment of partial blindness. Nat Med 4:1083-1087.

Katz LC (1999) What's critical for the critical period in visual cortex? Cell 99:673–676.

Kisvarday ZF, Beaulieu C, Eysel UT (1993) Network of GABAergic large basket cells in cat visual cortex (area 18). Implications for lateral disinhibition. J Comp Neurol 327:398-415.

Kisvarday ZF, Martin KAC, Whitteridge D, Somogyi P (1985) Synaptic connections of intracellularly filled clutch cells, a type of small basket cell in the visual cortex of the cat. J Comp Neurol 241:111-137.

Kisvarday ZF, Kim DS, Eysel UT, Bonhoeffer T (1994) Relationship between lateral inhibitory connections and the topography of the orientation map in cat visual cortex. Eur J Neurosci 6:1619-1632.

Kolb B, Gibb R (1993) Possible anatomical basis of recovery of function after neonatal frontal lesions in rats. Behav Neurosci 107:799-811.

Le Roux PD, Reh TA (1996) Reactive astroglia support primary dendritic but not axonal outgrowth from mouse cortical neurons in vitro. Exp Neurol 137:49-65.

Leslie FM (1993) Neurotransmitters as neurotrophic factors. In: Neurotrophic factors (Loughlin SE, Fallon JH, eds), p 607. San Diego, CA.: Academic Press.

Li Y, Jiang N, Powers C, Chopp M (1998) Neuronal damage and plasticity identified by microtubule-associated protein 2, growth associated protein 43, and cyclin D1 immunoreactivityafter focal cerebral ischemia in rats. Stroke 29:1972-1980.

Linden DJ, Wong KL, Sheu FS, Routtenberg A (1988) NMDA receptor blockade prevents the increase in protein kinase C substrate (protein F1) phosphorylation produced by long-term potentiation. Brain Res 458:142-146.

MacNeil MA, Lomber SG, Payne BR (1996) Rewiring of transcortical projections to middle suprasylvian cortex following early removal of cat areas 17 and 18. Cereb Cortex 6:362-376.

Massie A, Cnops L, Smolders I, Van Damme K, Vandenbussche E, Vandesande F, Eysel UT, Arckens L (2003) Extracellular GABA concentrations in area 17 of cat visual cortex during topographic map reorganization following binocular central retinal lesioning. Brain Res 976:100-108.

McGraw J, Hiebert GW, Steeves JD (2001) Modulating astrogliosis after neurotrauma. J Neurosci Res 63:109-115.

McGuire CB, Snipes GJ, Norden JJ (1988) Light-microscopic immunolocalization of the growth- and plasticity- associated protein GAP-43 in the developing rat brain. Brain Res 469:277-291.

McNamara RK, Routtenberg A (1995) NMDA receptor blockade prevents kainate induction of protein F1/GAP-43 mRNA in hippocampal granule cells and subsequent mossy fiber sprouting in the rat. Mol Brain Res 33:22-28.

Mir HM, Tatsukawa KJ, Carmichael T, Chesselet MF, Kornblum HI (2004) Metabolic correlates of lesion specific plasticity: an in vivo imaging study. Brain Res 1002:28-34

Michaelis EK (1998) Molecular biology of glutamate receptors in the central nervous system and their role in excitotoxicity, oxidative stress and aging. Prog Neurobiol 54:369-415.

Mittmann T, Eysel UT (2001) Increased synaptic plasticity in the surround of visual cortex lesions in rats. Neuroreport 12:3341-3347.

Mittmann T, Luhmann HJ, Schmidt-Kastner R, Eysel UT, Weigel H, Heinemann U (1994) Lesion-induced transient suppression of inhibitory function in rat neocortex in vitro. Neuroscience 60:891-906.

Montoro RJ, Diaz-Nido J, Avila J, Lopez-Barneo J (1993) N-methyl-D-aspartate stimulates the dephosphorylation of the microtubule-associated protein 2 and potentiates excitatory synaptic pathways in the rat hippocampus. Neuroscience 54:859-871.

Mountcastle VB (1957) Modality and topographic properties of single neurons of cat's somatic sensory cortex. J Neurophysiol 20:408-434.

Myers WA, Churchill JD, Muja N, Garraghty PE (2000) Role of NMDA receptors in adult primate cortical somatosensory plasticity. J Comp Neurol 418:373-382.

Neumann-Haefelin T, Witte OW (2000) Periinfarct and remote excitability changes after transient middle cerebral artery occlusion. J Cereb Blood Flow Metab 20:45-52.

Neumann-Haefelin T, Staiger JF, Redecker C, Zilles K, Fritschy JM, Mohler H, Witte OW (1998) Immunohistochemical evidence for dysregulation of the GABAergic system ipsilateral to photochemically induced cortical infarcts in rats. Neuroscience 87:871-879.

Nguyen TT, Yamamoto T, Stevens RT, Hodge CJ, Jr. (2000) Reorganization of adult rat barrel cortex intrinsic signals following kainic acid induced central lesion. Neurosci Lett 288:5-8.

Nieto-Sampedro M, Collazos-Castro JE, Taylor JS, Gudiño-Cabrera G, Verdú-Navarro E, Pascual-Piédrola JI, Insausti-Serrano R (2002) Trauma en el sistema nervioso central y su reparación. Rev Neurol 35:534-552.

Nudo RJ, Wise BM, SiFuentes F, Milliken GW (1996a) Neural substrates for the effects of rehabilitative training on motor recovery after ischemic infarct. Science 272:1791-1794.

Nudo RJ, Milliken GW, Jenkins WM, Merzenich MM (1996b) Use-dependent alterations of movement representations in primary motor cortex of adult squirrel monkeys. J Neurosci 16:785-807.

Orban GA, Vandenbussche E, Sprague JM, De Weerd P (1990) Orientation discrimination in the cat: a distributed function. Proc Natl Acad Sci U S A 87:1134-1138.

Payne BR, Lomber SG (2002) Plasticity of the visual cortex after injury: What's different about the young brain? Neuroscientist 8:174-185.

Payne BR, Peters A (2002) The concept of cat primary visual cortex. In: The cat primary visual cortex (Payne BR, Peters A, eds), pp 1-129. San Diego, CA.: Academic Press.

Payne BR, Berman NE, Murphy EH (1981) Organization of direction preferences in cat visual cortex. Brain Res 211:445-450.

Qu Y, Massie A, Van der Gucht E, Cnops L, Vandenbussche E, Eysel UT, Vandesande F, Arckens L (2003) Retinal lesions affect extracellular glutamate levels in sensory-deprived and remote non-deprived regions of cat area 17 as revealed by in vivo microdialysis. Brain Res 962:199-206.

Que M, Witte OW, Zilles K (2000) Transient up-regulation of gamma-aminobutyric acid(A) receptor binding by lubeluzole after neocortical specify lesion in rats. Neurosci Lett 296:125-128.

Que M, Schiene K, Witte OW, Zilles K (1999a) Widespread up-regulation of N-methyl-D-aspartate receptors after focal photothrombotic lesion in rat brain. Neurosci Lett 273:77-80.

Que M, Witte OW, Neumann-Haefelin T, Schiene K, Schroeter M, Zilles K (1999b) Changes in GABA(A) and GABA(B) receptor binding following cortical photothrombosis: a quantitative receptor autoradiographic study. Neuroscience 93:1233-1240.

Raivich G, Bohatschek M, Kloss CU, Werner A, Jones LL, Kreutzberg GW (1999) Neuroglial activation repertoire in the injured brain: graded response, molecular mechanisms and cues to physiological function. Brain Res Brain Res Rev 30:77-105.

Ramachandran VS, Gregory TL (1991) Perceptual filling-in of artificially induced scotomas in human vision. Nature 350:699-702.

Rauschecker JP, Tian B, Korte M, Egert U (1992) Crossmodal changes in the somatosensory vibrissa/barrel system of visually deprived animals. Proc Natl Acad Sci U S A 89:5063-5067.

Redecker C, Luhmann HJ, Hagemann G, Fritschy JM, Witte OW (2000) Differential downregulation of GABAA receptor subunits in widespread brain regions in the freeze-lesion model of focal cortical malformations. J Neurosci 20:5045-5053.

Ridet JL, Malhotra SK, Privat A, Gage FH (1997) Reactive astrocytes: cellular and molecular cues to biological function. Trends Neurosci 20:570-577.

Rumpel S, Hatt H, Gottmann K (1998) Silent synapses in the developing rat visual cortex: evidence for postsynaptic expression of synaptic plasticity. J Neurosci 18:8863-8874.

Rumpel S, Hoffmann H, Hatt H, Gottmann K, Mittmann T, Eysel UT (2000) Lesion-induced changes in NMDA receptor subunit mRNA expression in rat visual cortex. Neuroreport 11:4021-4025.

Sanchez C, Diaz-Nido J, Avila J (2000) Phosphorylation of microtubule-associated protein 2 (MAP2) and its relevance for the regulation of the neuronal cytoskeleton function. Prog Neurobiol 61:133-168.

Sanchez C, Ulloa L, Montoro RJ, Lopez-Barneo J, Avila J (1997) NMDA-glutamate receptors regulate phosphorylation of dendritic cytoskeletal proteins in the hippocampus. Brain Res 765:141-148.

Schieber MH, Hibbard LS (1993) How somatotopic is the motor cortex hand area? Science 261:489-492.

Schiene K, Staiger JF, Bruehl C, Witte OW (1999) Enlargement of cortical vibrissa representation in the surround of an ischemic cortical lesion. J Neurol Sci 162:6-13.

Schiene K, Bruehl C, Zilles K, Qu M, Hagemann G, Kraemer M, Witte OW (1996) Neuronal hyperexcitability and reduction of GABAA-receptor expression in the surround of cerebral photothrombosis. J Cereb Blood Flow Metab 16:906-914.

Schuett S, Bonhoeffer T, Hubener M (2001) Pairing-induced changes of orientation maps in cat visual cortex. Neuron 32:325-337.

Schweigart G, Eysel UT (2002) Activity-dependent receptive field changes in the surround of adult cat visual cortex lesions. Eur J Neurosci 15:1585-1596.

Sengpiel F, Stawinski P, Bonhoeffer T (1999) Influence of experience on orientation maps in cat visual cortex. Nat Neurosci 2:727-732.

Sengpiel F, Godecke I, Stawinski P, Hubener M, Lowel S, Bonhoeffer T (1998) Intrinsic and environmental factors in the development of functional maps in cat visual cortex. Neuropharmacology 37:607-621.

Sharma N, Kress Y, Shafit-Zagardo B (1994) Antisense MAP-2 oligonucleotides induce changes in microtubule assembly and neuritic elongation in pre-existing neurites of rat cortical neurons. Cell Motil Cytoskeleton 27:234-247.

Sharp FR, Lu A, Tang Y, Millhorn DE (2000) Multiple molecular penumbras aftercerebral ischemia. J Cereb Blood Flow Metab 20:1011-1032.

Shmuel A, Grinvald A (1996) Functional organization for direction of motion and its relationship to orientation maps in cat area 18. J Neurosci 16:6945-6964.

Shoham D, Hubener M, Schulze S, Grinvald A, Bonhoeffer T (1997) Spatio-temporal frequency domains and their relation to cytochrome oxydase staining in cat visual cortex. Nature 385:529-533.

Siesjo BK (1984) Cerebral circulation and metabolism. J Neuosurg 60:883-908.

Sillito AM (1974a) Proceedings: Effects of the iontophoretic application of bicuculline on the receptive field properties of simple cells in the visual cortex of the cat. J Physiol 242:127P-128P.

Sillito AM (1974b) Proceedings: Modification of the receptive field properties of neurones in the visual cortex by bicuculline, a GABA antagonist. J Physiol 239:36P-37P.

Sillito AM (1975a) The contribution of inhibitory mechanisms to the receptive field properties of neurones in the striate cortex of the cat. J Physiol 250:305-329.

Sillito AM (1975b) The effectiveness of bicuculline as an antagonist of GABA and visually evoked inhibition in the cat's striate cortex. J Physiol 250:287-304.

Singer W, Freeman B, Rauschecker J (1981) Restriction of visual experience to a single orientation affects the organization of orientation columns in cat visual cortex. A study with deoxyglucose. Exp Brain Res 41:199-215.

Skene JH (1989) Axonal growth-associated proteins. Annu Rev Neurosci 12:127-156.
Somogyi P, Freund TF, Cowey A (1982) The axo-axonic interneuron in the cerebral cortex of the rat, cat and monkey. Neuroscience 10:261-294.

Somogyi P, Kisvarday ZF, Martin KAC, Whitteridge D (1983) Synaptic connections of morphologically identified and physiologically characterized large basket cells on the striate cortex of cat. Neuroscience 10:261-294.

Spear PD, Tong L, McCall MA (1988) Functional influence of areas 17, 18, and 19 on lateral suprasylvian cortex in kittens and adult cats: implications for compensation following early visual cortex damage. Brain Res 447:79-91.

Strata P, Buffo A, Rossi F (1999) Mechanisms of axonal plasticity. Arch Ital Biol 137:181.

Stroemer RP, Kent TA, Hulsebosch CE (1995) Neocortical neural sprouting, synaptogenesis, and behavioral recovery after neocortical infarction in rats. Stroke 26:2135-2144.

Swindale NV, Matsubara JA, Cyander MS (1987) Surface organization of orientation and direction selectivity in cat area 18. J Neurosci 7:1414-1427.

Szele FG, Alexander C, Chesselet MF (1995) Expression of molecules associated with neuronal plasticity in the striatum after aspiration and thermocoagulatory lesions of the cerebral cortex in adult rats. J Neurosci 15:4429-4448.

Ts'o DY, Gilbert CD, Wiesel TN (1986) Relationships between horizontal interactions and functional architecture in cat striate cortex as revealed by cross-correlation analysis. J Neurosci 6:1160-1170.

Tusa RJ, Rosenquist AC, Palmer LA (1978) The retinotopic organization of area 17 (striate cortex) in the cat. J Comp Neurol 177:213-236.

Vandenbussche E, Sprague JM, de Weerd P, Orban GA (1991) Orientation discrimination in the cat: its cortical locus. I. Areas 17 and 18. J Comp Neurol 305:632-658.

Watson BD (1998) Animal Models of Photochemically Induced Brain Ischemia and Stroke. In: Cerebrovascular Disease (Ginsberg MD, Bogousslavsky J, eds), pp 52-73.

Woolsey TA, Wann JR (1976) Areal changes in mouse cortical barrels
following vibrissal damage at different postnatal ages. J Comp Neurol 170:53–66.

Zepeda A, Vaca L, Arias C, Sengpiel F (2003) Reorganization of visual cortical maps after focal ischemic lesions. J Cereb Blood Flow Metab 23:811-820.

Zihl J, von Cramon D (1985) Visual field recovery from scotoma in patients with postgeniculate damage. Brain Behav Evol 108:335-365.